THEME I

MECHANICAL PROPERTIES OF STEEL AND CONCRETE UNDER LOAD CYCLES IDEALIZING SEISMIC ACTIONS. STUDIES ON BOND BETWEEN CONCRETE AND STEEL.

PROPRIETES MECANIQUES DE L'ACIER ET DU BETON SOUS DES CYCLES REPRESENTATIFS DES ACTIONS SISMIQUES. ETUDES SUR L'ADHERENCE ACIER-BETON.

a) Steel – Acier

Reporter / Rapporteur: Ben KATO
University of Tokyo
Tokyo, Yapan

b) Concrete – Béton

Reporter / Rapporteur: Hiroyuki AOYAMA
University of Tokyo
Tokyo, Yapan

c) Bond between concrete and steel – Adhérence acier-béton

Reporter / Rapporteur: Theodosios P. TASSIOS
National Technical University
Athens, Greece

FORCE-STRAIN RELATIONSHIP OF REINFORCING BARS EMBEDDED IN CONCRETE UNDER REVERSED LOADINGS

Shiro MORITA
Kyoto University
Japan

Tetsuzo KAKU
Akashi Technological College
Japan

Eiji SUDO
Kyoto University
Japan

SUMMARY

The relationship between applied force and mean strain of a reinforcing bar embedded in a concrete prism subjected to repeated load reversals was determined theoretically by the use of the basic properties of the materials. The influence of the local contacts of cracked surfaces before the perfect closing of cracks at compressive loading was quantified from the reversed loading tests of concrete cylinders. In the theoretical determination, the local contact model of cracks and the bond-slip model under reversed loads were applied successfully. The agreement between experimental and theoretical results was good.

RESUME

La relation entre la force appliquée et l'effort principal dans une barre d'acier comprise dans prisme de béton soumis à des charges à alternation fréquente fut établi théoriquement en tenant compte des propriétés fondamentales des matériaux. La mesure quantitative de l'influence du contact local des surface fissurées avant leur-obturation sous compression fut déterminée par les expériences de charges alternées appliquées à des cylindres de béton. Dans la définition théorique, le modèle des contact local des fissure et le modèle du glissement-d'adhésion sous charges alternées furent appliqués avec succès. Les données expérimentales correspondaient suffisemment bien avec les estimation théorique.

INTRODUCTION

As a basic approach to predict the characteristic behaviors of reinforced concrete members, the relationship between applied force and mean strain of reinforcing steel embedded in concrete has been dealt with for monotonic and repeated loadings. Based on the results of these studies, a clear idealization of the behaviors was presented by Borges (1973)[1]. However, the exact understanding of the relationship was left unsolved especially for the transition from positive to negative strains or from negative to positive strains.

To predict the hysteretic behaviors of reinforced concrete elements under cycles of reversed loads, the rolls of bond between steel and concrete and of the compressive stress transfer across cracks due to local contacts should be taken into account. Compression and tension tests of cylinders of ordinary concrete and steel-fiber reinforced concrete were performed to

quantify the local contact effects of cracked surfaces and the deterioration of the properties in tension due to the histories of compressive strain. The idealized results of cylinder tests were used as the properties of the materials in the theory to predict force-strain relationship of a steel bar embedded in a concrete prism. The bond-slip model under reversed loadings proposed by Morita and Kaku (1973)[3] was also applied to the theorization.

To verify the validity of the theoretically obtained behaviors, compression and tension tests of reinforced concrete prisms were carried out. A prismatic concrete specimen of 9.5 x 9.5 x 50cm reinforced axially with a 16 mm diameter bar was used. The theoretically predicted behaviors agreed with the test results. The results of the investigation can be easily applied to describe the behavior of tension zones in beams and columns subjected to load reversals.

COMPRESSION AND TENSION TESTS OF CONCRETE CYLINDERS

Though a large number of test results have been reported on the stress-strain relationship under repeated compressive load histories, none of these aimed to investigate the behaviors at the transition from compression to tension or from tension to compression loads. In beams and columns subjected to reversed loading, concrete behaves always passing through this transition. Once cracks have occurred in the previous tensile loading, some compressive stress may be transferred across the cracks before they entirely close in the proceeding compressive loading. In addition, tensile strength of concrete may decrease owing to high compressive strain histories.

To examine the above mentioned behaviors, reversed loading tests were performed on 10 x 18cm cylinders. Upper and lower end portions of 10 x 20cm test cylinders were cut off to make sure of bonding to end steel plates by epoxy. Tension was applied through high strength steel bolts threaded into the end plates. Fig. 1 shows the testing arrangements. Ordinary concrete and steel-fiber concrete (fiber contents = 2 vol. %, dimension of crimped fiber = 0.25 x 0.50 x 25mm) were tested. Average compressive strengths were 250 kgf/cm^2 and 500 kgf/cm^2 for each concrete. Loading histories were as follows; (1) tension loading to failure and then compression loading, (2) compression loading to various strain levels and then tension to failure and compression again. Fig. 2 shows the typical stress-strain curves obtained. The strain measurement by wire resistance gages showed that concrete behaved elastically within the uncracked portion. Therefore, the deviation of the stress-strain curve in compression measured in the 16cm gage length spanned across a crack from that measured without any tension cracks can be regarded as the local contact effects between cracked surfaces. Then the crack width can be assumed as the deviated strain times the 16cm gage length. The crack width thus assumed might have some errors especially for the specimen to which a high compressive strain history was given before testing in tension and then again in compression. The cause is that some irrecoverable strain at tension loading exists owing to the deterioration in tension. Fig. 3 shows the inflence of compressive strain histories on the stress-strain curves in tension. The significant deterioration was observed in the tensile strengths and

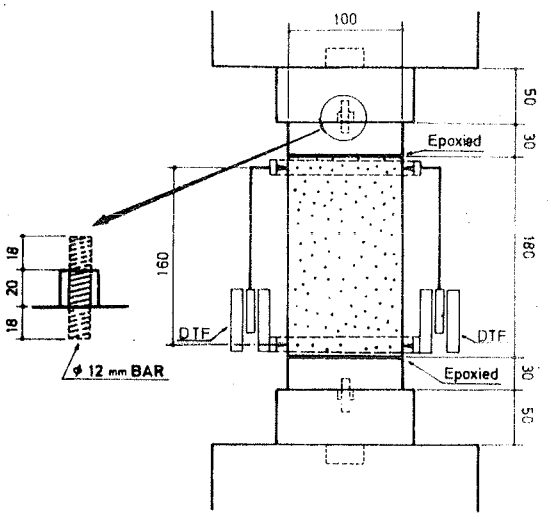

Fig. 1 CYLINDER TEST ARRANGEMENT

in the stress-strain curves.

Based on the test results shown in Fig. 2 and Fig. 3, the local contact effect of cracked surfaces and the deteriorated behaviours in tension due to compressive strain histories were idealized as shown in Fig. 4 and Fig. 5, respectively. Fig. 5 indicates that when unloading starts from the peak stress in compression strength and elastic modulus in tension decrease to one-half the values at testing first in tension, and that when unloading starts from a intermediate compressive strain the corresponding values are given by linear interpolation. The above idealized behaviors are shown in Fig. 2 combined with the assumption mentioned later in Fig. 10, along with the experimental curves.

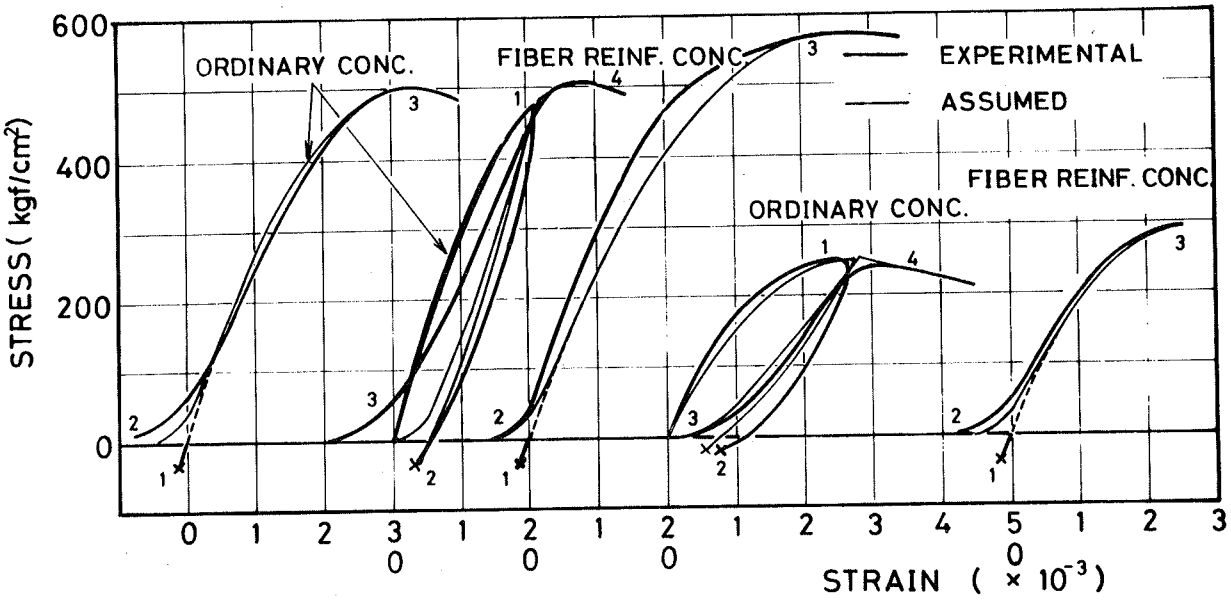

Fig. 2 STRESS-STRAIN CURVES OF CONCRETE UNDER REVERSED LOADINGS

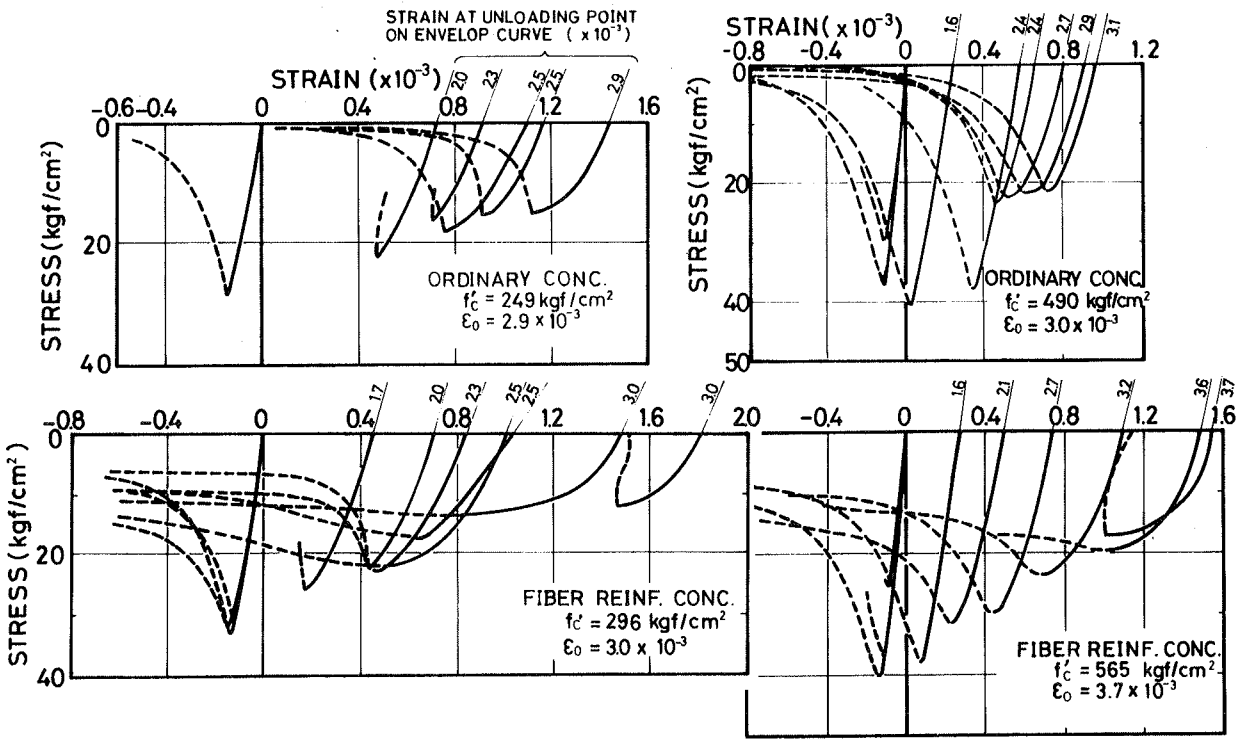

Fig. 3 DETERIORATION IN TENSILE STRESS-STRAIN CURVES DUE TO COMPRESSIVE STRAIN HISTORIES

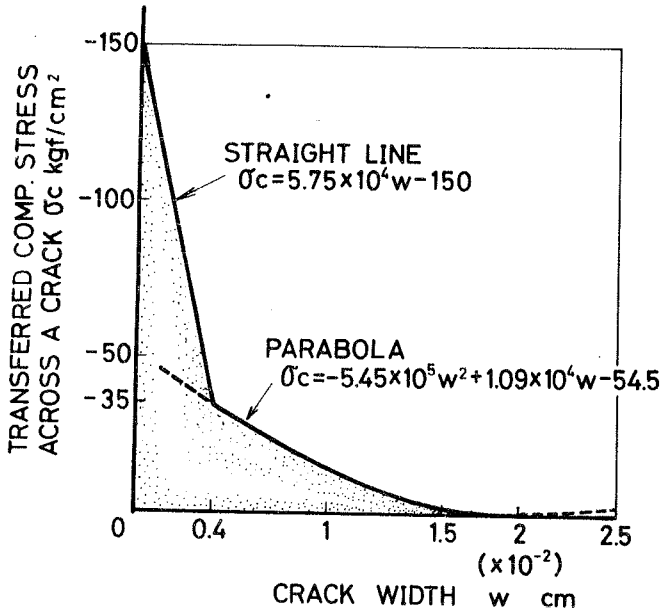

Fig. 4 MODEL FOR LOCAL CONTACT EFFECTS

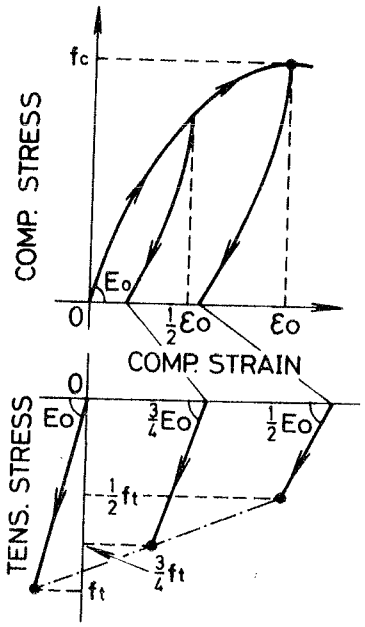

Fig.5 MODEL FOR DETERIORATION IN TENSION

DERIVATION OF THE BEAHVIORS OF REINFORCED CONCRETE PRISMS

The deformability of reinforced concrete prisms at monotonic tension loadings was analyzed in detail by Morita and Kaku (1975)[4]. In their derivation, the force-strain curve of a bar embedded in concrete was represented by the curve OABCD in Fig. 6. Based on the bond-slip relationship the contribution of surrounding concrete to reducing the mean steel strain was evaluated by the $k_1k_2f_tA_c$ value in Fig. 6, where f_t and A_c denote the tensile strength of concrete and concrete cross sectional area, respectively. The values of k_1k_2 were calculated and plotted against the mean steel strain as shown in Fig. 7. The bold line in Fig. 7 is the experimental equation obtained from tension tests of reinforced concrete prisms[4]. Contrary to the satisfactory explanation of the behavior in the monotonic tension loading, the behavior at transition from tension to compression or from compression to tension still remains unsolved. When unloading starts at point C in Fig. 8, the force-strain curve follows line CEFG and joins line OGH at point G. Line OGH denotes the compressive force-strain curve of reinforced concrete prisms at monotonic loading. If the effect of local contacts of craked surfaces is disregarded the unloading curve will pass through points CEG* and the sudden change in rigidity must be observed at point G*. However, such a sudden change can not be realized. Before cracks entirely close, some compression can be transferred across cracked surfaces owing to local contacts. Therefore, the effect of the local contacts can be shown by the shaded area in Fig. 8.

The above explanation is only qualitative. The main object of this investigation is to quantify the behaviors of reinforced concrete prisms under load reversals. The assumption used in the theorization are;

1. The bond-slip model proposed by Morita and Kaku (1973)[3] is applicable. (The model is briefly shown in Fig. 9 with six parameters used in this investigation)
2. The idealized contact effect of cracked surfaces shown in Fig. 4 is also applicable.
3. Concrete behaves elastically in tension. Deterioration in tensile

strength and elastic modulus due to compressive strain histories can be estimated by Fig. 5.

4. The stress-strain curve of concrete in compression is represented as shown in Fig. 10. (The experimental equation, proposed by Karsan and Jirsa (1967)[2], for the relation between S_E and S_P was used in this study.)
5. Concrete stress distribution in a cross section is uniform.

Concrete prisms of 9.5cm x 9.5cm in cross section and 50cm in length reinforced axially by a 16mm diameter deformed bar were analyzed using the properties of materials obtained in the verification tests; compressive strength of concrete prisms f_c = 334 kgf/cm^2 (=0.86f_c'), strain at the peak stress ε_o = 0.2%, tensile strength f_t = 17.9 kgf/cm^2. Every segment bounded by adjacent cracks were divided into 40 intervals and the uniform bond stress distribution was assumed within each interval. Step by step calculations were iterated to

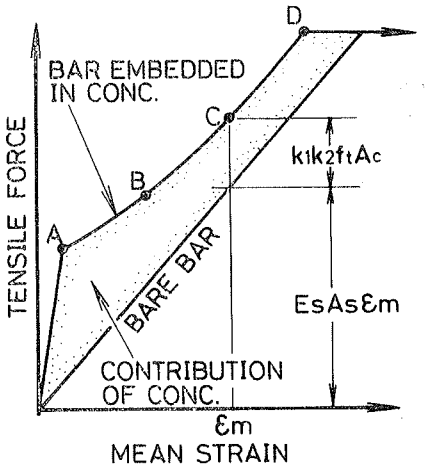

Fig.6 IDEALIZED FORCE-STRAIN CURVE OF STEEL IN CONCRETE

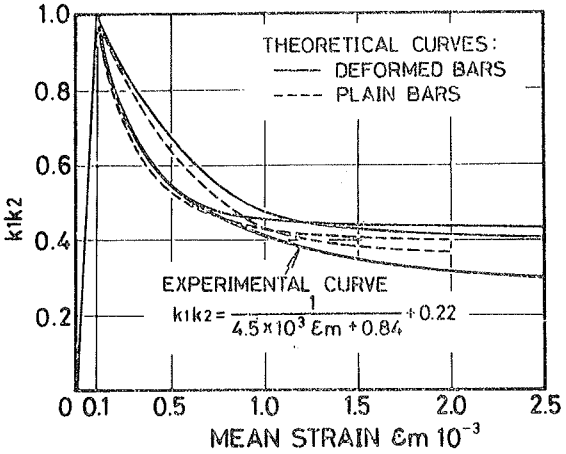

Fig. 7 k_1k_2 - ε_m DIAGRAM

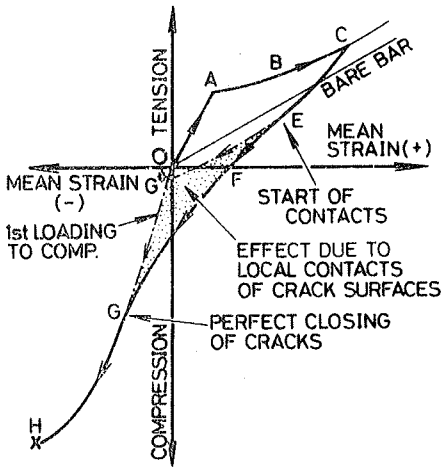

Fig.8 SCHEMA FOR TRANSITION FROM TENSION TO COMPRESSION STRAIN

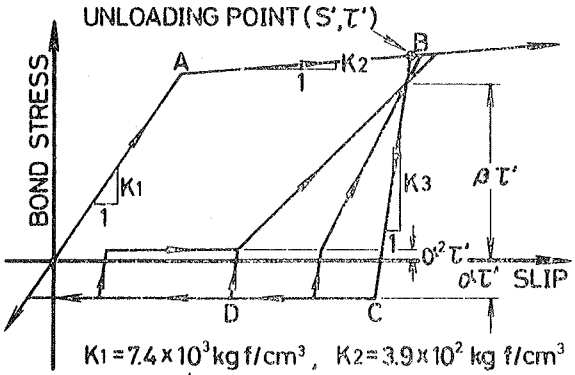

Fig. 9 BOND - SLIP MODEL

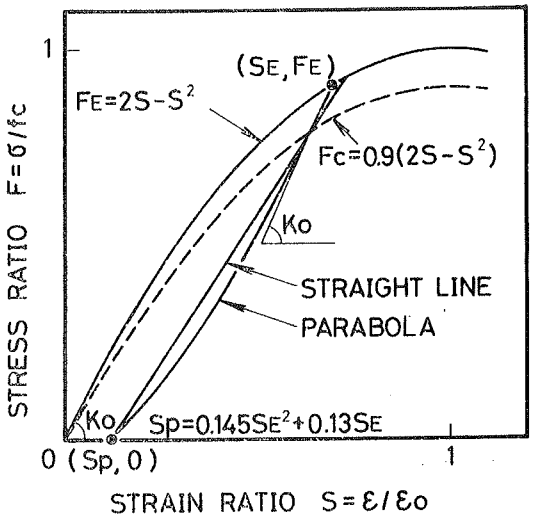

Fig. 10 ASSUMED STRESS-STRAIN CURVE OF CONCRETE

satisfy end conditions. The loading histories adopted in the verification tests were followed in the theoretical derivation.

The derived force-strain curves are shown in Fig. 11 (a),(b),(c) by broken lines. Fig. 11(d) shows the steel force distribution of specimen PD3 along the axis of the segment at various loading stages.

Though the predicted average crack spacing at the stabilized cracking stage tended to 12.5cm, the crack spacing was limited at least to 16.7cm in the theory to give the reasonable comparisons between the predicted and experimental behaviors. The reason is that two cracks were observed in the specimens to give the average spacing of 16.7cm in the experiments and the crack spacing gives the important influence on the evaluation of the local contact effects.

REVERSED LOADING TESTS OF REINFORCED CONCRETE PRISMS

Tests were performed on fifteen reinforced concrete specimens to verify the predicted behaviors. The variables in the experiment were; type of concrete (orinary or fiber reinforced), surface characteristic of bars (plain or deformed). The results of six specimens among them were selected to compare with the predicted behaviors.

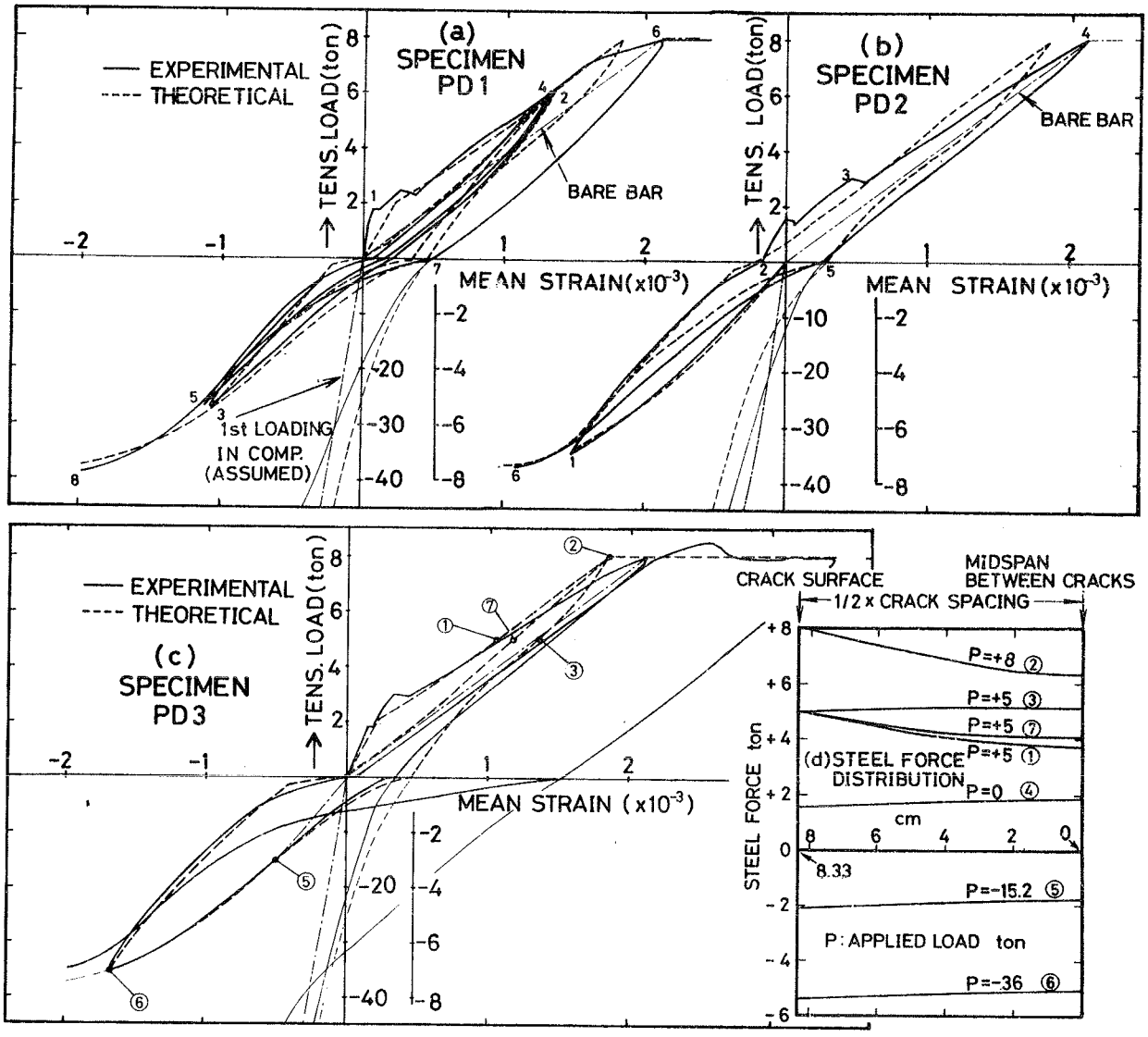

Fig. 11 COMPARISON BETWEEN THEORETICAL AND EXPERIMENTAL FORCE-STRAIN CURVES

Fig. 12 shows the test specimen. Load reversals were applied to steel end plates through threaded rods. The embedded bar was butt-welded at both ends to end plates. The specimens were cast in a horizontal position and cured in a moist condition until three days before testing.

The concrete mix proportions were 1 : 3.2 : 2.4 with water-cement ratio of 55% for ordinary concrete and with water-cement ratio of 64% for fiber reinforced concrete of 2 vol.% fiber contents. The maximum gravel size was 10mm for both concretes. Cylinder strengths at the test age were 399 kgf/cm^2 for ordinary concrete and 427 kgf/cm^2 for fiber concrete.

The mean strain of the specimens was obtained from the total deformation measured by differential transformers spanned between end plates. Moving head speed of the Instron-type testing machine was set at 0.3 mm/min. The designations of the specimens were noted in such a manner that; the first letter indicates the type of concrete (P: ordinary concrete, F: fiber reinforced concrete), the second letter indicates the type of bars of 16mm diameter (D: deformed bars, R: plain round bars) and the last number, if any, indicates the number of the specimen of the same kind.

The test results were plotted in Fig. 11, Fig. 13 and Fig. 14. As can be seen in Fig. 11, the theoretical predictions can describe the behaviors obtained in the tests. The deviation of the test curve from the theoretical one at high tensile loads near yielding was probably caused by the loss of bond at the end parts of the segment due to the formation of internal cracks. The effects of local contacts of cracked surfaces were

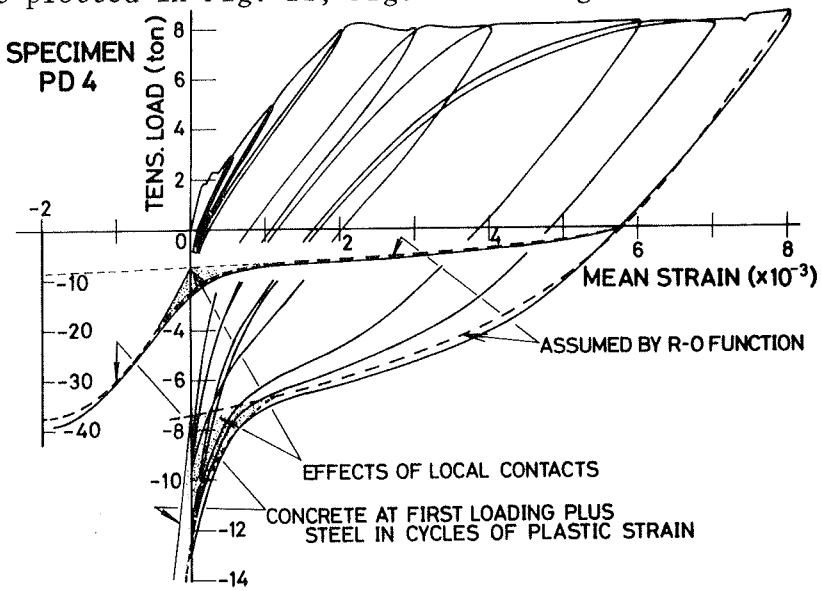

Fig. 13 FORCE-STRAIN CURVE INCLUDING LARGE PLASTIC STRAIN HISTORIES

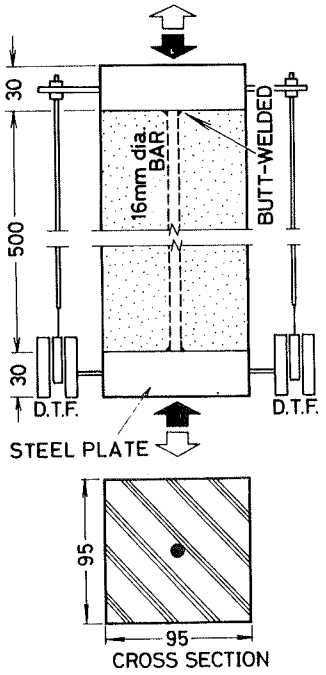

Fig. 12 TEST SPECIMEN

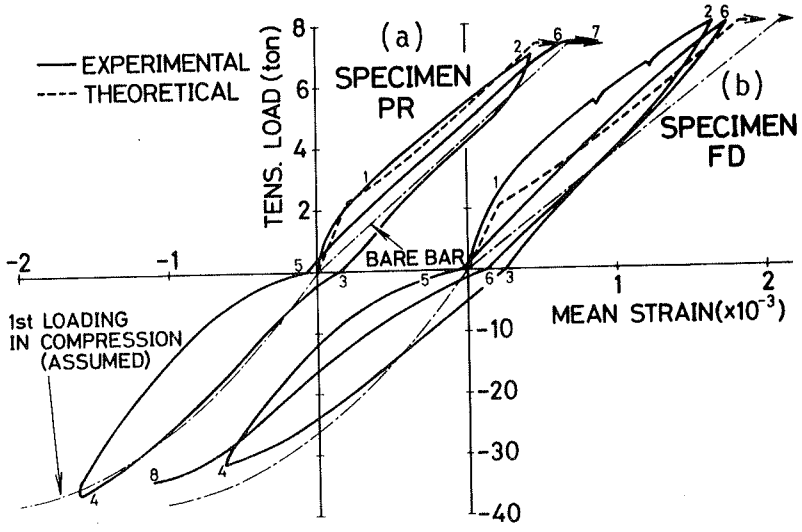

Fig. 14 FORCE-STRAIN CURVES OF PR AND FD SPECIMEN

somewhat exaggerated in the predicted curves, though it seems to be underestimated at the cylinder tests as shown in Fig. 2.

The contribution of concrete in tension can be disregarded in the region well into the plastic strain of steel, but the local contact effects are still clearly observed in the transition from tension to compression strain as shown in Fig. 13. This contribution can be successfully estimated without the consideration of stress transfer by bond as shown in Fig. 13 by the shaded area. This estimation was done by adding the local contact model to the force-strain curve of steel alone which was assumed to follow the Ramberg-Osgood function. Fig. 14 (a) shows the test result of the specimen reinforced by a plain round bar, along with the predicted curve for the deformed bar specimen under monotonic loading in tension. In this specimen any cracks could not be observed at all. Though it is said that the contribution of surrounding concrete in tension is lowered in the case of round bars, Fig. 14 (a) shows the almost equivalent contribution of concrete for both bars. The reason is, as pointed out by Morita and Kaku (1975)[4], that the effect of good bond is mainly realized in shortening the crack spacing not in reducing the mean steel strain. Fig. 14 (b) shows the test curve of fiber reinforced concrete having a deformed bar axially at the center. In this case, the contribution of concrete in reducing the mean steel strain is emphasized owing to the tensile stress transfer across the cracks even after the tensile fine cracks have occurred.

CONCLUDING REMARKS

The force-strain relationship under reversed loadings of reinforcing steel embedded in concrete was predicted by the use of the local contact model and the bond-slip model. The predicted relationships were verified by the tests of axially reinforced concrete prisms. From the comparisons between theoretical and experimental results, the following conclusions were obtained.

1. The proposed model for the quantitative estimation of the local contact effects between cracked surfaces gives the tool to describe the behaviors in the transition from tension to compression strains of reinforced concrete elements.
2. The proposed model of bond-slip relationship under reversed loadings is applicable to predict the effect of the deterioration of bond on the behaviors of reinforced concrete elements under load reversals.
3. Further improvements of the local contact model should be needed to set up in general the reasonable idealization of the force-strain relationship of bars embedded in concrete.

REFERENCES

1) Borges, J. Ferry; Structural Behavior under Repeated Loading, European Committee for Earthquake Engineering, Dec., 1973.
2) Karsan, I. D. and Jirsa, J. O.; Behavior of Concrete under Compressive Loadings, Proc. of ASCE, ST.12, Dec., 1969.
3) Morita, S. and Kaku, T.; Local Bond Stress-Slip Relationship under Repeated Loading, Lisbon IABSE Symposium, Sep., 1973.
4) Morita, S. and Kaku, T; Cracking and Deformation of Reinforced Concrete Prisms Subjected to Tension, Liege Colloquium Inter-Association, Jun., 1975.

BEHAVIOUR OF CONCRETE UNDER LOW CYCLE REPEATED LOADINGS

Vladimir CERVENKA
Building Research Institute
Technical University
Prague, Czechoslovakia

SUMMARY Experimental investigation of concrete under repeated loading with load level near the strength of material is described. A special method based on load-volumetric strain curve was developed for determination of appropriate load level for each specimen ensuring that loading is within the low cycle fatigue. Results include derivation of fatigue curve and determination of the stability limit.

RESUME Les éprouvettes du béton ont été exposées aux charges répétées sur le niveau proche à la résistance du béton respectif. Une méthode particulière était utilisée dans les essais - méthode fondée sur la loi "charge-déformation volumétrique". Le but de l'évaluation simultanée était la détermination de niveau de charge approprié pour chaque éprouvette pour obtenir sa rupture après un petit nombre de répetitions de la charge. Comme résultats des essais on a obtenu la courbe S-N et la limite de stabilisation dans le domaine de petit nombre des cycles.

1. INTRODUCTION

Behaviour of concrete under repeated loading with load level approaching the monotonous strength is characterized by damage which occurs as an increment of permanent deformation after each load cycle. The failure of material is reached after relatively low number of cycles. Similar works were performed early by SINHA (1964) et al. and by KARSAN and JIRSA (1969). They investigated stress-strain curves for repeated loading of concrete and established envelope curve and stability limit for low cycle loading.

The aim of present investigation is two-fold:

1. Derivation of fatigue curve in the range from 0 to 20 cycles.
2. Determination of stability limit.

Careful analysis of pilot tests led to the development of a new method for controlling the load level near the strength. This was necessary in order to avoid premature failure of specimens and ensure that all tests will fall within low-cycle fatique range.

2. METHOD OF TESTING

A standard approach is to perform monotonic loading tests on a certain number of specimens from the series and the remaining specimens are subjected to repeated loadings. The average strength found from monotonic tests is then assumed as a reference value for all specimens under repeated loadings. However, due to natural random variation of concrete properties the strength of each specimen differs from the average value. This becomes an important effect when the load level falls within the interval of scatter of the strength, and causes that some of specimens either fail prematurely or are loaded below stability limit. The probabilistic analysis of this situation disclosed that only 30% of tests would be useful. Therefore the standard method was rejected and it was decided to predict strength for each specimen individually.

For this purpose a new method was developed based on load-volumetric strain curve (Fig.1). (Volumetric strain ε_v is the sum of principal strains.) This curve well illustrates the process of gradual deterioration of concrete by crack propagation (also called microcracking) as was already proved by BERG (1965), SHAH (1966), STROEVEN (1972) and others. Under the initial loading material compresses almost linearly. As the load increases the cracking initiates and causes pronounced turn in positive direction of the upper part of volumetric curve. The peak point C (point of minimal volume) can be considered as the approximate border between undamaging and damaging load. Any load beyond the peak point causes permanent damage to the concrete due to cracking. Therefore the upper branch of volumetric curve was used for controlling load level and also for prediction of strength.

The measure of damage is defined as

$$\gamma = (\varepsilon_{vc} - \varepsilon_v)/\varepsilon_{vc} \qquad (1)$$

(See Fig.1). The load parameter is defined as

$$y = (P_u - P)/(P_u - P_c) \qquad (2)$$

From Eq.2 follows the expression for estimate of load level

$$F_m = P_m/P_u$$

$$F_m = (1-y)/(1-y\ P_c/P_m) \qquad (3)$$

The function

$$y = f(\gamma) \qquad (4)$$

was derived experimentally.

The procedure is following: The specimen is loaded monotonically from zero to P_m (where P_u P_m P_c) while volumetric strains are recorded. The value of γ is found from Eq.1 and corresponding y from Eq.4. Then the load level F_m is found from Eq.3.

3. TEST SPECIMENS AND HARDWARE

The test specimens were prisms 15x15x40 cm made from ordinary concrete with natural aggregate. All specimens were nominally identical with average prism strength at time of testing 37 N/m^2. Sulphur caping was provided to ensure uniform contact on loading planes.

The loading machine was Amsler 5000 kN hydraulic test machine. Longitudinal and transverse strains were measured by strain gagues G 350 (50 mm length) in the middle part of specimens. Total longitudinal deformations were also measured by potentiometers. Two diagrams, for longitudinal and volumetric strains, were recorded simultaneously by X-Y plotters. The loading was under constant rate of strain 0,4% per minute approximately.

4. TEST RESULTS

4.1 Monotonic Loading Tests

In total 37 specimens were tested under monotonously increased longitudinal strain. The average load-longitudinal strain and load-volumetric strain curves were derived from these tests with following parameters:
Peak values of longitudinal strain curve are stress $\sigma_u = 37{,}6$ N/mm, strain = -0,00185 and peak values (at point C) of volumetric curve are $F_c = 0{,}825$, volumetric strain $\varepsilon_{vc} = -0{,}000533$.

For the purpose of determination of load level from Eq.3 the upper branch of volumetric curve (between points C and O, Fig.1) was found by the least square method as well described by exponential function

$$y = \exp(-2{,}24\ \gamma^{0{,}55}) \qquad (5)$$

This function with average values and standard deviations of experimental curves at seven points are shown in Fig.2. It is interesting to note that the standard deviation of the load parameter y is maximum 10% of the interval $P_u - P_c$ or 2% of strength P_u. This shows good invariant properties of this curve with respect to strength.

4.2 Repeated Loading Tests

72 specimens were subjected to 20 cycles of loading between upper load level P_m and lower load level $P_d = 0{,}12P_u$. The load level P_m was found during the first cycle as a load corresponding to a prescribed value of γ_m. Thus the amount of damage γ was actually the controlling parameter and the load level was a function of it (according to Eqs. 3,4).

Out of 72 specimens only 40 specimens failed due to repeated loading within 20 load cycles. Results of these tests are plotted in Fig.3. The points indicate number of cycles to failure for corresponding load level Fm of specimens.

Examples of recorded data for a typical specimen are shown in Figs. 4, 5, .6. The relationship between load level F_m and the number of cycles to failure N (usually called S-N curve) was derived from these experiments in the form of exponential function by the least square method (Fig.3)

$$F_m = \exp(-0,128\ N^{0,45}) \qquad (6)$$

The shape of the function was chosen simillar to the curves of KARSAN and JIRSA (1969).

The stability limit was determined from observation of volumetric strain increments in load cycles. These increments indicate damage of concrete due to cracking. It was observed that the damage is higher in the first few cycles and shortly before failure than in the middle cycles. When load level decreases to the load F_c the increments vanish. The volumetric strain seems to be more feasible for this observation, then longitudinal ones. Thus the stability limit is coincident with load at the peak of monotonic volumetric curve. The envelope curve was found in agreement with KARSAN and JIRSA (1969) as identical with monotonic load-longitudinal strain curve.

5. CONCLUSIONS

1. The method based on monotonic load-volumetric strain curve was successfully applied for determination of upper load level of repeated loading tests of concrete.

2. Fatigue curve for one type of concrete (37 N/mm^2 prism strength) was derived in the form of Eq.6.

3. Stability limit is at the load level corresponding to the peak of monotonic load-volumetric strain curve. This implies that the stability limit can be predicted from monotonic tests. Validity of this conclusion should be examined for other types of concrete with diferent strengths.

6. REFERENCES

BERG, O.J.: Physical Foundations of the Strength Theory of Concrete, (In Russian), Moscow, 1961

KARSAN, I.D., JIRSA, J.O.: Behaviour of Concrete Under Compressive Loadings, Journal of the Struct.Div. ASCE, Dec.1969, p.2543

SHAH, S.P., WINTER, G.: Response of Concrete to Repeated Loading, RILEM Int.Symp., Mexico City, Spt.1966

SINHA, B.P., GERSTLE, K.H., TULIN, L.G.: Stress-Strain Relations for Concrete Under Cyclic Loading, Journal ACI, Feb.1964

STROEVEN, P.: Some Aspects of the Micromechanics of Concrete, Report, Stevin Laboratory, T.U.Delft, 1972

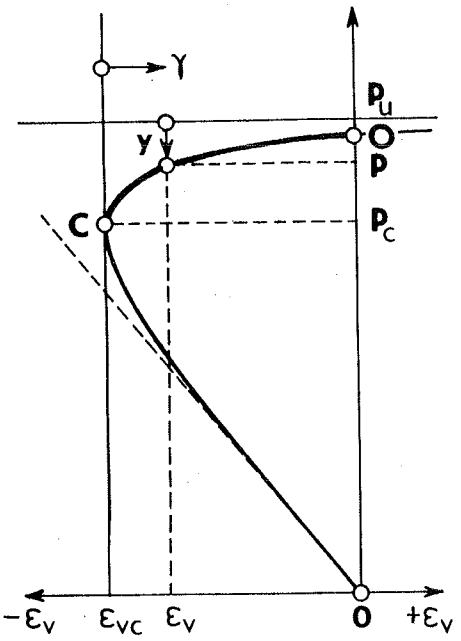

Fig.1. Load-Volumetric Strain Curve

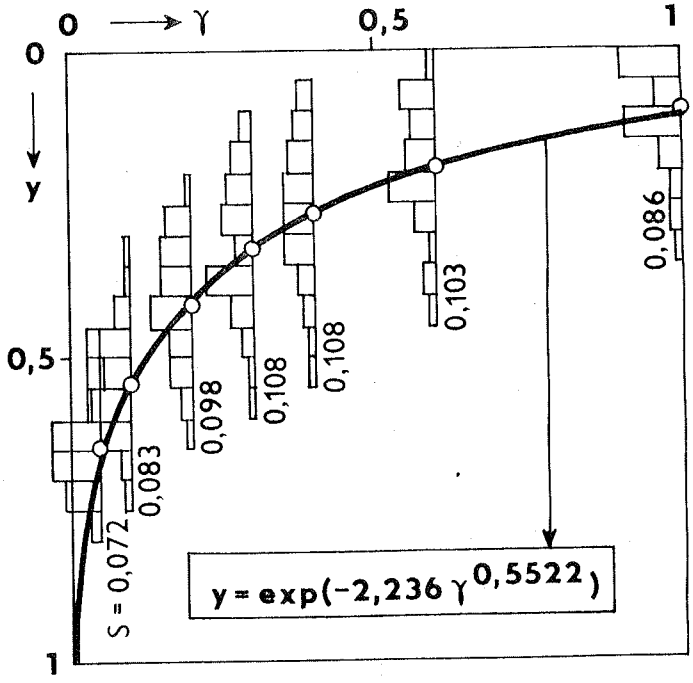

Fig.2. Upper Branch of Volumetric Strain Curve

O Average Values
S Standard Deviations

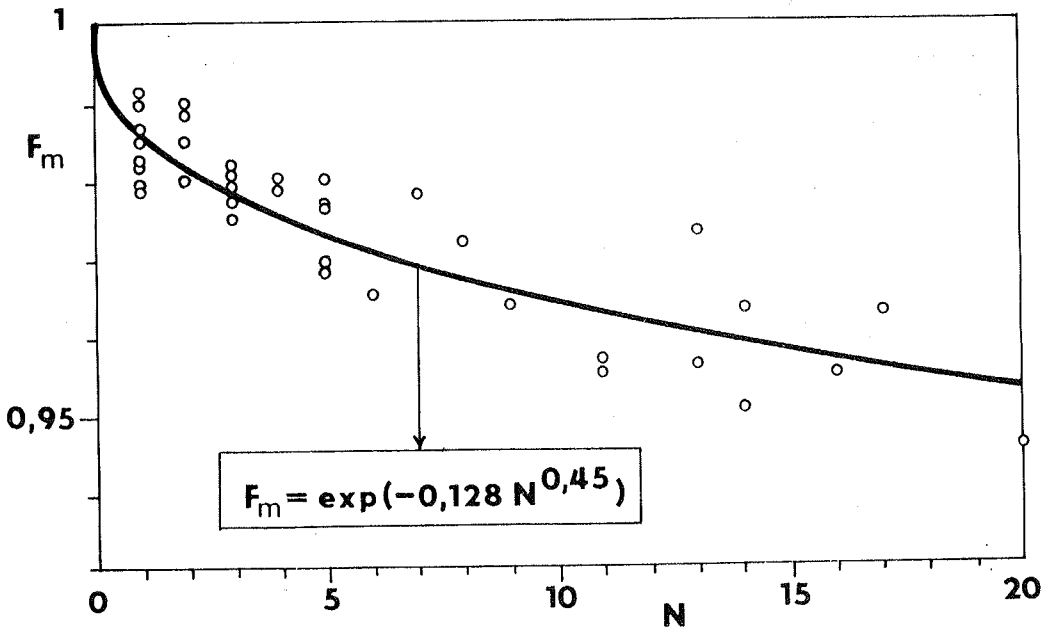

Fig.3. Fatigue Curve For the Test Specimens

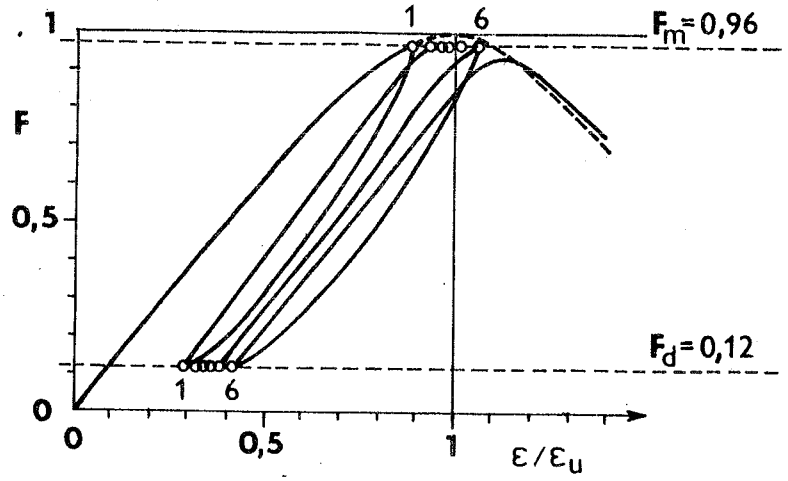

Fig.4. Load-Longitudinal Strain Curve for the Specimen 109

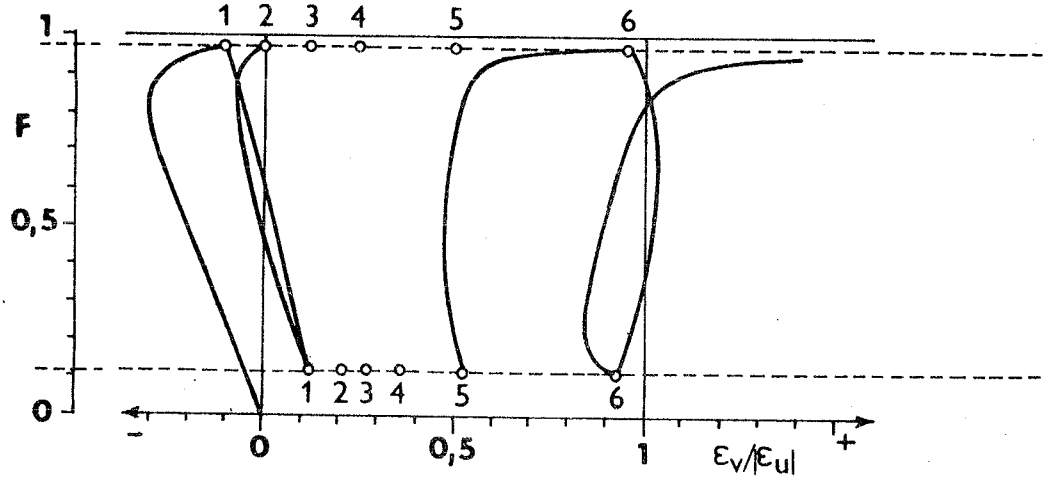

Fig.5. Load-Volumetric Strain Curve for the Specimen 109

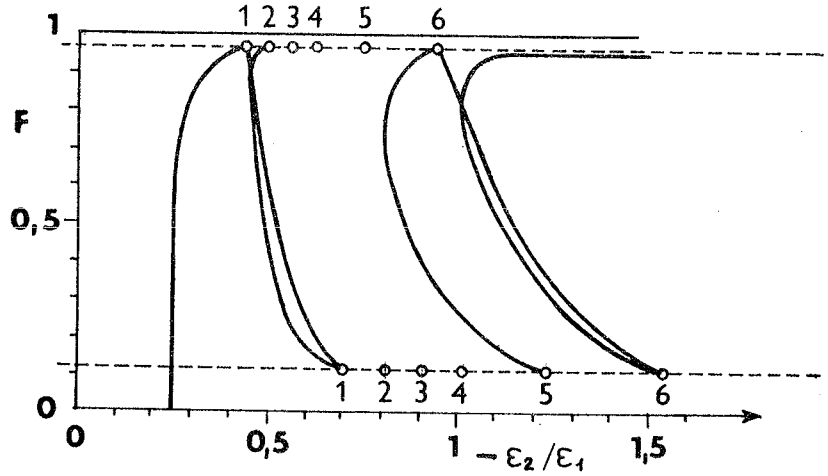

Fig.6. Load-Poisson's Ratio Curve for the Specimen 109

EFFET DES ACTIONS DE TYPE SISMIQUE SUR LA RESISTANCE ET DEFORMABILITE DES BETONS

Luis Julián LIMA
Universidad Nacional de La Plata
La Plata, Argentina

RESUME.- Il est étudié l'influence,sur la résistance et déformabilité du béton,d'un ensamble d'importantes charges répétées appliquées dans une courte période,mais que,par son nombre inssufisant,ne configurent pas un phénomene de fatigue.Ils sont analysées diférentes histoires de charge avant et aprés les charges répétées.Il est proposé une interpretation du phénomene.

SUMMARY.- There is estudied the action,on the strength and deformability of concrete,of a cyclic load of high magnitude applied during a short time,that have not the characteristics of a fatigue phenomenon due to his little number.One annalyse quite differents historys of load applied before and after the cyclic load.There is proposed an explication of the facts.

1.- INTRODUCTION

1.1.Les actions de type sismique ne sont pas directement classifiables parmi les phénomenes de fatigue mais plutôt dans des procés de la même famille que l'on peut designer par *de désorganisation progressive* du béton.
1.2.Etant ces procès intimmement ligués a l'histoire des charges appliquées et d'une facon moins nette aux caractéristiques de l'ambiance,il est trés importante de chercher une loi générales de comportement por sustituer l'hypothèse de Mines que n'a pas été confirmée par l'expérimentation.
1.3.Dans cette communication on analyse l'influence,sur la résistance et defórmabilité du béton,d'un ensamble d'importantes charges répétées,appliquées dans une courte période,mais que,par son nombre insuffisant ne configurent pas un phénomène de fatigue,et qui peuvent être précédées par n'importe quel histoire de charges.
1.4.On suppose que les charges appliquées correspondent a celles produites par les mouvements du terrain d'origine sismique et non pas par la période propre de la structure.
1.5.Comme aprés un sisme on peut trouver des élément fortement comprimés on a étudié aussi la rupture du béton dans ces conditions.
1.6.On propose enfin une interpretantion de la rupture du béton,avec l'idée de que serve d'appui a des nouvelles recherches plutôt que cherchant une interpretacion ajustée du phénomène.

2.-RESULTATS EXPERIMENTALES EXISTANTS

2.1. Malgré que la recherche sur l'action des charges répétées dans la résistance du béton,sur tout celle vinculée aux phénomènes de fatigue,elle est nombreuse,elle commence l'an 1898 avec Considère et De Joly,la plupart des résultats ne sont pas utilisables car il manque une information précise sur les méthodes et materiaux utilisés.

Dans la suite ils sont résumés les résultats les plus interessants.On pourra trouver une information plus complète par example dans (17).

2.2. Si les charges répétées sont toutes de la même valeur σ'_n,le nombre n de répétitions necesaires pour arriver à la rupture il peut être exprimé par (10)

$$\sigma'_n = f'_c.(1,2 - \log n)$$

2.3. La rupture par fatigue elle est progressive et elle est due à l'accumulation de damages permanentes dans la structure interne du béton,originées par les contraintes et déformations variant avec le temp (4).

2.4. La velocité de chargement (fréquence) a une influence trés petite dans la valeur de σ'_n;malgré que les valeures les plus basses elles sont en générale associées a moindres valeures de σ'_n et plus grandes des déformations permanentes (10;15;17).

2.5. La forme du diagramme (σ'-ε') est modifié avec n,et d'une concavité vers l'axe des déformations dans les premières chargements elle tourne vers l'axe des contraintes aprés un certaine nombre de répétitions.La valeur de cette concavité peut être un indicateur des domages eues par le materiel.Un autre indicateur peut être le module de déformation sécant dont la valeur diminue en augmentant n,car avec n augmentent aussi bien les déformations permanentes et les élastiques (16;17).

2.6. Si l'on n'arrivera pas à la rupture l'augmentation de ε' tend à se stabiliser et au cas contraire elle s'intensifie.Dans tous les cas les déformations permanentes s'accroissent plus rapidement que les élastiques et, à partir d'une certaine valeur de n,commencent a être plus grandes;dans les bétons jeunes cet phénomène arrive plus tôt et la stabilisation plus tard que dans les plus agés (17).

2.7. Sur la valeur des déformations de rupture il n'y a pas accord car, tandis que pour (20) elle est la même pour charges répétées que pour l'essai normalisé,pour (2) elle augmente en diminuant $\sigma'_{máx}$.

2.8. Dans la résistance a fatigue l'âge de l'eprouvette et les conditions de conservation ont une importante influence (17),tandis qu'on ne connaît pas d'influences du retrait et des caracteristiques des agrégats (14).Le comportement des bétons saturés est pire que ces des conservés a l'air pour n'importe quel histoire de charge (21)

2.9 S'il n'y a pas de fatigue les charges répétées augmentent f'_c en 5% (5) et n'influent pas dans la securité des éléments structuraux (1).

2.10. L'hypothèse de Mines ne se vérifie pas dans le béton car les caracteristiques de sa rupture sont fortement influencées par l'histoire de charges: en flexion l'existence de charges répétées plus grandes avant l'essai de fatigue augmentent σ'_n,si elles sont plus basses la diminuent et si l'essai est fait avec charges hautes et basses alternées σ'_n diminue en augmentant le nombre des cycles hautes (14);en compression charges initiales basses augmentent σ'_n et si elles sont hautes la diminuent (5;16;17); courtes periodes de déchargement (de non plus de 5') augmentent σ'_n jusque en 10% (14);courtes periodes de charge constante,si elle ne dépasse pas la valeur $0,75.f'_c$,augmentent σ'_n (2).

2.11. Dans la surface des éprouvettes on peut trouver fissures,même pour valeures de n assez petites,et sa ne signifie pas que dans tous les cas on va a arriver a la rupture (17).

2.12. S'il n'y a pas de tractions,la charge de compression centrée est celle qui donne les plus petites valeures de σ'_n dans tous les cas (2).

2.13. Le module de Poisson diminue en augmentant le nombre des charges(17).

3.- RESULTATS EXPERIMENTALES OBTENUES

3.1. Nous avons essayé en compression des éprouvettes cylindriques de 15 cm de diamètre par 30 cm de hauteur, fabriquées et conservées selon (12). Les essais de charge variable et ces de rupture ont été faites avec una presse *LOS* de 350 tn; les charges constantes de longue durée ont été appliquées moyennant des machines a ressort de 40 tn.

3.2. les histoires de charge que ont été étudiés sont ces de (fig.1). La vitesse d'application des charges a été mantenue constante et donc la période a oscillé parmi 20'' et 45''.

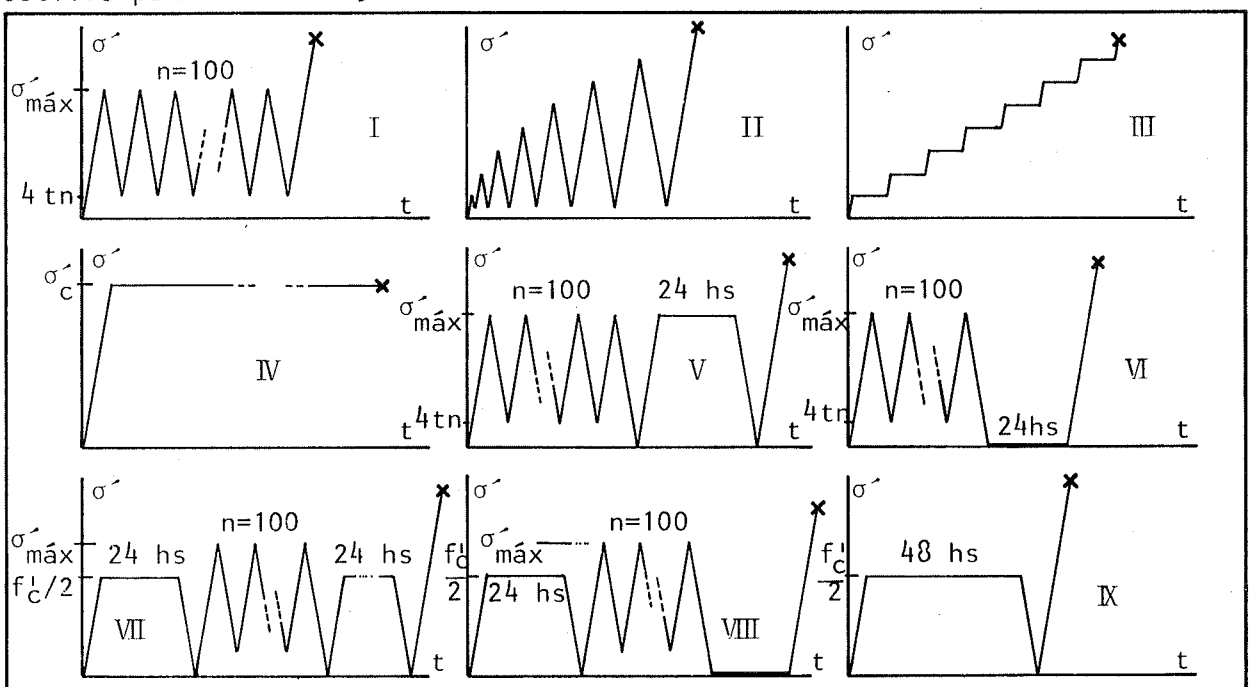

FIG.1 HISTOIRES DE CHARGE

3.3. Comme résultat général on peut dire qu'existe une limite au dessous de laquelle le béton ne souffre pas des modificationes importantes dans sa résistance et deformabilité, tandis que au dessus d'elle on est dans ce qu'on peut définir comme *procès de rupture*. La valeur de cette limite est une fonction, au moins, des contraintes appliquées, des déformations eues et de l'histoire des charges. Si cette limite n'a pas été dépassé on dira que le béton est en *état I*, si elle a été dépassé, en *état II* (21). La limite elle même sera denommé *limite de stabilité* (LE).

3.4. Pour les histoires de charge de type I (n=100) la limite LE se trouve approximativement en $\sigma'_{max}=0,9.f'_{cm}$ et $\varepsilon'_c= 2$ à $2,2$ °/₀₀ (table 1). En diminuant σ'_{max}, pour arriver a LE on doit augmenter n, et ε'_c augmente aussi.

TABLE 1

EPROUVETTES QUE SE SONT ROMPUE SOUS CHARGE REPETE

épr.	$\frac{\sigma'_{máx}}{f'_{cm}}$	f'_{cm} N/cm²	n° de la charge de rupture	ε'_c (‰) 1ere charge	ε'_c (‰) dern. charge	initiation du procés de rupture n_i	initiation du procés de rupture ε'_c	$E/\sqrt{f'_c}$ n=2	$E/\sqrt{f'_c}$ n_i	$E/\sqrt{f'_c}$ n_{u-1}
R.3.10	0,905	19,1	39	0,95	3,16	30	2,26	21700	20200	12900
R.4.7	0,907	17,5	78	0,90	2,72	60	1,925	25500	22700	15900
R.4.8	0,842	17,5	156	0,95	3,65	125	2,485	23600	20300	12600

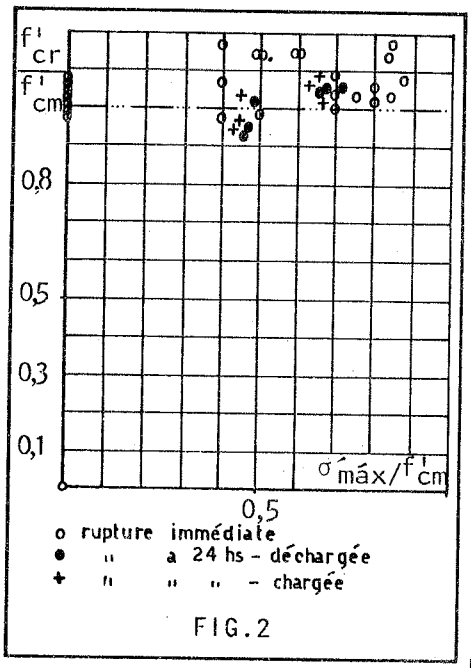

FIG.2

Si LE n'est pas surpassé, l'augmentation de f'_c peut arriver jusqu'a 15% (fig.2). Pour valeures de σ'_{max} qui ne depassent pas $0.8.f'_c$ la déformabilité totale a le même ordre de grandeur que celle de l'essai normal (1,6 a 1,8 °/₀₀), donc en augmentat σ'_{max} augmente ε'_{cn} et diminue ε'_{cr} (fig.3) Pour des valeures plus grandes de σ'_{max}, les courbes. $(\sigma'-\varepsilon')$ ont la même allure que celle de $0,8.f'_c$ et par conséquence la déformabilité totale augmente. LE n'est pas une limite bien définie, elle comprend plutôt toute une zone dans laquelle la structure interne du béton commence a se désorganiser.

3.5. Pour les cas V et VI on a trouvé: avec $\sigma'_{max}=0,5.f'_c$ une réduction de la résistance du 4% et pour $0,7.f'_c$ une augmentation d'elle même du 5%. Pour la déformabilité reste valable ce qu'on a dit dans (3.4). Malgré que il faudrait faire un nombre plus grand d'essais por l'affirmer, pour le premier cas la dispertion a été moindre dans l'histoire V et pour le deuxieme dans la VI.

3.6. Pour les histoires VII; VIII, et IX: avec $\sigma'_{max}=0,7.f'_c$ on trouve le meilleur comportement dans VII, avec trés peu de dispertion et une augmentation de la résistance du 9%; dans les autres la dispertion est plus grande et la resistance augmente seulement du 3%. Pour la déformabilité reste valable (3.4). Avec $\sigma'_{max}=0.8.f'_c$ on est aux environs de la zone LE. Pour les éprouvettes que restent dans l'état I, il est valable ce qu'on a dit au paragraphe précédent; celles qui passent a l'état II se desorganisent et rompent; et celles qui restent dans le zone LE ont un comportement tout particulier: aprés les charges répétées elles ont une fissuration importante (fissures verticales de 3 à 4cm de longeur et jusqu'a o,4mm de largeur), ses deformations sont grandes et elle augmentent beaucoup sous la charge soutenue du cas VII, malgré tout la résistance est ancore $1,09.f'_c$, mais la déformation ultime peut surpasser le 2,7 °/₀₀.

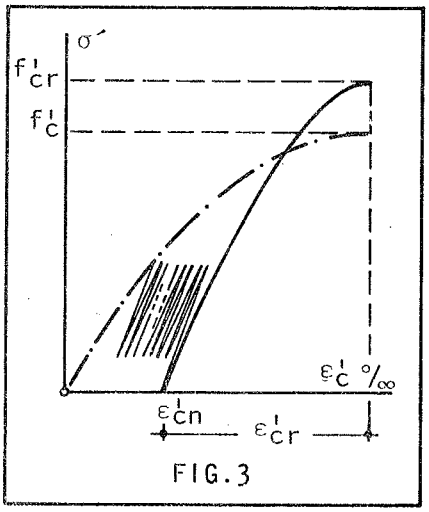

FIG.3

3.7. Les résultats des essais de charge soutenue sont indiqués dans la (fig.4) et la table 2. On arrive a la limite LE pour une certaine couple de valeures ε'_{c1} et t_1 associées selon (fig.5). L'existance d'une charge préalable de $0,5.f'_c$ durant 3 heures conduit a résultats meilleures.

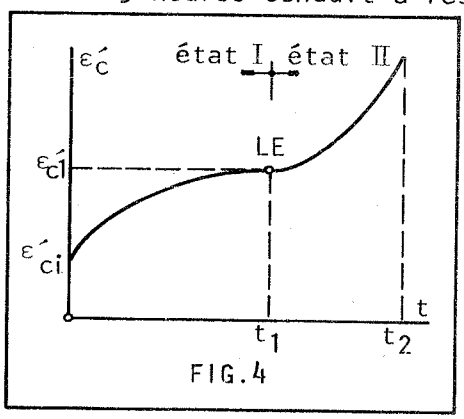

FIG.4

4.- UNE INTERPRETATION DU PROCES DE RUPTURE DU BETON

4.1. Pour parler de la rupture du béton il va être necesaire préciser au préalable certaines idées, car il ne s'agite pas d'un fait instantané mais d'un procès que a un déclenchement et une culmination plus ou moine définis. Certaines histoires de charge, comme la rupture sous charge soutenue, ils pérmetent aprecier bien le déroulement du procès.

4.2. On doit tenir présent un fait trés impor-

tanto pour l'analyse du phénomène en étude: la rupture du béton a son point de départ dans le niveau le plus bas de sa microstructure (22) et là le materiel est absolument hétérogène.

TABLE 2

EPROUVETTES QUE SE SONT ROMPUE SOUS CHARGE CONSTANTE

épr.	σ'_c N/cm^2	$\frac{\sigma'_c}{f'_{cm}}$	déf. initial (‰)	init. de la rupture t_1 (min)	ε'_{c1} (‰)	$\frac{\varepsilon'_c}{\varepsilon'_i}$	$\frac{t_1}{t_2}$	rupture t_2 (min)
4.9	14,8	0,85	0,90	65	2,40	2,67	0,88	73,7
4.10	16,8	0,96	0,95	0,7	1,45	1,53	0,44	1,58
5.4	17,8	0,94	0,90	32	2,20	2,44	0,73	43,9
5.5	17,1	0,915	1,195	0,75	1,82	1,52	0,60	1,25
5.6	16,5	0,873	0,90	9	1,83	2,03	0,54	16,7
5.7	16,5	0,871	0,90	180	2,60	2,89	0,57	314
5.8	15,6	0,826	0,90	ne s'est pas rompue				
5.9	16,8	0,891	0,90	26	2,03	2,26	0,60	43,3
5.10	18,3	0,969	0,90	60	2,23	2,48	0,69	86,5

Elles sont hétérogenes les caractéristiques phisiques et géométriques des particules, et par consequence il l'est le champ des forces de liaisson entre elles. Ce champ est qui donne unité a l'ensemble, car du point de vue de la résistance la *phase tobermorite* doive être consideré plutôt comme un système continue de forces d'interaction que comme une structure continue de particules solides (7). Avec l'âge ou aprés certaines charges, cet hétérogénité s'atténue un peu.

Elles son aussi trés hétérogènes, par consequence, la grandeur et distribution des vides ou pores. Lesquels, par sa grandeur mayonne, peuvent être classés en: pores interieures des particules et pores capilaires, étant les premiers toujours continus et les autres pas toujours (21), ce que accentue de plus l'hétérogéneité du corp. Cette constatation est trés remarcable car dans les pores on y trouve un élément que a un rôle important dans le procès de rupture: l'eau.

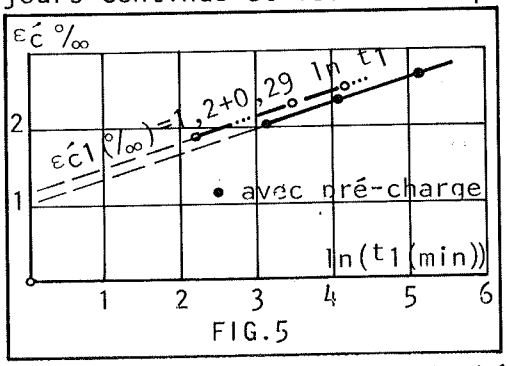

FIG.5

Si le béton est chargé, la distribution des sollicitations, dans le niveau ou on est en train de faire l'analyse, va être aussi trés hétérogène.

Il y a d'une part hétérogénité dans la résistance, et d'autre dans la distribution interne des sollicitations.

4.3. On doit adjouter que le béton a toujours un grand nombre de microfissures que s'originent dans le niveau en analyse (11;22), même dans des spécimens que n'ont pas été jamais chargés. Il y a fissures dans la pâte de ciment, dans les agrégats et dans l'interface. Pour des charges croissantes la quantité relative des premières augmente (22).

4.4. Le teneur d'eau evaporable du béton durci est a peu prés du 30% en volume. Toute elle est movile sous un gradient de pression, mais sa viscosité est variable a cause de la variation des forces d'adsortion (malgré que toute, ou presque toute, l'eau est adsorbé, les molecules plus proches des particules solides elles le sont de plus). Donc tout changement dans l'état de sollicitation du béton cause une rédistribution de l'eau évaporable (19). Cet écoulement se produisse en accord avec la loi de Darcy (11):

$$i = K.p/h$$

(i=débit; h=larguer du béton; p=pression), mais K n'est plus une constante, elle varie avec p et aussi avec la température.

4.5. Les déformations du béton se composent de deux termes: les déformations propres de la structure interne et la microfissuration; elles sont aussi accompagnées de mouvements de l'eau interstitielle dont la présence les affecte de facon diverse en diminuant les déformations et en augmentant la

microfissuration.
4.6. Dans un proces de charges répétées on observe des boucles d'hystérésis dont la surface interne diminue avec l'accroissement de n et augmente aux environs de la rupture (5;20).Cette surface représente une énergie de déformation irreversible qui est dépensé en déformations plastiques du materiel, écoulements de l'eau interstitielle,fissures et frictions internes;aux environs de la rupture ces dernieres sont prédominants.L'apparent plasticité du béton est toujours accompagné par destructions locales de la cohésion qui représentent une certaine dégradation interne.
4.7. Pour arriver a la désintegration d'un corp on doit le donner de l'énergie,et dans les procès de rupture du béton qu'on est en train d'analyser cette énergie est mecanique.L'énergie nécessaire pour en arriver sera celle qu'amene l'énergie de liaison des particules aux niveaux de la désintégration.Une fracture en échelle macroscopique est liée a l'accumulation d'une certaine quantité critique d'énergie potentiel,qui ne peut pas être dépensé comme chaleur avant que se produise la separation et que soit transformé en énergie superficielle (7).
4.8. Les charges répétées ou soustenues occasionnent une propagation progresive des fissures internes.Jusqu'une certaine valeur des contraintes $K_e.f'_c$, la propagation est lente et tend vers la stabilisation.Dans ce cas on dira que le béton est dans l'état I.Si l'on depasse cette valeur de la contrainte on entre dans l'état II,qui est toujours associé à la rupture,et dans lequel la fissuration augmente beaucoup plus rapidement (sa vitesse augmente à mesure qu'on s'approche à la rupture).Parmi les deux états décrits il existe une zone de transition,qu'on a appelé *limite de stabilité* LE (3.3),ou le procès de fissuration se dés-stabilise et on arrive a un état de deséquilibre interne.
Les valeures de K_e trouvées par nous mêmes sont indiquées en (3.3) à (3.7). Pour éprouvettes saturées et charges répétées (21) trouva K_e=0,7.
La grande variation des valeures de K_e est due aux nombreuses variables que les affectent,à la hétérogéneite du materiel et au caractère aléatoire des phénomènes qu'interviennent.
4.9. Dans l'état I nous avons trouvé que,si aprés n'importe quel histoire de charge on applique une charge rapide jusqu'a la rupture (comme dans l'essai normal) on y arrive avec une déformation qui est a peu prés la même qu'on trouve dans l'essai normal et sous une contrainte en peu plus grande que f'_c. Dans les éprouvettes qui ont arrivé a la zone limite LE,la rupture sous charge rapide elle se produit pour valeures de la contrainte un peu plus grandes que f'_c,mais maintenant avec des déformations ultimes beaucoup plus grandes que ces de l'essai normal.
Dans l'état II le procès de rupture,qui est irreversible,il est dejà déclenché et la résistance est chaque foi plus petite.
4.10. La rupture du béton n'est pas determinée ni par les contraintes qu'actuent ni par les déformations que ont eu lieu,elle dépend fondamentelement de l'état de fissuration interne,lequel est de sa part fonction de l'histoire des charges.Cet a dire que la rupture ne depend pas du travail donné au corp mais de la part de celui-ci dépensée en cassures permanentes de sa structure interne.
4.11. Il ne paraît pas raisonnable d'étendre l'application de la thèorie de Griffith au niveau microscopique ou sub-microscopique où commencent les procès de rupture,car ici on ne peut pas considerer le materiel ni élastique,ni homogène,ni continue.Mais les idées de base de cette thèorie elles si sont applicables et elles nous permettrons d'expliquer le passage de l'état I à l'état II.
4.12. Quand on applique une charge au béton elle se distribue parmi sa structure interne et l'eau interstitielle.La première se transmet par les parti-

cules solides et produit déformations dans la masse,l'autre produit pression dans l'eau et tend a la faire écouler.La transmission des charges a travers la structure solide n'est pas uniforme car,due a l'hétérogénéite du materiel, les lignes de charge se divisent et croissent (22) donnant origine a des fortes concentrationes de forces de traction qui agissent,la plupart,sur des plans paralels à la charge externe.La présence de nombreuses microfissures accentue,cette situtation en concentrant les tractions dans ses bouts.La pression del l'eau interstitielle n'est pas constante non plus et sa valeur dépend des posibilités d'écoulement qu'elle trouve a cahque endroit.

4.13. Dans ces conditiones le mécanisme résistant du béton sous charges répétées ou soutenues doit être régie par deux façteurs antagoniques: l'un que tend a augmenter la resistance due a une augmentation des forces de Van der Waald et l'autre que tend a la diminuer a travers de la formation de fissures.Selon lequel soit prédominant l'état sera ou non stable.

4.14. Si la valeur des charges est tel que le béton reste dans l'état I,la plupart des pics de contrainte de la structure interne se dissipent moyennant déformations plastiques et les surpressions de l'eau par écoulements et migrations vers des zones où se trouvent des vides avec air.Seulement ils se produirant des fissures (qui sont toujours de traction) dans certaines endroits ou coïncident des fortes tractions,basses résistances et hautes pressiones d'eau;et une foi libéré l'excès d'énergie elles se stabilisent.Sous laction de nouvelles charges le materiel no présente pas traits de désorganisation.

Si les charges son importantes,les tractions et les pressions d'eau augmentent et le nombre des fissures s'accroître.Un phénomène semblable se produit si les charges se répétent un certain nombre de fois.

On est dans l'état II quand les tractions dans les particules solides et la pression de l'eau interstitielle arrivent a des valeures telles que l'énergie libéré pendant la formation d'une fissure ne peut plus être équilibré par l'énergie superfitielle des nouvelles aires,plus la dépensé en frictions, déplacements et nouvelles déformations plastiques,et donc la fissure est instable,elle ne s'arrête plus;et on a arrivé à l'étape de rupture.Le fait que ces fissures puissent se produire aussi dien dans la pâte de ciment,dans les agrégats ou a l'interface complique de plus le problème.

4.15. Les critères de Griffith (non pas sa thèorie)peuvent être appliqués au béton;il manque mettre a point les concepts thèoriques et les valeures experimentales.

5.- COMPORTEMENT DU BETON SOUS DES ACTIONS SISMIQUES

5.1. Les actions de type sismique produisent des déformations permanentes dans le béton,lesquelles se compossent par déformations plastiques de la structure interne,écoulements d'eau et fissures.Seulement ce dernier part des deformations permanentes peut être une mesure de la dégradation souffert par le béton.Il faudra donc orienter la recherche vers des méthodes que permissent les mettre en évidence.

5.2. En relité por pouvoir juger sur la securité d'une structure qu'a été soumise a des actions sismiques el est necessaire un peu moins:il sera suffisant de connaitre si dans un endroit quelconque le béton a abandonné l'état I.Si l'on peut constater que le béton n'a abandonné dans aucune de ses parties l'état I ,on peut être sûr que f'_c et la defomrabilité ultime sont au moins égales aux originales,et par consequence que la securité ne s'est pas abaissé.

Si dans quelque point le béton est sortie de l'état I,l'analyse qu'il faudrai faire échappe aux limites de cette comunication,mais ce fait n'indique pas que la structure soit forcement hors service.

5.3. Si,aprés un sisme,une piece quelconque en béton résulte aves une force de compression plus grande que celle pour laquel elle avait été dimensionée il faudra prendre toutes les mesures de securité nécessaires,car une rupture sous charge soustenue est rapide une foi étant le béton dans l'état II,mais peut se produire aprés un période assez longue depuis le sisme.
5.4. Les structures bien conçues et rationellement utilisées sont soumises, dans sa vie outile,a des histoires de charge que,en general,améliorent sa capacité pour s'opposer aux actions sismiques.

NOTATIONS

σ '=contrainte normal de compression
ε '=deformation relative de compression
n =nombre des charges appliquées
t =temp
f'_c =résistance du béton en compression (essai normal)
f'_{cm}=résistance moyenne (en général de 3 eprouvettes)
f'_{cr}=résistance en compression d'eprouvettes soumises à une histoire de charge quelconque.

REFERENCES

1)Aas-Jakobse,Lenschow(1973)*Behav.of reinf.columns subj. to fatigue load.* ACI Jnl.3/73;2)Aci Committee 215 (1974)*Cons. for design of conc. struc. sub. to fatigue load*-ACI Jnl.3/74; 3)Antrim,Mac Laughlin (19)*Fatigue study of air-entr. conc.*-ACI Jnl. ; 4)Bastgen,Hermann(1977)*Exp. made in det. the static mod. of elast. of concr.*-M&C n°60; 5)Bennet (1974) *La fatiga en el concreto*-IMCYC n°71; 6) Desay (1977) *Fract. of concr. in comp.*-M&C n°57; 7) Freudenthal (1950) *The inel. bahav. of eng. mat. and struc.;* 8) Giovambattista Violini (1977) *Evoluc. de las caract. de los hormig. endurecidos* -Asoc. Arg. de Tecnol. del Horm.; 9)Kaplan (1961) *Crack propag. and fract. of conc.*-ACI Jnl 12/61; 10)Korcinski,Poliakov,Bihovski,Duzinkevici,Pavlik (1964) *Bazele Proiectării Clădirilor în Regiuni Seismici*; 11)L'Hermite (1966)*Course CHEBAP CHEC-Paris;* 12)Lima (1979) *Resist. y def. del horm. bajo dif. hist. de carga* Fac. de Ingeniería-UNLP-(en préparation); 13)Lima (1979) *Consideraciones sobre la rotura del horm.*-Fac. de Ing.-UNLP(en preparation); 14) LLoyd,Lott, Kesler (1968)*Fatigue of concrete*-Univ. of Illinois; 15)Murdock (1965) *A crit. review of res. on fatigue of plain concr.*-Univ. of Illinois; 16)Neville (1972) *Prop. of concr.*-London; 17) Nordby(1958) *Fatigue of concr.- A review of res.* -ACI Jnl 8/58; 18)Peltier (1955) *Notes sur la courbe intr. des bét.* A.des p. et Ch. 11/55; 19)Powers,Mann,Copeland(1940) *Flow of watr in hard. Port. cement paste* -High.Res.Bd.Sp.Rep. n°40;20)Raju (1970) *Comparative study of the fatigue behav. of concr.mortar and paste in uniax. comp.*-Aci Jnl 6/70; 21)Shah,Chandra (1970) *Fract. of concr. subj. to cyclic and sust. loading.* -ACI Jnl 10/70; 22)Stroeven (1972) *Some aspects of the micro-mechanics of concrete.*Delf Univ.

****

NEW DATA ON SEISMIC PROPERTIES OF AERATED CONCRETE

V. V. MAKARICHEV
Concrete and Reinforced
Concrete Research Institute
Moscow, U.S.S.R.

O. P. VINOKUROV
Concrete and Reinforced
Concrete Research Institute
Moscow, U.S.S.R.

Summary

Gas concrete, based on cement, as well as gas concrete on a combined binding, volumetric mass 500-900 kg/m^3 and having the design cubic strength 1,5-7,5 MPa correspondingly, were subjected to the tests on non-often repeated dynamic loads.

The tests specimens-prisms 10x10x30 cm in size were conducted on two force frames by means of hydraulic jacks with 10t and 20t capacity. The jacks were supplied from hydropulsator, creating a necessary load with loading frequency 300 cycles per min.

In all more than 200 specimens were made and tested. As a result of the tests the linear correlation dependences, which can be given on average for all the tested concretes in the following form σ max = Rpr (1,257 - 0,094 log n).

Measurements of longitudinal and transverse deformations have shown that the more the cycles the greater the deformations and failure does not take place all of a sudden. Therefore some authors' statement concerning the brittle failure of aerated concrete is not well-grounded.

Résumé

Les bétons au gaz sur la base du ciment ainsi que le béton au gaz sur la base du liant mixte ayant la masse volumique de 500-900 kg/m^3 et des types projet d'après la résistance à la compression respectivement 1,5-7,5 MPa ont été soumis aux essais de non-multiples mises en charge dynamique.

Les essais des éprouvettes-prismes aux dimensions de 10x10x30 sm ont été réalisé sur les deux installations de force à l'aide des vérins hydrauliques de capacité de 10 et 20t. Les vérins s'alimentaient de hydropulsateur créant la charge nécessaire avec la frequence de la mise en charge de 300 cycles/min

On a produit et essayé plus de 200 éprouvettes. Les dépendances linéaires en corrélations ont été déterminées par ces essais. Ces dépendances en moyenne pour les bétons essayés peuvent être présentées sous la forme suivante $\sigma max = Rpr(1,257 - 0,094 \log n)$.

Les mesures des déformations longitudinales et transversales ont moutré que l'augmentation de la quantité des cycles mène à l'augmentation des déformations et la destruction n'est pas brusque. Voilà pourquoi la confirmation de certains auteurs sur la rupture fragile du béton cellulaire n'est pas tout à fait bien-fondée.

Introduction

At present the work in the field of studying strength and deformable characteristics of progressive building materials, attracts investigators' attention. One of such building materials is aerated concrete. Owing to such qualities as lightweight in spite of comparatively high compressive strength, comparative cheapness and possibility of mass production on a factory level, the aerated concrete finds wider application both in the USSR and abroad.

It should be noted that for economical raising of seismic buildings erection it is very important to reduce structures weight which results in reducing inertial seismic loads. A considerable reducing of structures weight can be obtained by using of autoclaved aerated concretes for walls and floor units.

However, wideler use of aerated concrete in such extensive districts of our country as seismic ones, occupying a great part of territory of the USSR, is kept back by unsufficient studying of seismic properties of aerated concretes and structure of this made of them and lack of suitable standard Recommendations.

In 1968 S.V.Polyakov and Yu.I.Kotov submited a contribution concerning dynamic properties of gas silicates and perlite concretes to the International Congress on Lightweight Concrete in London.

New experimental investigations on dynamic properties of gas concrete were conducted in NIIZhB Gosstroy USSR in 1977-1978 (Vinokurov O.P., Makarichev V.V., 1978).

Materials and testing methods

Aerated concretes are divided into 24 varieties, yet 90% of the whole production of autoclaved aerated concretes belong to gas concrete, where a main binding is cement or a combined binding (lime + cement). At present autoclaved gas concrete with volume weight of 600-800 kg/m^3 and a design compressive strength not lower than 25 is more widely used in building practice.

Taking into account the above mentioned 5 series of test specimens of autoclaved gas concrete having volume weights of 500, 600, 700, 800, 900 kg/m^3 and design compressive strength 15, 25, 35, 50 and 75 correspondingly, were produced for experimental investigations.

Specimens-prisms 10x10x30 cm in size were cut out of blocks, made both in laboratory and in production conditions. The choice of dimensions for specimens is stipulated by the reason that many authors (Polyakov S.V., Kotov Y.I., 1968; Samsonova G.V., 1976; Potapova T.V., Polyakov S.V., 1965) conducted analogous investigations with specimens of the same dimension. Raw material compounds for making the test specimens are given in table 1. Before testing the specimens were stored in natural conditions up to attainment of an equilibrium moisture of about 3-9%.

Table 1

Place of test specimens production	Composition of raw material			Specific surface of sand (cm^2/g)	B/T
	Cement %	Burnt lime %	Sand %		
Laboratory of aerated concrete and structures NIIZhB	47,5	5	47,5	2000	0,5
Luberetsky combinat of building materials and structures	27	19	54	1940	0,4

For more uniform distribution of stresses along the surface section of upper and lower specimens bases, the metal heads in gypseous mortar were set upon the abuts of specimens.

Investigations of strength characteristics change for gas concrete on influence of non-multiply repeated load were conducted under central compression. Before pulsating tests, a part of preproduction models was tested up to destruction by static load. The results of static tests are given in table 2.

Tests on non-multiply repeated load were conducted on two force frames by means of hydraulic jacks with 10t and 20t capacity connected hydropulsator.

Numerous experimental investigations show that constructions can vibrate with frequency complying with the frequence of

their dead vibrations independently of external affects frequency. Most of buildings and constructions have periods of free vibrations of 0,1-2,0 sec., therefore the frequency of dynamic load on construction under earthquake will be in the range from 0,5 to 10 hz (Korchinsky I.L., 1971). In the given investigations the frequency of loading was assumed as 5hz that is within the rate corresponding the rates of seismic loads.

Asymmetry coefficient i.e. coefficient of critical stresses of cycle $\rho = \sigma$ min/ σ max influences greatly on dynamic characteristics of materials. The worst results of strength characteristics of materials are obtained at $\rho = -1$, the best ones are at $\rho = 1$ i.e. at limiting maximum stress of sycle equal to strength under static loading. Most of authors (Polyakov S.V., Kotov Y.I., 1968; Samsonova G.V., 1976; Potapova T.V., Polyakov S.V., 1965; Korchinsky I.L., 1971) assumed $\rho = 0 \div 0,3$ in investigations of concrete strength characteristics on affecting of non-multiply repeated loading. It is explained by the wish of approaching tests to actual work of material during seismic affects as well by taking into account the available equipment for testing. In order to compare the test results asymmetry coefficient of sycle was assumed as $0,1 \div 0,2$. Maximum stress of sycle σ max was assumed as $0,6 \div 1,2$ from a mean static strength.

Control of load was carried out by calibrated strain gauges, glued on a metal dynamometer, with their readings recorded on photopaper with the help of intensifier 8 ANT and loop oscillograph N 700. The construction of pulsator did not allow to apply pulsating load right away with a required amplitude of stress and some time was needed for getting a needed amplitude. In the long process of getting the amplitude of stress (making up some hundreds of sycles in certain authors' works) the specimen is subjected, up to a set regime of testing, to considerable pulsating load which results in earlier destruction of specimen.

In our investigations we succeeded in to shorten the time of putting jack to a required amplitude of stress up to 8-20 sec which corresponds to 40-100 cycles of loading.

This gave the possibility of approaching, considerably, experimental investigations to actual work of material i.e. to reduce preliminary overloading of specimens. The recorded example of getting the amplitude of stresses is given on figure 1.

A number of cycles, before the destruction of specimen, was determined in the following way: 1/3 part of number of cycles required for putting pulsator into action was added to the number of cycles with constant amplitude of stresses.

In the course of pulsating tests with the purpose of determination the character of specimens failure, the development of longitudinal and transverse strains was recorded on the

oscillograph tape by means of wire strain gauges with 50 mm base, glued as a cross on each side of prisms. The scheme of strain gauges joint allowed to determine the mean strain of the prism four sides.

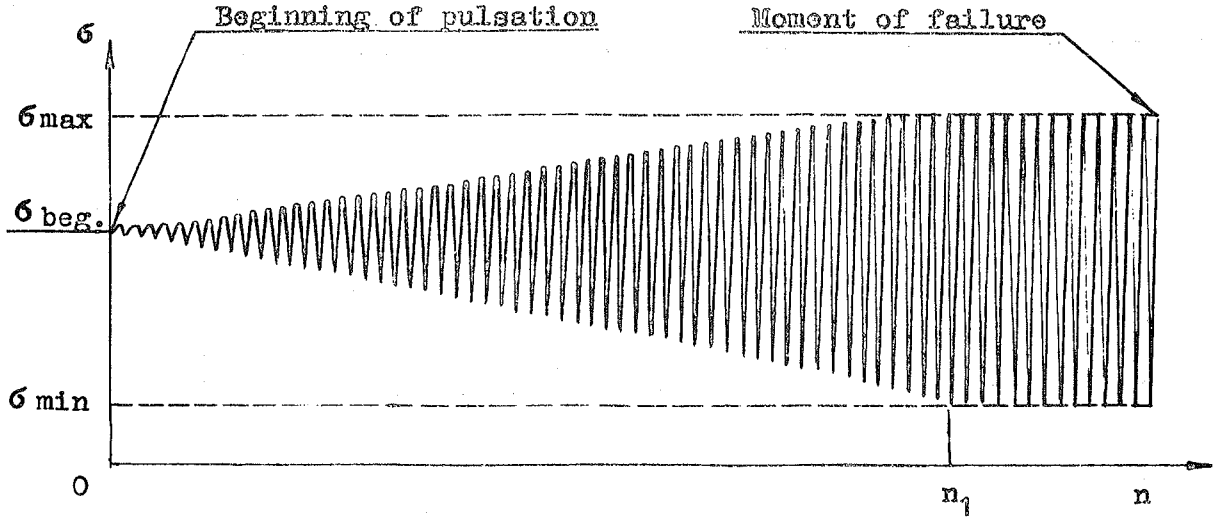

Figure 1: Oscillogram of forces transfered to the test specimens in testing on non-multiply repeated load.

n - number of cycles; σ - stress; n_1 - number of cycles required for putting pulsator into action.

Test results

As a result of the tests for each series of specimens the linear correlation equations of

$$\sigma \text{ max} = Rpr(a - b \log n)$$

form connecting relative stresses of pulsation σ max/Rpr with the number of load cycles n to the moment of specimens destruction were obtained. The results of statistical treatment of test data are given in table 2. Reliability of the results obtained can be seen out of the ratio of coefficient correlation (r) to its mean error ($\pm m_r$). If this ratio is 3 or more, the coefficient correlation can be assumed as reliable, i.e. the connection between σ max/Rpr and n is considered to be proved.

Test results with regard to all the experimental data are given on figure 2 in the form of correlative direct line i.e. the correlative direct line for autoclaved gas concrete with volume weight 500-900 kg/m3.

The relation of maximum stress under pulsation σ max to a mean prism strength Rpr is shown along vertical axis on figure 2 and along a horisontal axis - a member of loading in the logarithmic order under which the specimens were destroyed.

Table 2

N series	Mean volume weight (kg/m^3)	Mean prismatic strength (MPa)	a	b	$\frac{r}{m_r}$	A number of tested specimens
I	489	2,50	1,245	0,092	9,5	45
II	603	3,58	1,249	0,062	4,2	24
III	689	4,53	1,231	0,093	10,9	25
IV	813	5,56	1,234	0,098	10,3	61
V	895	5,87	1,285	0,103	18,8	41

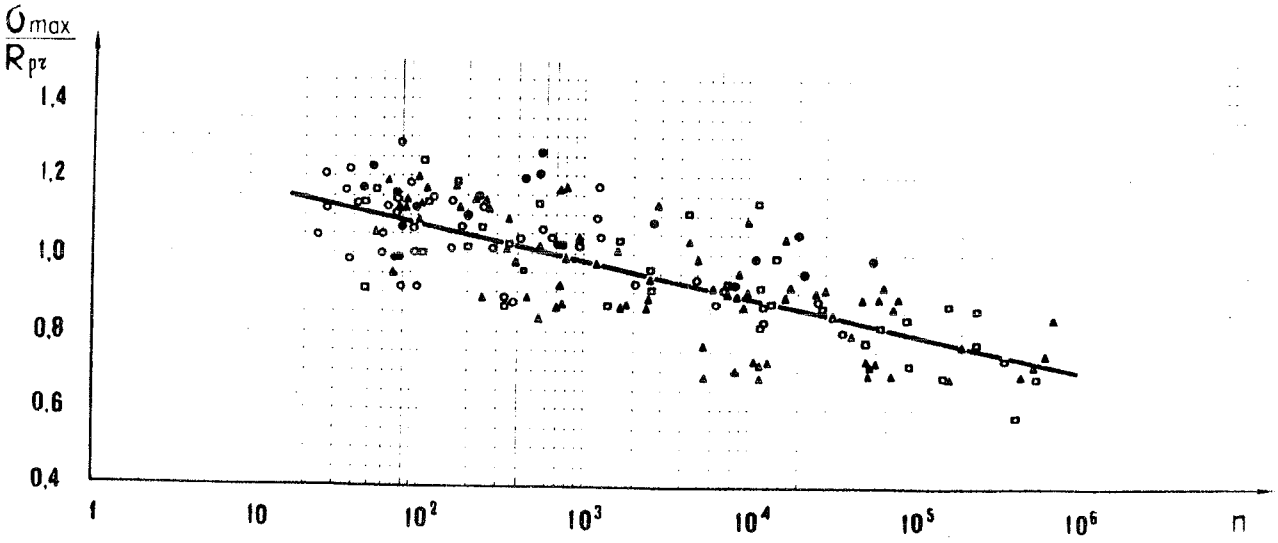

Figure 2: Test results of gas concrete with volume weight 500÷900 kg/m^3 on non multiply repeated load.

○ - specimens of I series; ● - specimens of II series; △ - specimens of III series; ▲ - specimens of IV series; □ - specimens of V series.

As we can see on this diagram prisms, having about 500 cycles of repeated loadings, can carry pulsating load with maximum stress σ max exceeding their static limit of strength Rpr.

The results of other authors' investigations obtained at close parameters of tests for different concrete sorts are given in the form of correlative direct lines on figure 3. Comparison of test results show that as far as the cycle strength autoclaved gas concrete behaves not worse than normal heavy concrete under pulsating loads.

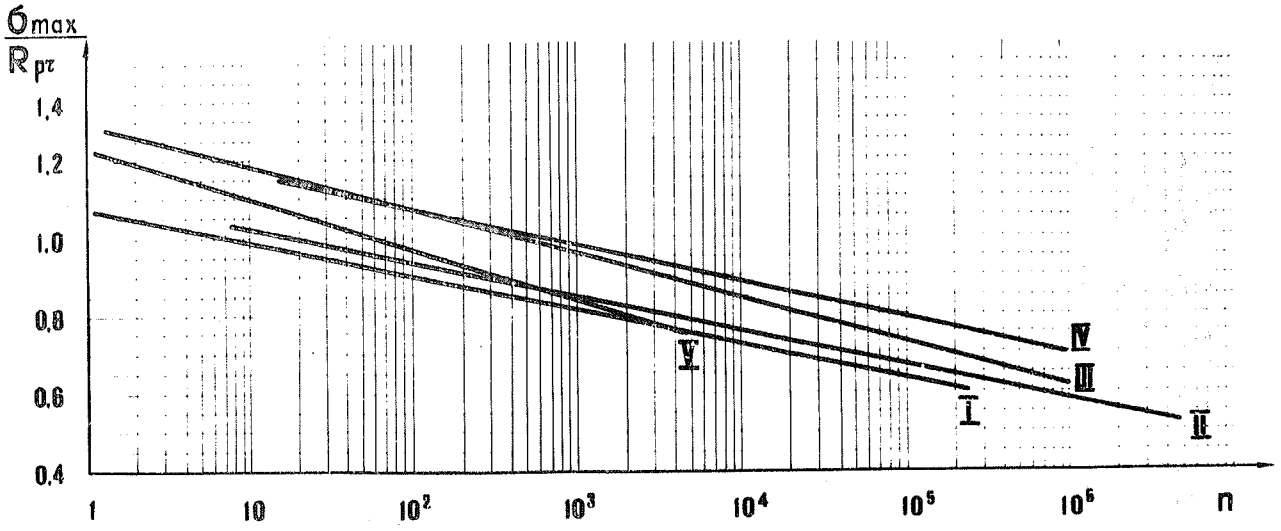

Figure 3: Relative strength of concretes under repeated loadings according to data of different authors.

I - Yu.I.Kotov's tests with gas silicates on the base of barkhan sands; II - T.V.Potapova's tests with dense silicate concrete; III - G.V.Samsonova's tests with ceramsite concrete; IV - The author's tests with gas concrete; V - G.V.Becheneva's tests with heavy cement concrete.

A pronounced brittle character of gas silicates destruction on the base of barkhan sands, distinguishing by lacking of preliminary strain development which characterize common cement concrete, was determined by tests (Polyakov S.V., Kotov Y.I., 1968). This is an unfavourable factor for work of material in the conditions of seismic affects.

The example of oscillogram records obtained in the test of autoclaved gas concrete on non-multiply repeated compressive affects is shown in figure 4. As it can be seen on figure 4 the preliminary development of longitudinal and especially transverse deformations, precede gas concrete destruction. Therefore, we can come to the conclusion that character of gas concrete destruction is not brittle.

Conclusions

The tests of autoclaved gas concrete conducted on affecting of non-multiply repeated compressive loads (like seismic) have shown that this material may be recommended in seismic construction for external wall structures and coefficient of work conditions, taking into account a short-term action of seismic load (m_{kr}), can be assumed for gas concrete the same as for normal heavy concrete which according to chapter SNiP II-A.12-69^{x} (p. 2.13) is equal to 1,2.

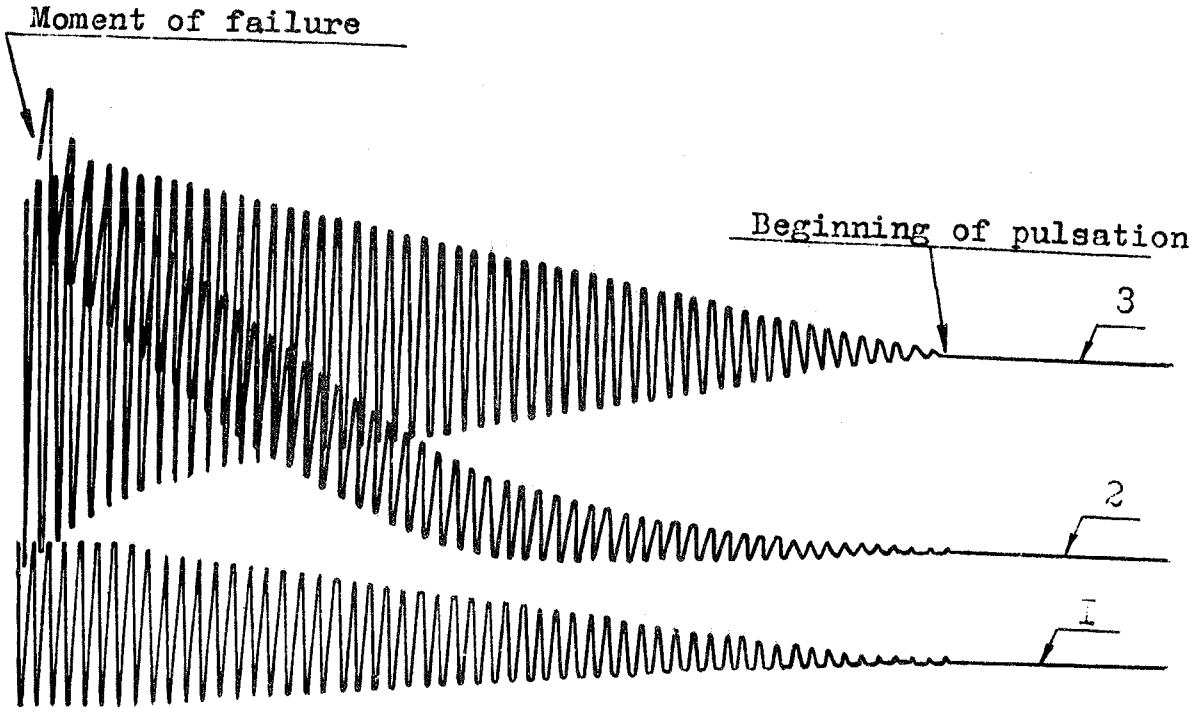

Figure 4: Example of test oscillogram.

1 - load; 2 - transverse strains; 3 - longitudinal strains.

REFERENCES

1. KORCHINSKY I.L. Seismic construction of buildings. Edition of "High School". M., 1971. (In Russian.)

2. POLYAKOV S.V. and KOTOV Y.I. The strength and deformation of aerated and lightweight-aggregate concrete under repeated dynamic loads. Proceedings of the 7-erst International Congress on Lightweight Concrete, May, 1968. Volume 2, London, Cement and Concrete Association.

3. POTAPOVA T.V., POLYAKOV S.V. The strength of silicate concrete under repeated loadings. Building Materials N 6, 1965. (In Russian.)

4. SAMSONOVA G.V. Ceramsite Concrete on local aggregates for seismic vertical enclosure constructions. Building and Architecture of Uzbekistan, N 7, 1976.(In Russian.)

5. VINOKUROV O.P., MAKARICHEV V.V. Application of cellular concretes in seismic areas. Concrete and reinforced concrete. N 11, 1978. (In Russian.)

V.V.MAKARICHEV

O.P.VINOKUROV

21.XII.78

STUDY ON IMPROVING THE FLEXURAL AND SHEAR DEFORMATION CAPACITY OF CONCRETE MEMBER BY USING LATERAL CONFINING REINFORCEMENT WITH HIGH YIELD STRENGTH

Hiroshi MUGURUMA
Kyoto University
Japan

Fumio WATANABE
Kyoto University
Japan

Hitoshi TANAKA
Kyoto University
Japan

Kazuo SAKURAI
Kyoto University
Japan

Eiichi NAKAMURA
Kyoto University
Japan

SUMMARY: Concentric and eccentric loading tests were carried out on concrete cylinder and square column specimens confined by lateral reinforcement having 1650 ~ 13000 kgf/cm^2 in yield strength. Test results showed that the use of high yield strength hoop reinforcement results in excessively large improvement of concrete compressive ductility. Similar results were obtained from beam flexural loading tests. In addition, from the shear tests on column specimens, it was concluded that the yielding of web reinforcement should be avoided for preventing the sudden failure in shear under cyclic loading.

RESUME: Des essais de charge concentrique et excentrique furent effectués sur de spécimens en béton de cylindre et de colonne carée, contraints par armatures latérales ayant une limite d'ecoulement de 1650 ~ 13000 kgf/cm^2. Les résultats en montraient que l'usage d'armature à étrier ayant une grande limite d'écoulement s'est produit d'amélioration excessivement large de ductilité compressive de béton. Des résultats semblables furent obtenus aussi par des essais de charge flexionelle en poutre. En outre, selon les essais de cisaillment sur colonne-spécimens, fut-it conclu que l'écoulement d'armature de cisaillement devrait être évité pour empêcher la rupture soudaine à cisaillement sous charge répétée.

1. INTRODUCTION

Many experimental studies[1] had been presented in the past on the confining effects of lateral hoop reinforcement upon the compressive strength and the compressive ductility of concrete. In these studies, however, the use of relatively lower yield strength of hoop reinforcement, for instance, 2400 to 4000 kgf/cm^2, induces the early release of lateral confining of concrete due to yielding of confining reinforcement. Thus, the yielding of lateral hoop reinforcement may be not desirable to induce the full efficiency in ductility improvement. Similarly, the yielding of shear reinforcement may result in the widening of shear crack width of concrete member subjected to the shear load and as a result the sudden failure of member may be caused under the cyclic high-over shear loading. In this study, to investigate the necessity of high yield strength hoop reinforcement for ductility improvement of concrete under compression or shear, axial compressive loading tests were firstly carried out on concrete cylinder and square column specimens confined by lateral hoop reinforcement having various yield strengths from 1640 to 13000 kgf/cm^2. And further from the cyclic high-over repeated loading tests the effects of high-over cyclic load upon the compressive ductility improvement

were investigated. Also, from the monotonic flexural loading tests on reinforced concrete beams with and without confining lateral reinforcement the possibility of improving the compressive ductility of concrete at flexural compression zone were discussed. Finally, the combined cyclic flexural and shear loading tests were carried out under constant axial load in reinforced concrete square column specimens with high yield strength web reinforcement. Test results were discussed in terms of failure mode, ultimate strength and ductility compared with those from ordinary yield strength of web reinforcement.

2. FUNDAMENTAL COMPRESSION BEHAVIOR OF CONCRETE CONFINED BY HIGH YIELD STRENGTH HOOP

The specimens used in the concentric loading tests are 24-ϕ15 x 30 cm concrete cylinders laterally confined by circular spiral hoop reinforcement and 36-19.4 x 19.4 x 40 cm square columns by square one. The confining hoop reinforcements used in the tests are from 1640 to 13000 kgf/cm^2 in yield strength and are 6, 7 and 9 mm in diameter. The pitches were varied from 2.5 to 32 cm in correspondence to the volumetic ratios, p_s = 0.4 to 3.3 %. The target compressive concrete strength at the test age was 300 kgf/cm^2, excepting that it was 250 to 600 kgf/cm^2 in some test series for obtaining the effect of concrete strength upon the confinement. The compressive concrete strains were measured over the central 25 cm for cylinder specimens and over the 35 cm for square column specimens by linear differential transformer. The strain of hoop reinforcement was also measured by wire strain gages to obtain the confining stress.

Typical stress-strain curves and corresponding confining stress obtained are shown in Fig. 1. In this study, the confining stress σ_L induced in the concrete was calculated from the measured strain of hoop reinforcement by using the following equation[2].

$$\sigma_L = 2A_s \cdot f_s / s \cdot D \qquad (1)$$

A_s: Sectional area of hoop reinforcement
f_s: Tensile stress in hoop reinforcement calculated from measurement of hoop strain
s : Pitch of hoop reinforcement
D : Diameter of cylinder specimen or width of square column specimen

As can be seen from Fig. 1, the yielding of hoop reinforcement takes place at the concrete strain of 0.3 ~ 0.4% in case of ordinary yield strength hoop reinforcement and after that considerable strain softening had taken place because of the release of lateral confining. On the contrary, in case of high yield strength hoop reinforcement, linear increase of hoop tension can be recognized with a little or without any decrease of axial compressive stress over the remarkably large compressive strain of concrete. This phenomenon well suggests that lateral reinforcement should confine the core concrete elastically without any release or yielding to fully improve the compressive ductility of concrete. From the measurements of tensile strain in lateral reinforcement it can be recommended to use the steel having the yield strength more than 8000 kgf/cm^2.

As a reference, the degree of improving the compressive ductility of concrete was estimated by the axial compressive strain of concrete at which the average stress in stress-strain curve becomes maximum. In this study, such strain is defined as the available limit of compressive strain. The values obtained from measured stress-strain relations are shown in Fig. 2, which indicates that the available limit of compression strain obtained

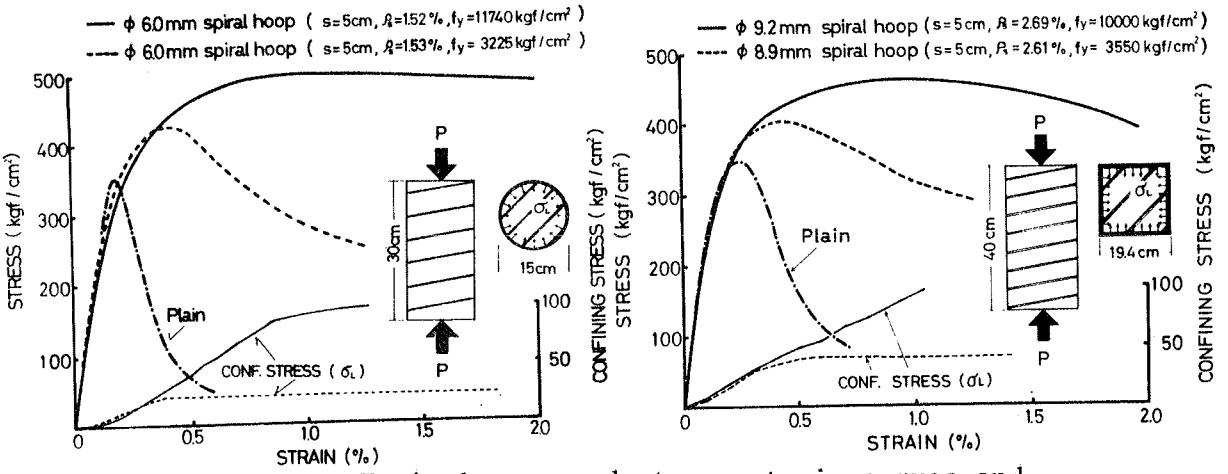

Fig. 1 Typical measured stress-strain curves and corresponding confining stress

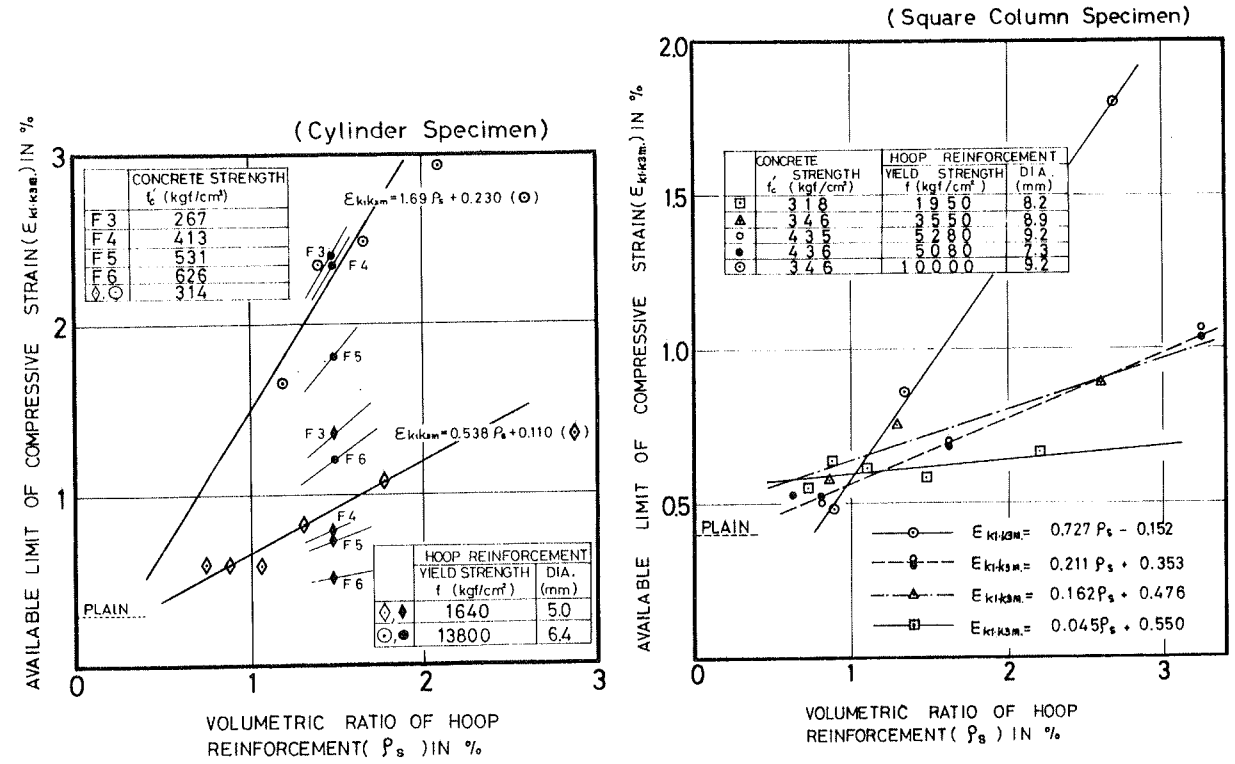

Fig. 2 Available limit of compressive strain of concrete obtained from monotonic concentric loading tests

from the specimen with high yield strength hoop reinforcement becomes more than 4 times that obtained from ordinary yield strength one in the cylinder specimen and more than 2 times in the square column specimen, when the amount of hoop reinforcement is sufficient.

3. BEHAVIOR UNDER CYCLIC HIGH INTENSITY REPEATED LOADINGS

From the view point of aseismic design of concrete structure, the beha-

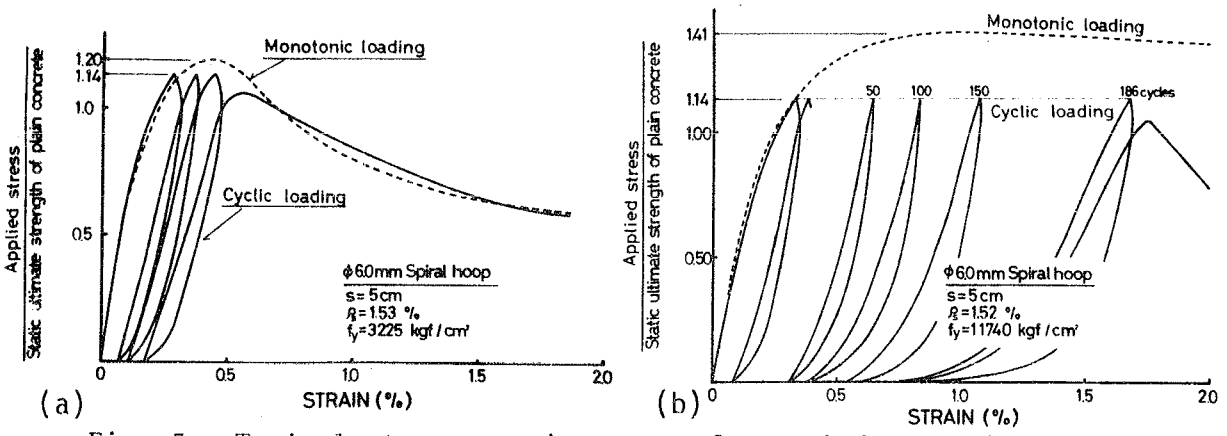

Fig. 3 Typical stress-strain curves for cylinder specimens under cyclic highpintensity repeated loadings

vior of confined concrete under cyclic high intensity repeated axial loading may be most important to discuss the effects of laleral confining. In this study, some of confined cylinders were tested under high intensity repeated axial loading. In Fig. 3, typical stress-strain curves obtained from the specimen with high yield strength hoop reinforcement are compared with those with ordinary yield strength one, where the maximum stress applied is 1.14 times the compressive strength of plain (unconfined) concrete. In case of ordinary yield strength hoop reinforcement the specimen can withstand the the cyclic loads until the drift of strain at the maximum load level attains at the post peak stress-strain skelton curve under monotonic loading. This may be owing to the gradual deterioration of lateral confinement created by excessive yielding elongation of hoop reinforcement under cyclic load. Contrarily, in the case of high yield strength hoop reinforcement, failure of specimen was taken place by compressive fatigue crushing of concrete after larger load cycles without the strain drift attaining at skelton curve. However, it can be recognized from strain measurement in hoop reinforcement that the yielding of hoop reinforcement also began to occure at several cycles of loading before failure. Considering such failure mode, it may be concluded that the concrete confined by high yield strength hoop reinforcement exhibited the full potential load carrying capacity. As the fatigue failure cycles concern, the specimen shown in Fig. 3(b) withstood 186 cycles of loading without failure, while that in Fig. 3(a) only 3 cycles. As a reference, the fatigue life curves obtained from the cylinder specimens confined with various yeild strength hoop reinforcement are shown in Fig. 4

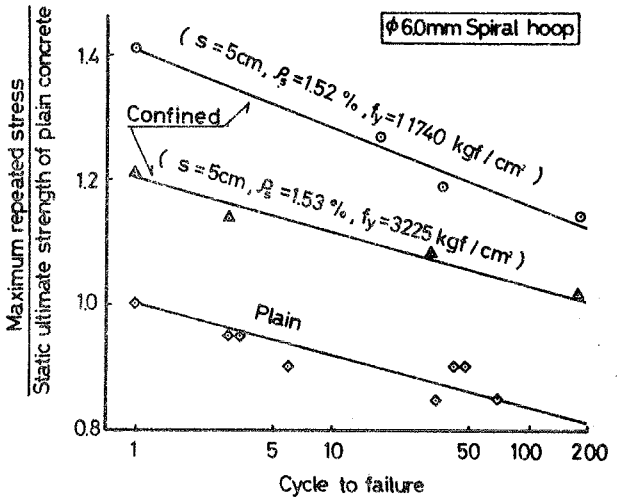

Fig. 4 Stress-fatigue life curve in cylinder specimens

4. VERIFICATION OF IMPROVEMENT OF COMPRESSION DUCTILITY OF CONCRETE BY BEAM FLEXURAL TESTS

To verify whether the lateral confinement by high yield strength hoop

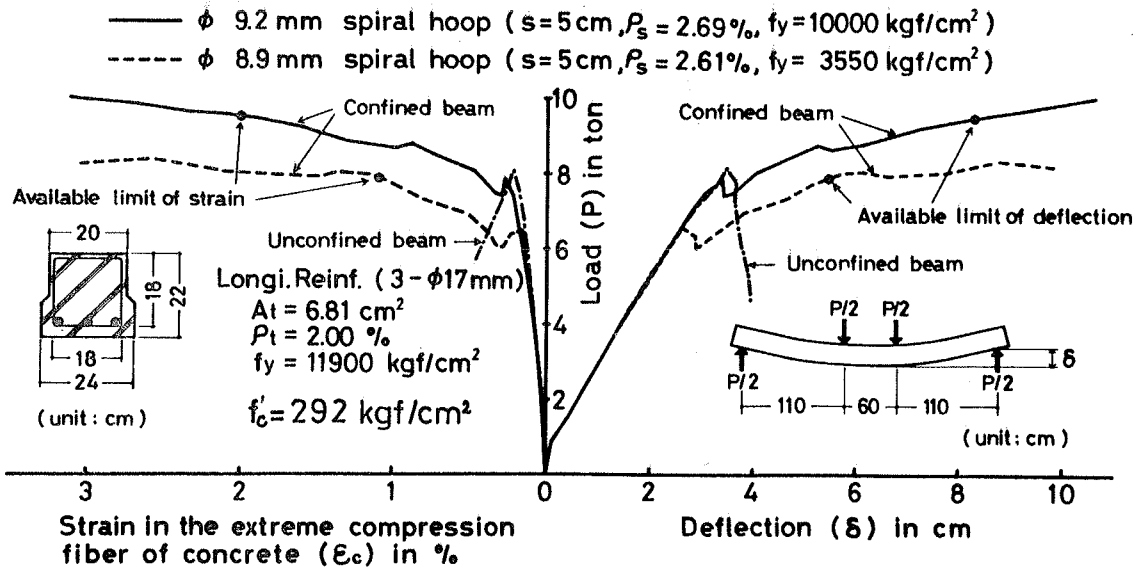

Fig. 5 Effects of high yield strength lateral reinforcement on flexural behavior of beams

reinforcement is effective or not for improving the rotating ductility of concrete beam section, flexural loading tests were carried out on reinforced concrete beams confined laterally by high yield strength hoop reinforcement. As the tensile reinforcement, 3-φ17 mm in diameter non-stressed prestressing bar having nominal yield strength of 11000 kgf/cm^2 were used for avoiding the yielding of tensile reinforcement until flexural failure. Typical midspan deflection curve and extreme compressive fiber strain at midspan section are shown in Fig. 5 with the details of beam section and loading condition. Also, measurements on beams laterally confined by ordinary yield strength hoop reinforcement and those on unconfined beams are plotted in Fig. 5. For quantitative comparison of confining effects, available limit of compressive fiber strain of concrete was calculated by using measured tensile strain in reinforcement, concrete fiber strain and depth of neutral axis. where, referring to the definition proposed in Section 2, the fiber strain at which the average compressive stress in compression zone becomes maximum was defined as available limit in the case of beam flexure. These values are 2 % for beam with high yield strength hoop reinforcement and 1.1 % for that with ordinary one as indicated in Fig. 5. In Fig. 6, the increase of available limit of compressive strain of concrete by using high yield strength lateral reinforcement is shown in comparison with those obtained from concentric loading tests described in Section 2. In addition, results obtained from eccentric loading tests on confined square column specimen is also plotted in Fig. 6. From Fig. 6 it can be noted that the available limit of com-

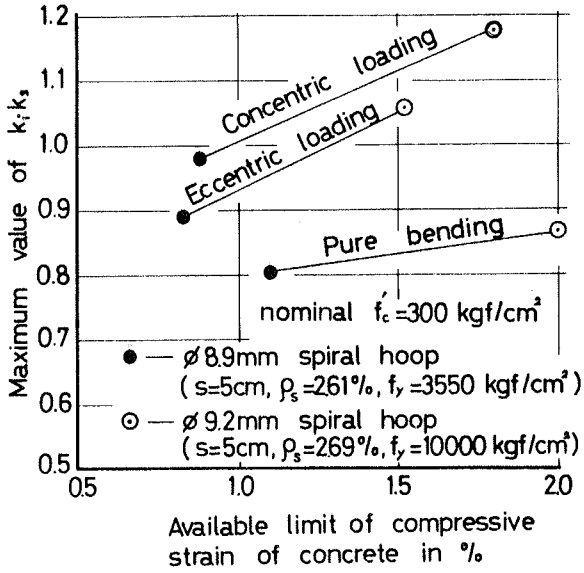

Fig. 6 Increase of available limit of compressive strain by using high yield strength hoop reinforcement

pressive strain of concrete can be significantly increased by using high yield strength lateral reinforcement even in case of pure flexure of beam.

5. IMPROVING OF SHEAR DEFORMATION CAPABILITY OF REINFORCED CONCRETE COLUMN

In the aseismic design failure of column in shear should be prevented by providing adequate shear reinforcement because of its brittleness. Especially when column is subjected to reversed cyclic high over shear force with flexure, the yielding of web reinforcement may cause the sudden failure in shear due to the degradation of aggregate interlocking action along the shear crack and of shear resistance of concrete in compression zone.

Thus, in this study, to investigate the effects of high yield strength web reinforcement upon the shear failure behavior, monotonic and cyclic shear loading tests were carried out on column specimens shown in Fig. 7. Eight specimens having 25 x 25 cm square section and 60 cm in column height were used. The column was reinforced longitudinally by 4 - D19 mm in diameter deformed bars with the yield strength of 3850 kgf/cm^2. For avoiding the bond slippage, the longitudinal reinforcement were anchored mechanically on top and bottom surfaces. As the web reinforcement, 6 mm in diameter closed hoops having 3000 and 11200 kgf/cm^2 in yield strength were arranged in a pitch from 5 to 10 cm, which corresponds to the ratio of web reinforcement, p_w = 0.224 to 0.45 %. Tests were carried out at the age of 26 days. The compressive and tensile strength of concrete at the test age were 267 and 25.1 kgf/cm^2, respectively. Prior to the loading test, the concrete base cast in monolithic at the column foot was fixed rigidly on the testing floor by prestressing. As shown in Fig. 7, lateral load was applied at the top side of column by servo controlled hydraulic jack so as to have the shear span-total depth ratio of 2.0, where the axial compressive load was held in constant in one-sixth of static compressive strength of column section during lateral loading. Column deflection was measured at the level of lateral loading by linear transformer. In the cyclic high over lateral loading tests, applied load was controlled on the basis of the lateral deflection at initial yielding of column foot section. That is, after applying

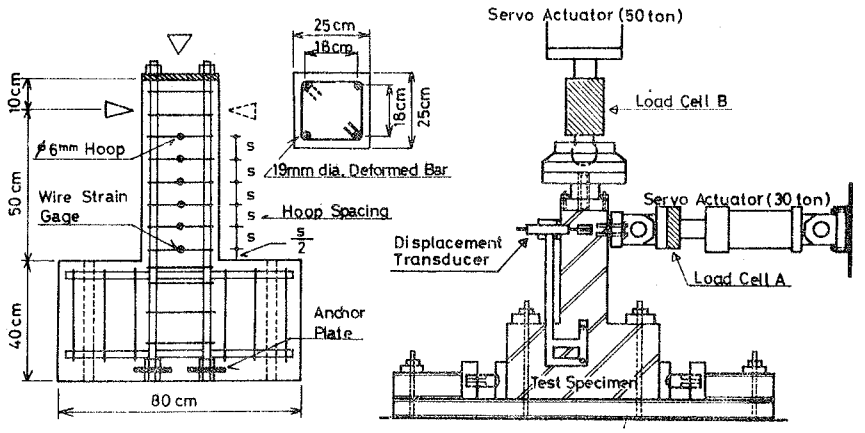

Fig. 7 Specimen and loading method of column shear test

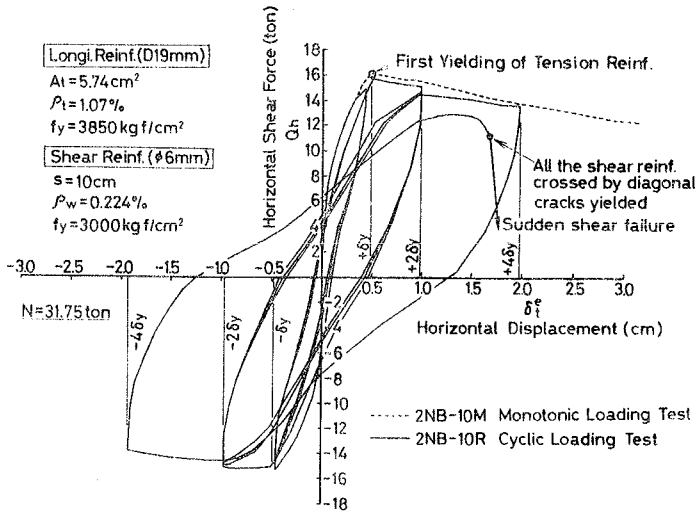

Fig. 8 Shear force-deflection curves of column having low yield strength web reinf.

3 cycles of reversed cyclic load with the maximum deflection level at initial yielding, next 3 cycles were followed under the maximum lateral deflection amplitude of 2 times the yielding deflection. And then the deflection amplitude was increased to 4 times the yielding.

Shear force-lateral deflection hysteretic curves measured are shown in Fig. 8 to Fig. 11, respectively, by solid line. Skelton curves obtained from monotonic lateral loading tests are also plotted in those figures by dotted line. As can be seen from these figures, excessive large post peak lateral deformation was observed for each specimen under monotonic loading. And further, the skelton curve in Fig. 4 is quite close to that in Fig. 2, while higher yeild strength of web reinforcement is used in the former. However, under reversed cyclic loading, different load-hysteresis curves as well as different failure characteristics were obtained between the specimen with high and low yield strength web reinforcement, especially when the loading cycles with the deflection amplitude of 4 times that at yielding of column foot section were being applied. That is, in the case of low yield strength web reinforcement the increase of tensile strain in web reinforcement was observed under cyclic loading and when it attains at its yielding strain in all the web reinforcement crossing the inclined cracks at column foot section, sudden failure in shear takes place (See Fig. 2 and Fig. 3). This may be explained by

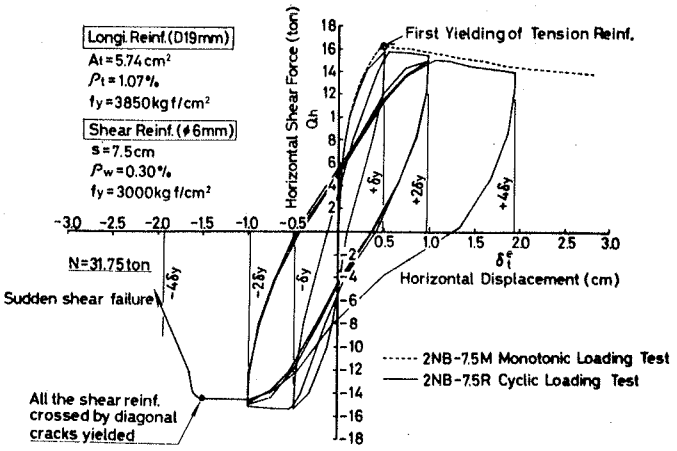

Fig.9 Shear force-deflection curves of column having low yield strength web reinf.

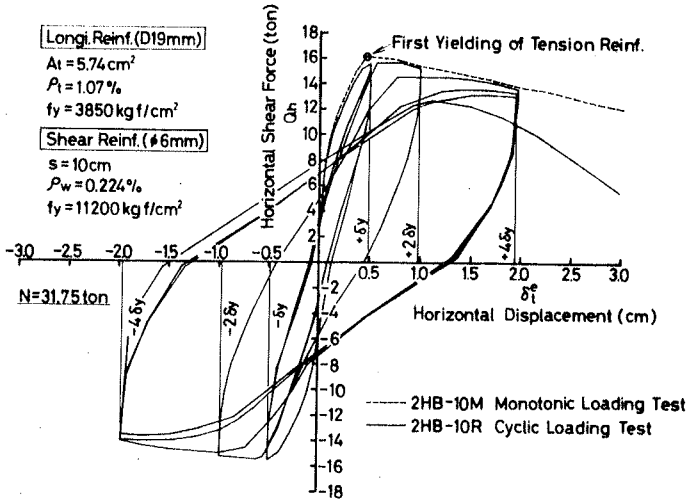

Fig.10 Shear force-deflection curves of column having high yield strength web reinf.

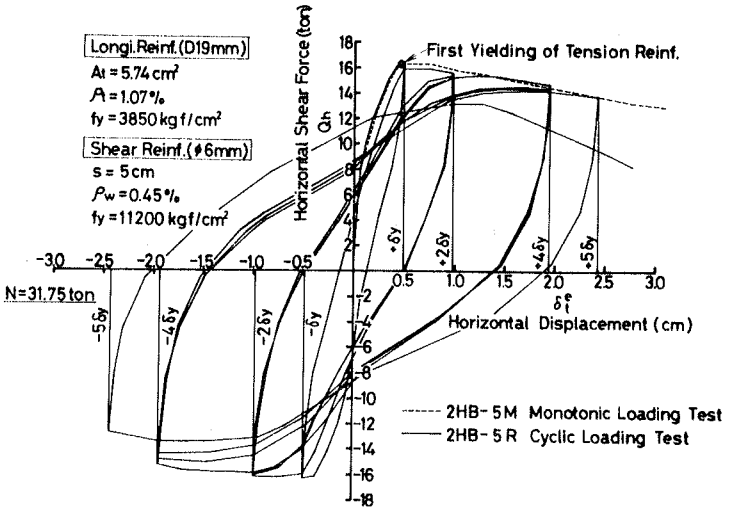

Fig.11 Shear force-deflection curves of column having high yield strength web reinf.

the reason that the yielding of web reinforcement mainly results in excessive degradation or loss of aggregate interlocking action. On the contrary, in the case of high yield strength web reinforcement the specimen failed by crushing of concrete at column foot section without any yielding in web reinforcement, which may result in more stable hysteresis loops under reversed cyclic loadings and more steady post peak deflection curve after failure (see Fig. 4 and Fig. 5). As a reference, the progress of measure strain of web reinforcement on typical column specimen (2NB-10R and 2-10R) under high over cyclic loading is shown in Fig. 12

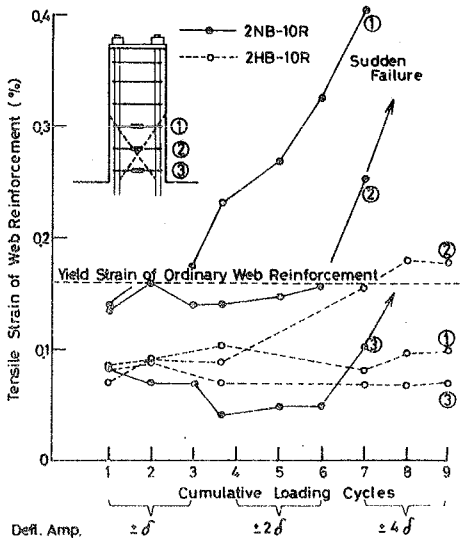

Fig. 12 Measured strains of web reinforcements during repeated cyclic loading tests

6. CONCLUSIONS

From this study, the following conclusions were derived.

1. Lateral confinement concrete by high yield strength lateral reinforcement can remarkably enhance the compressive ductility of concrete subjected to uniaxial compression. In this study, even in the square column specimen confined by square hoop reinforcement, the use of high yield strength square hoop reinforcement showed at least two times available limit of compressive strain by ordinary yield strength one when the amount of lateral reinforcement is sufficient, while the cylinder columns confined by circular one showed more than four times.
2. Elastic lateral confinement of concrete by high yield strength hoop reinforcement is very effective for preventing the early failure in fatigue of concrete.
3. The use of lateral confinement by high yield strength hoop reinforcement also enables to improve the compressive ductility of concrete in compression zone of beam section subjected to pure flexure. In this study, the available limit of extreme compressive fiber strain attained 2 % for beams with square spilal hoop reinforcement having high yield strength and 1.1 % for that ordinary one.
4. As the test results obtained concern, the use of lateral reinforcement having the yield strength more than 8000 kgf/cm^2 is recommended for full improvement of concrete ductility.
5. In addition the use of high yield strength web reinforcement can much enhance the shear deformation capability of reinforced concrete column subjected to combined bending moment and shear force. In this study, column specimen having high yield strength web reinforcement showed the stable hysteretic load deflection curves under cyclic high over load without any sudden failure in shear, while sudden failure had taken place in case of ordinaly yield strength one.

7. REFERENCE

1) For instance, K.T.S.R. Iyenger et al.: Magazine of Concrete Research, Vol. 22, No. 72, September, pp.173-184 (1970)
2) F. E. Richart et al.: University of Illinois Engineering Experiment Station Bulletin, No. 190, Urbana, April (1929)

CONFINEMENT EFFECTS OF REINFORCEMENT ON REINFORCED CONCRETE ELEMENTS UNDER CYCLIC LOADING

I. PASKALEVA
Geopsycal Institute
Bulgarian Academy of Sciences
Sofia, Bulgaria

S. SACHANSKI
Department Seismic Mechanics
Bulgarian Academy of Sciences
Sofia, Bulgaria

SUMMARY

The paper presents the results of a research on reinforced concrete prisms and columns with different cross reinforcement. tested for repeated and cyclic loading.

The load -deformation hystereses loops, stress-strain relations concerning concrete and ties in reinforced concrete prisms are analysed.

Reinforced concrete columns with different ties are tested for axial compression and cyclic shear and bending. The hystereses loops, strength capacity, limit deformations are analysed by using the results of the test.

Analytical expression for influence of cross reinforcement on bearing capacity of columns is established.

RESUME

La communicassion expose les résultats de la recherche sur des prismes et des colonnes armés d'armature transversale de quantités diverses.

On analyse les courbes d'hystérésis de charge - déformation du béton et de l'armature transversale des prismes et des colonnes.

Des colonnes armées sont éprouvées par rapport à la pression axiale et à la coupe et la flexion cyclique. Les résultats sont analysés et une formule de détermination de la résistance portante des colonnes est déduite.

Introduction

The significance of confined concrete on improving the earthquake resistance of columns has been established both through the damages in the constructions during earthquakes and numerous tests.

The results of the investigations of various authors on the influence upon the cross reinforcement on the bearing capacity of confined concrete show great differences - from 0 to 70% /I,2,3,4/. That is why the investigations in this field should continue under conditions similar to those of the confined concrete of structures.

Regardless of the different results concerning the increase of the bearing capacity of confined concrete there is no doubt that the cross reinforcement increases the ductility factor of the columns to a great extent and brings forth conditions for the redistribution of the stresses in structures and increase of the earthquake resistance. That is why the influence of the cross reinforcement on the bearing and deformable capacity of the columns in the nonelastic stage should continue.

I. Experimental Investigations on Prisms

The investigated reinforced prisms 20/20/40 cm represent a physical model of the upper or lower end of the concrete column reinforced by longitudinal reinforcement 4 Φ I2 and with different distance between the ties / I9, 9 and 6 cm /. Prisms that have no reinforcement, prisms with longitudinal reinforcement /without any cross reinforcement/ and prisms with longitudinal and cross reinforcement have been investigated.

The prisms have been tested under repeated compression at different speed of loading with normal pressure of the steel plates of the machine on the concrete and by decreasing the friction between the compressed surfaces.

The deformations of the concrete, ties and longitudinal reinforcement by means of strain gages have been measured.

The hystereses loops and their envelope for the concrete of a prism are giv en in Fig. I. Some of the hystereses loops of the deformations in the ties located in the middle of the prisms are represented in Fig. 2.

The following important conclusions have been drawn from the experimental investigations:

- the longitudinal reinforcement which is not connected with the ties does not increase the ultimate strength and deformations of the concrete;

- the increase of the number of ties leads to the increas of the bearing and deformative capacity of the prisms to 50% / Fig. 3 /.

- the ties in close proximity with the plates of the testing machines have less strain because of the friction and limitation of deformation in the concrete;

- the prisms with reduced friction between the concrete and the plates have IO to 20% reduced bearing capacity;

- the speed of loading the prisms exerts influence on the ultimate strength, deformations and way of destruction. The ultimate strength increases to 35% by increasing the speed of loading. The ultimate deformations decrease in this case;

- the destruction of the concrete depends on the number of ties / Fig. 4 /. When the number of ties is smaller the destruction is realized by shearing along one plane. When the number of ties is greater the confined concrete is destroyed;

- the ultimate deformations of the confined concrete increase twice compared to the concrete that has no cross reinforcement;

- some ties made in the common way unfold at the hooks without being in the position to undertake great stresses. The problem of folding the ties is rather important for the increase of their eff ectiveness;

The results of testing the prisms have been used for the investigation of columns subjected to combined loading.

2. Experimental and Theoretical Investigations on Columns at Cyclic Loading

The columns in the frame buildings with infilling walls during earthquake are subjected to additional bending and shearing not only as a result of the $p - \delta$ effect but also as a result of the resistance of the infilling walls during horizontal displacements. That is why some experimental investigations on columns subjected to compression and additional cyclic exitation of bending and shearing have been carried out / Fig. 5-a /. Columns with cross section I2/I2 cm and I2/20 cm with different distances between the ties - 5, I0 and I5 cm have been tested.

The deformations of the concrete, the longitudinal reinforcement and the ties have been measured by strain gages.

The hystereses loops of one of the columns are given in Fig. 5-b.

On the basis of the theoretical investigations and comparison of the results with the experiments the following formula for determining the destructive bending moment in columns subjected to axial compression has been drawn:

$$M = W\left[\frac{a}{h}\,\frac{A_{st}\,R_{st}}{A} + 0{,}5\,\frac{N}{A}\left(1 - \frac{N}{A\,R_c}\right) + \frac{R_{st}^{t}\,\ell_t\,A_{st}^{t}}{A_{cc}\,S}\right]$$

where:

W -resistance moment of inertia of the cross concrete section:

a - distance between compressional and tensional reinforcement;

Ast, Rst - cross section and ultimate strength of longi-

tudinal reinforcement;

A - cross section of the column;

A^t_{st}, R^t_{st} - cross section and ultimate strength of the ties;

Acc - cross section of the confined concrete;

l_t - length of ties;

s - distance between ties;

The first term in brackets of this formula determines the contribution of the longitudinal reinforcement, the second - of the concrete and the third - of the cross reinforcement of the bending moment.

The ultimate bending moments calculated according to the formula above give values quite similar to those obtained in the experimental way.

3. Conclusion

The following basic conclusions have been drawn from the theoretical and experimental investigations:

The ties in the compressed columns decrease the lateral deformations in the concrete and strengthen it. They prevent the longitudinal reinforcement from buckling and increas its contribution during earthquakes. The ties increase the ductility of columns and help the formation of plastic hinges. That is why the distance between the ties of the upper and lower ends of the columns should be reduced from 5 to 10 cm and regulated to the standards.

The destructive bending moment of the columns with taking into account the influence of the cross reinforcement can be determined according to the above-given formula. This formula can also be used at the analyses of buildings damaged by earthquakes.

The results of the investigations presented in this paper can be used for taking into consideration some other factors at the analyses of destructions in reinforced concrete buildings during earthquakes. Some of the conclusions will be used for working out new programmes for investigations.

Refernces

I. Sheik S.A. Uzumeri S.M.; Concrete Confinement by Rectangular Ties, Proc. Sixth European Conf. on E.E., Dubrovnik I I978.

2. Umemura H. Aoyama H., Evaluation of Inelastic Seismic Deflections of Reinforced Concrete Frames Based on the Tests of Members, Proc. 4WCEE Chile I969.

3. Otoni S., Sozen M., Behaviour of Multistory Reinforced Concrete Frames During Earthquakes, University of Ilinois Series No 392, I972 Urbeena, Ilinois.

4. Bertero N.V., Vollenas S., Confined Concrete - Research and Development Needs, University of California, Berkeley I977.

5. Paskaleva I., Analyses of Structural Elements and Buildings in Nonelastic Stage for Harmonic and Seismic Exitation, Tesses for PhD. Bulgarian Academy of Sciences, Geophysical Institute, Sofia.

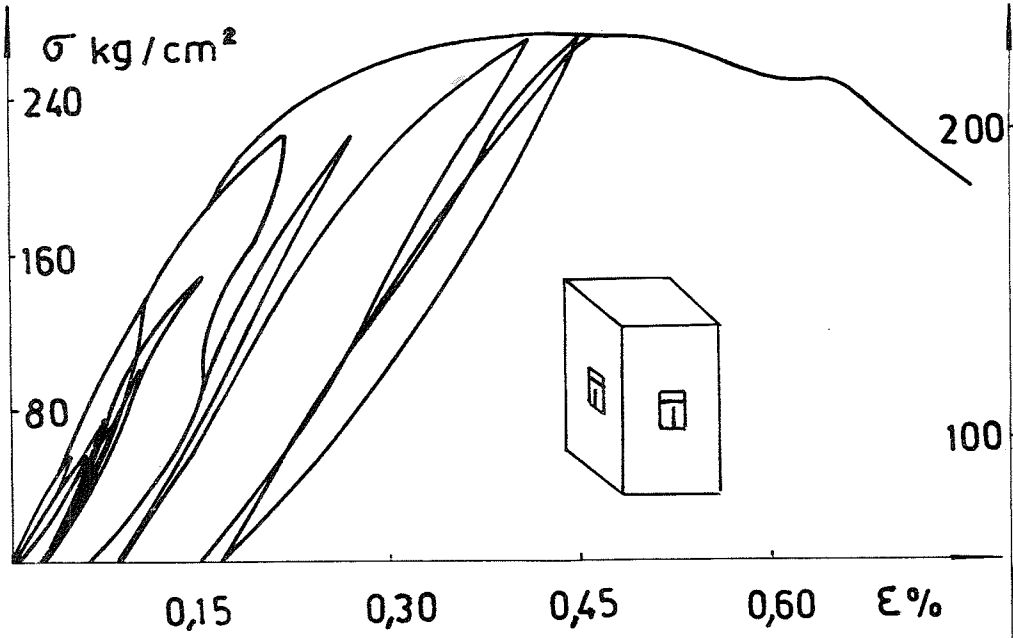

fig. 1

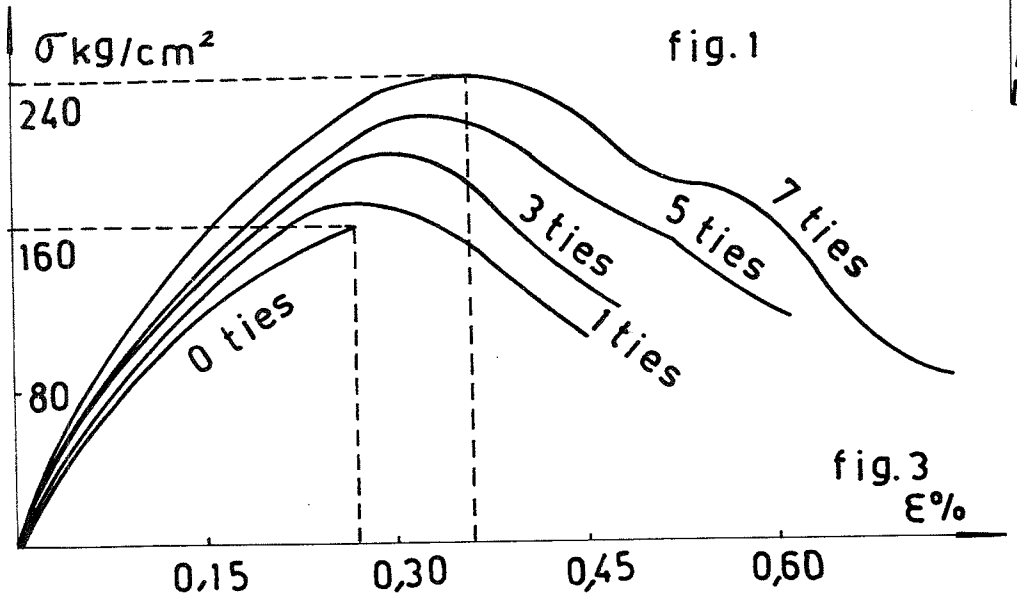

fig. 3

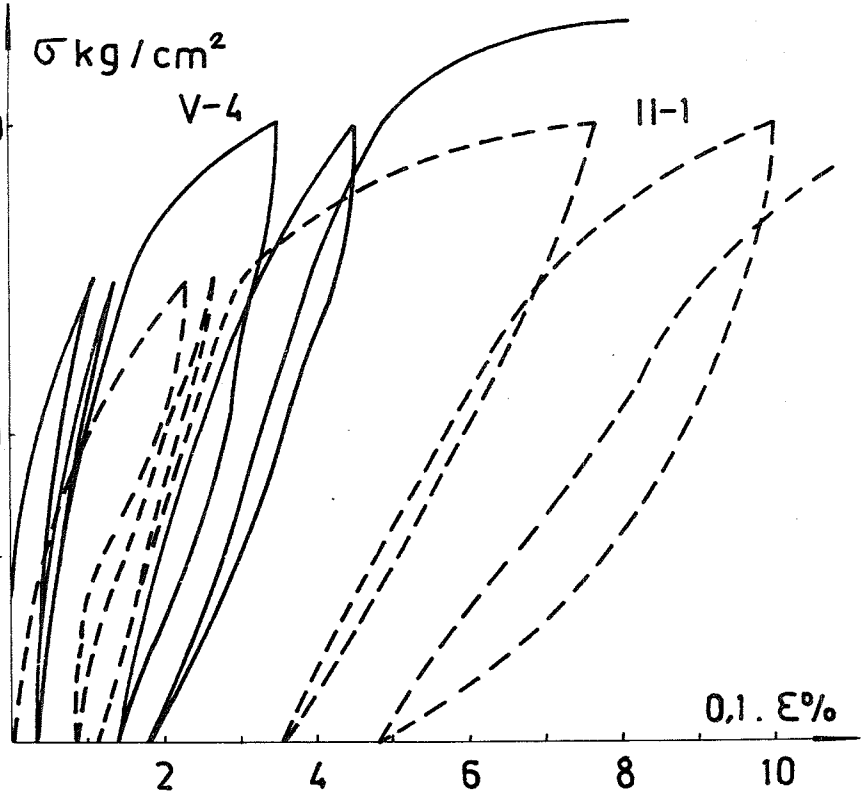

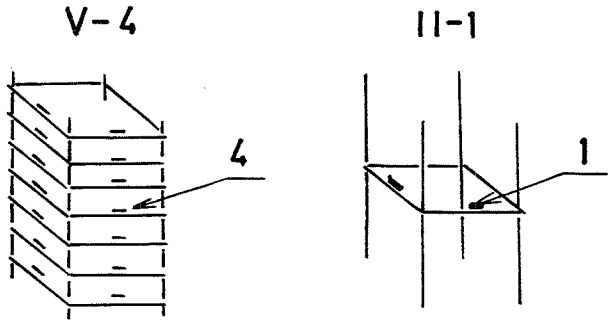

fig. 2

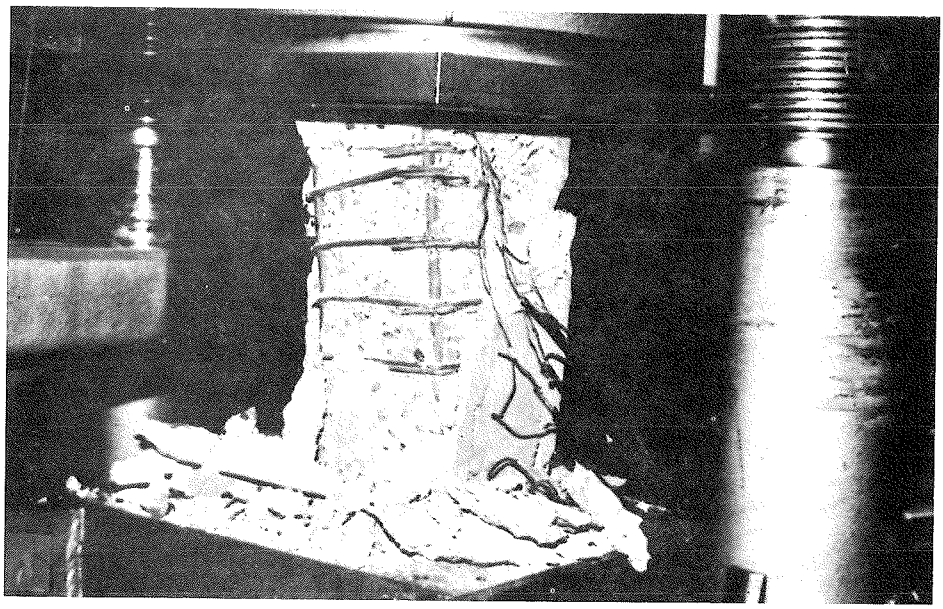

fig.4

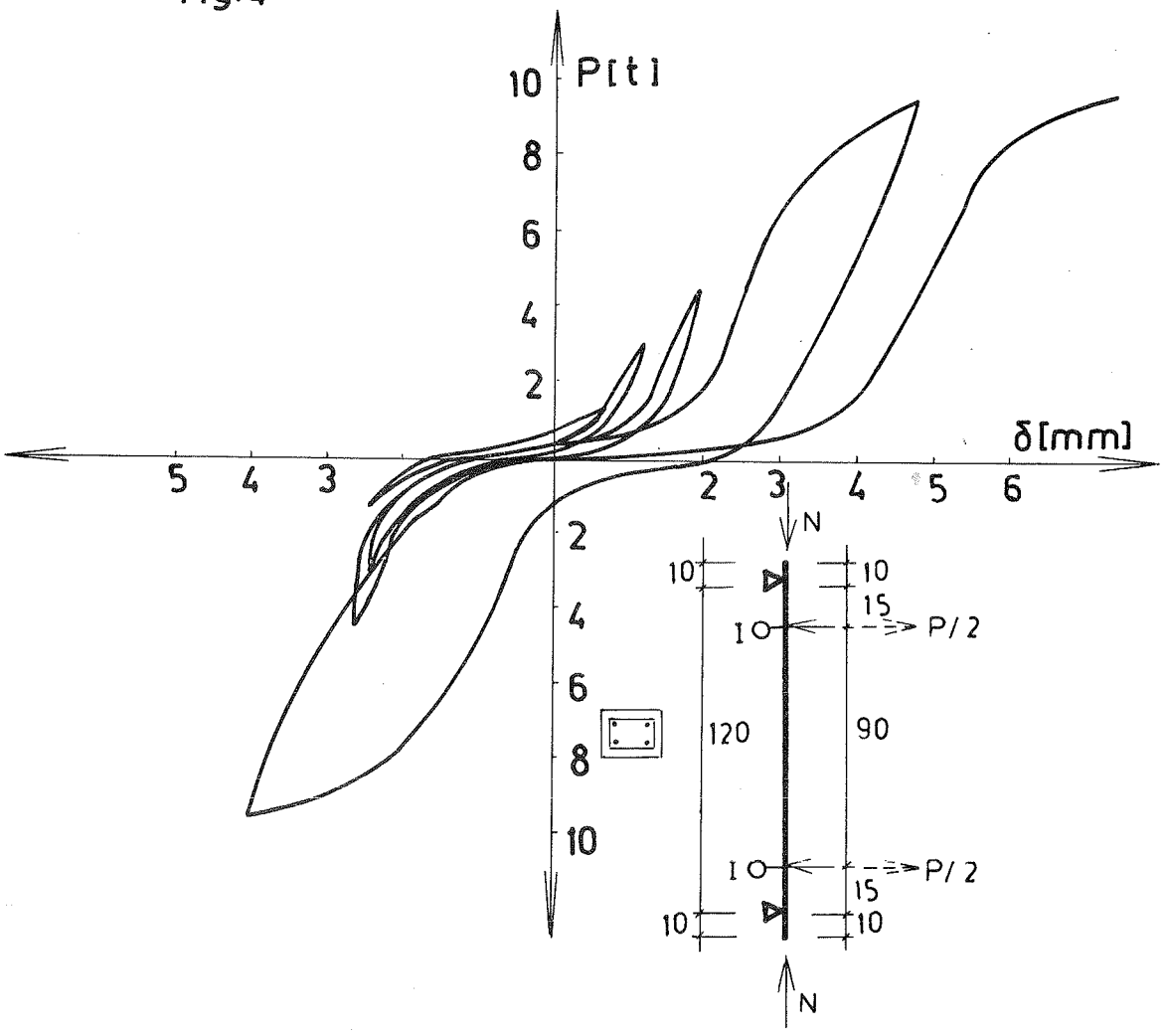

fig. 5

PROPERTIES OF CONCRETE CONFINED BY RECTANGULAR TIES

S. A. SHEIKH
SWR Engineering Limited
Toronto, Canada

S. M. UZUMERI
University of Toronto
Toronto, Canada

SUMMARY

The research reported in this paper is directed towards the experimental and analytical determination of the stress vs. strain curve of concrete confined by rectangular ties. The experimental part of the study involved the testing of 24 columns, 12 x 12 in. (305 x 305 mm) in section, and 6'-5" (1956 mm) high, with core dimensions of 10.5 x 10.5 in. (267 x 267 mm) (centre to centre of the perimeter tie). Columns were cast vertically and tested under monotonic axial compression. The test variables included the tie arrangement resulting from the distribution of the longitudinal steel around the core perimeter, the tie spacing, the amount of lateral and longitudinal steel and the strength of the lateral steel.

An analytical model has been developed to predict the behaviour of concrete confined by rectangular ties when subjected to axial compression. A comparison of the experimental and the predicted results for the Toronto tests and for tests reported by various researchers shows that the proposed model is capable of predicting very well, the effects of different variables.

La recherche décrite dans cet article a pour but la détermination expérimentale et analytique de la relation entre la contrainte et la déformation du béton contenu par des étriers rectangulaires. Du côté expérimental, les essais ont porté sur 24 colonnes, de section 12" x 12" (305 mm x 305 mm) et de hauteur 6'-5" (1956 mm). Les dimensions du noyau, mesurées à partir de l'axe des étriers, étaient de 10.5" x 10.5" (267 mm x 267 mm). Après le coulage vertical du béton, les colonnes étaient soumises à une compression axiale monotone. Les paramètres variables de l'expérience comprenaient la disposition des étriers selon la distribution de l'acier longitudinal autour du noyau, l'espacement des étriers, la quantité d'acier latéral et longitudinal, et les caractéristiques de l'acier latéral.

Un modèle analytique a été developpé pour prédire le comportement du béton contenu par des étriers rectangulaires et soumis à une compression axiale. La comparaison des tests de Toronto, ainsi que d'autres tests rapportés par divers chercheurs, avec les résultats prédits par le modèle, montre que le modèle est capable de très bien prédire les effets de divers paramètres.

LIST OF SYMBOLS

A_c = core area (measured to centre of perimeter hoop)
A_g = gross area of column
A_s = area of longitudinal steel
b = core dimension measured from centre to centre of the perimeter hoop
c = centre to centre distance between the longitudinal bars
d = diameter of tie steel
f'_c = strength of unconfined concrete, as determined from standard cylinder test
f_{cc} = strength of confined concrete in the specimen
f_{cp} = strength of unconfined concrete in the specimen
f_s = steel stress at the strain level considered
f'_s = stress in the lateral steel
f_y = yield point of longitudinal steel
K_s = ratio of the strength of confined concrete to the strength of plain concrete
P_{cmax} = maximum test load carried by the concrete: $(P_{test} - P_{st})$
P_{conc} = $(P - P_{st})$, load carried by concrete
P_o = $P_{oc} + A_s f_y$
P_{oc} = $0.85\ f'_c\ (A_g - A_s)$
P_{occ} = $0.85\ f'_c\ (A_c - A_s)$
P_{st} = force resisted by the column steel
P_{test} = maximum axial force resisted by the column
s = spacing of sets of ties
ε_{oo} = average longitudinal strain corresponding to the maximum stress in plain concrete
ε_{pmax} = average longitudinal strain corresponding to P_{test}
ε_{s1}, ε_{s2} = minimum and maximum average longitudinal strains corresponding to the maximum stress in concrete
ε_{s85} = average longitudinal strain corresponding to 85% of the maximum stress in concrete on the unloading part of the curve
η = a constant used in the proposed model - equals the number of longitudinal bars in the specimens tested during this investigation
ρ = A_s/A_g or A_s/A_c
ρ_s = ratio of volume of lateral (tie) steel to the volume of core

INTRODUCTION

When concrete is subjected to cyclic compression simulating seismic action, the stress vs. strain curves exhibit strength and stiffness decay, but the envelope curve thus obtained is almost identical to the stress vs. strain curve of concrete under monotonic axial compression. Further, provided that the "envelope curve" is available, there are adequate mathematical models to develop the stress vs. strain curve under cyclic compression.

The primary requirement in seismic design is the capacity of the structure to absorb and dissipate energy by post-elastic deformations. It is generally accepted that spiral confinement reinforcement increases the strength and ductility of confined concrete. It is also generally accepted that the concrete confined by rectangular ties exhibits increased ductility. However, there is a divergence of opinion on the quantification of this increased ductility, and more important, there is no agreement regarding the possible increase in the strength of concrete due to the confinement provided by rectangular ties. In the research reported here an experimental

and analytical study was carried out to study the effects of different variables in the mechanism of confinement provided by rectangular ties.

EXPERIMENTAL WORK

The experimental part of the study involved the testing of twenty-four 12" (305 mm) square, 6'-5" (1960 mm) high columns, under monotonic axial compression. Columns were cast vertically. In all the specimens the core dimension (centre to centre of the perimeter tie) was 10.5 in. (267 mm) square. Specimens with four different tie configurations were tested (see inset of Fig. 1). Some of the details of the specimens are given in Table I. The test program was carried out such that the effects of the primary variables can be evaluated by comparing the columns with only one factor as the primary variable, e.g. columns 2C5-17 and 2C6-18 have the same amount of longitudinal steel and almost equal amount of lateral steel contents. The primary variable between the two columns is the spacing of the sets of ties.

VARIABLES

Following is a brief summary of the variables examined during this investigation:

1. Distribution of Column Steel Around Perimeter. If the longitudinal bars are well distributed around the core perimeter which also determines the tie configuration, the efficiency of the confinement mechanism should improve. To investigate the significance of this effect, columns with 8, 12 or 16 uniformly distributed longitudinal bars were studied. The resulting sections and tie configurations are shown in Figure 1.

2. Amount of Lateral Reinforcement. Higher transverse steel contents mean a higher confining pressure capability. The effect of this variable is examined by varying the volumetric ratio of tie steel (ρ_s). Values used in the tests were approximately 0.8, 1.6 or 2.4% of the volume of the core concrete.

3. Tie Spacing. The ratio of the tie spacing to the dimensions of the confined core is an important parameter in determining the column behaviour. A number of pairs of columns have been tested with tie spacing as a variable while keeping the volumetric ratio of transverse steel constant.

4. Amount of Longitudinal Reinforcement. The ratio of the area of longitudinal reinforcement to the gross section area was varied between 0.017 and 0.037. This variable was investigated by comparing columns with otherwise identical characteristics.

RESULTS

The results are presented in the form of curves of concrete contribution vs. average longitudinal strain in the column test region. The concrete contribution obtained from the tests is non-dimensionalized with respect to the theoretical total force in concrete (P_{oc}) in the initial stages of loading when the concrete cover is still effective in carrying the load. After the cover is completely spalled off, the experimental concrete force is non-dimensionalized with respect to the theoretical core concrete force (P_{occ}). Between the onset and the completion of the cover spalling, a transition curve joins the initial and final parts of the relation. The detailed procedure to determine the complete relationship is explained

elsewhere (Sheikh and Uzumeri, 1978).

The effects of some of the variables are shown in Figures 1 to 3, which show the relations between the force in concrete and the average column strain.

ANALYTICAL WORK

The analytical models proposed by various researchers were used to predict the results of the experimental program reported here. It was observed that none of the available equations satisfactorily predicted the behaviour of concrete confined by rectangular ties (Sheikh, 1978). Despite the fact that numerous parameters have been studied by different researchers, none of the models takes the distribution of the longitudinal steel and the resulting tie configuration into account.

A model was developed to include all significant variables affecting the confinement. The relationship shown in Figure 4 is suggested to represent the behaviour of concrete in the core. The increase in the strength of confined concrete is calculated on the basis of the 'effectively confined' concrete area. This reduced area is a function of the tie configuration and tie spacing. It increases with the increase in the number of longitudinal bars supported by a bend of a tie and with the reduced spacing. Due to lack of space the development of the model can not be presented here but the final equations for square column and core sections are given below. The constants were determined empirically from a regression analysis using the experimental data obtained during this investigation.

$$K_s = 1.0 + \frac{b^2}{140\ P_{occ}} \left\{\left(1 - \frac{\eta\ c^2}{5.5b^2}\right)\left(1 - \frac{0.5s}{b}\right)^2\right\} \sqrt{\rho_s f'_s} \qquad (1)$$

$$\varepsilon_{s1} = 80\ K_s\ f'_c\ \times\ 10^{-6} \qquad (2)$$

$$\frac{\varepsilon_{s2}}{\varepsilon_{oo}} = 1.0 + \frac{248}{c}\left(1 - 5.0(s/b)^2\right) \frac{\rho_s f'_s}{\sqrt{f'_c}} \qquad (3)$$

$$\varepsilon_{s85} = \varepsilon_{s2} + .225\ \rho_s \sqrt{b/s} \qquad (4)$$

where P_{occ} is in kN; f'_c and f'_s in MPa and linear dimensions are in mm.

In Figure 5, the ratios of the strength of confined concrete to the strength of unconfined concrete obtained from the tests and calculated from the analytical model are compared. Figure 6 compares the experimental stress-strain curve of concrete for column 4B6-21 with the analytical curve obtained by using the above equations.

CONCLUSIONS

The following conclusions can be drawn from the experimental and analytical research reported here.

1. Concrete when confined with rectangular ties and longitudinal steel exhibits a very significant gain in strength (up to 70% in the tests

reported) as well as increased ductility.

2. The area of the effectively confined concrete is less than the nominal core area bounded by the centre line of the exterior tie and is determined by tie configuration and its spacing.

3. A closely knit cage both in the longitudinal and the lateral direction increases the efficiency of confinement.

   Well distributed longitudinal steel around the core perimeter - and the resulting tie configurations - enchances the strength and ductility of the confined core. Reduced tie spacing results in higher concrete strength and ductility despite the fact that the stiffness of the tie steel is reduced by reducing the tie diameter to maintain the same volumetric ratio.

4. The amount of lateral reinforcement has a very significant effect on the behaviour of the confined core. However, the change in the lateral steel contents results in less than proportional change in the strength and ductility of the confined concrete. A similar conclusion can be drawn for the effect of changing the strength of the lateral steel.

5. Within the range used in the tests, the amount of longitudinal reinforcement appears to have little effect on the behaviour of the confined concrete.

ACKNOWLEDGEMENTS

Research reported is supported by a National Research Council of Canada Grant (NRC A4273). Experimental work was conducted in the Structures Laboratory of the Department of Civil Engineering of the University of Toronto.

REFERENCES

Sheikh, Shamim A., "Effectiveness of Rectangular Ties as Confinement Steel in Reinforced Concrete Columns", Ph.D. Thesis, Department of Civil Engineering, University of Toronto, Toronto, Canada, June, 1978, 256 pp.

Sheikh, Shamim A., and Uzumeri, S.M., "Concrete Confinement by Rectangular Ties", Proceedings of the 6th European Conference on Earthquake Engineering, Sept. 18-22, 1978, Dubrovnik, Yugoslavia, 8 pp.

TABLE I

AXIALLY LOADED SHORT COLUMNS

305 x 305 x 1956 mm; Core: 267 x 267 mm (to $\mathcal{C}_L$ of hoop)

SPECIMEN	COLUMN STEEL					LATERAL STEEL			CONC.	COMPUTED			EXPERIMENTAL			$\frac{P_{cmax}}{P_{occ}}$
	No. & Size	A_s (mm^2)	f_y (MPa)	ρ (%) Gross	ρ (%) Core	d_h (mm)	s (mm)	ρ_s (%)	f'_c (MPa)	P_o (kN)	P_{oc} (kN)	P_{occ} (kN)	P_{test} (kN)	P_{cmax} (kN)	ε_{pmax}	
2A1 - 1	8 #5	1600	367	1.72	2.25	4.76	57.1	0.80	37.5	3498	2910	2216	3416	2829	0.0036	1.28
2A1H- 2	8 #5	1600	367	1.72	2.25	4.76	57.1	0.80	37.0	3461	2873	2188	3358	2771	0.0048	1.27
4C1 - 3	16 #5	3200	367	3.44	4.50	3.17	50.8	0.76	36.4	3951	2775	2101	3780	2606	0.0033	1.24
4C1H- 4	16 #5	3200	367	3.44	4.50	3.17	50.8	0.76	36.7	3972	2796	2117	2825	2647	0.0026	1.25
4C6 - 5	16 #5	3200	367	3.44	4.50	4.76	38.1	2.27	35.0	3841	2665	2018	4706	3313	0.0170+	1.64
4C6H- 6	16 #5	3200	367	3.44	4.50	4.76	38.1	2.27	34.3	3793	2618	1982	4225	3047	0.0093	1.54
4A3 - 7	8 #7	3097	386	3.33	4.35	7.94	76.2	1.66	40.9	4316	3121	2364	4270	3078	0.0044	1.30
4A4 - 8	8 #7	3097	386	3.33	4.35	4.76	28.7	1.59	40.8	4311	3115	2360	4412	3220	0.0057	1.37
4A5 - 9	8 #7	3097	386	3.33	4.35	9.52	76.2	2.39	40.5	4290	3094	2344	4096	2904	0.0050	1.24
4A6 - 10	8 #7	3097	386	3.33	4.35	6.35	35.1	2.32	40.7	4300	3105	2352	4336	3123	0.0103	1.33
4C3 - 11	16 #5	3200	403	3.44	4.50	6.35	95.2	1.62	40.7	4390	3101	2348	4261	2971	0.0051	1.27
4C4 - 12	16 #5	3200	403	3.44	4.50	3.17	25.4	1.52	40.8	4400	3112	2356	4915	3434	0.0205	1.46
4A1 - 13	8 #7	3097	438	3.33	4.35	4.76	57.1	0.80	31.3	3745	2389	1810	3789	2428	0.0045	1.34
2A5 - 14	8 #5	1600	400	1.72	2.25	9.52	76.2	2.39	31.5	3085	2445	1862	3224	2571	0.0110	1.38
2A6 - 15	8 #5	1600	400	1.72	2.25	6.35	35.1	2.32	31.7	3101	2461	1874	3469	2766	0.0215	1.48
2C1 - 16	16 #4	2065	407	2.22	2.90	3.17	50.8	0.76	32.5	3352	2512	1910	3465	2624	0.0056	1.37
2C5 - 17	16 #4	2065	407	2.22	2.90	7.94	101.6	2.37	32.9	3379	2539	1930	3522	2637	0.0157	1.37
2C6 - 18	16 #4	2065	407	2.22	2.90	4.76	38.1	2.27	33.1	3395	2555	1942	4465	3309	0.0280	1.71
4B3 - 19	12 #6	3406	392	3.67	4.79	7.94	101.6	1.80	33.4	3878	2543	1924	4092	2757	0.0061	1.43
4B4 - 20	12 #6	3406	392	3.67	4.79	4.76	38.1	1.70	34.7	3973	2638	1996	4368	3034	0.0080	1.52
4B6 - 21	12 #6	3406	392	3.67	4.79	6.35	47.6	2.40	35.5	4036	2701	2043	4617	3140	0.0144	1.54
4D3 - 22	12 #6	3406	392	3.67	4.79	7.94	82.5	1.60	35.5	4036	2701	2043	4301	2966	0.0041	1.45
4D4 - 23	12 #6	3406	392	3.67	4.79	4.76	28.6	1.70	35.9	4062	2727	2063	4514	3180	0.0076	1.54
4D6 - 24	12 #6	3406	392	3.67	4.79	6.35	38.1	2.30	35.9	4062	2727	2063	4723	3362	0.0177	1.63

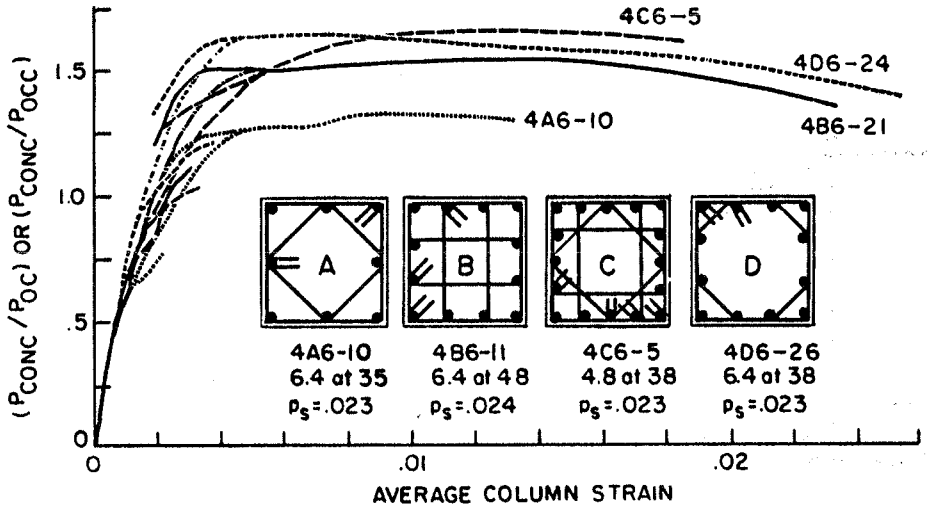

Fig. 1: Effect of tie configuration

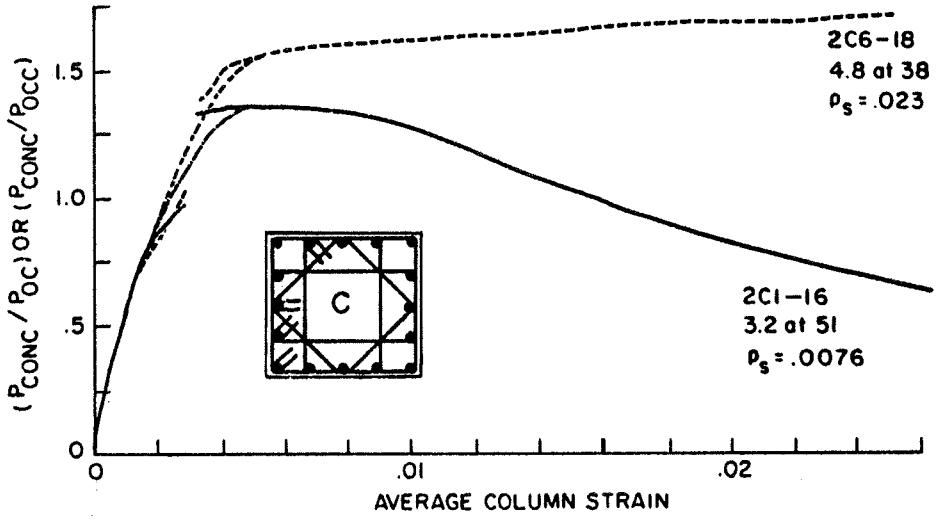

Fig. 2: Effect of amount of lateral reinforcement

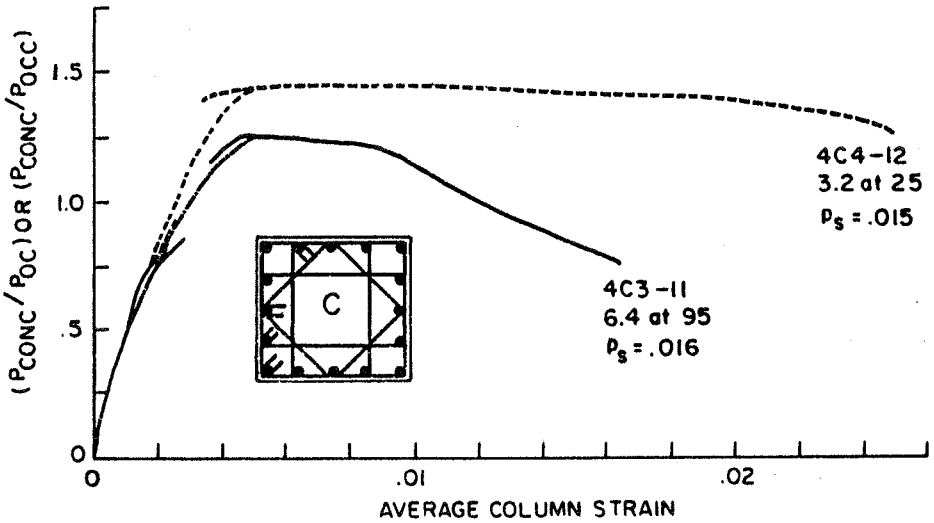

Fig. 3 Effect of tie spacing

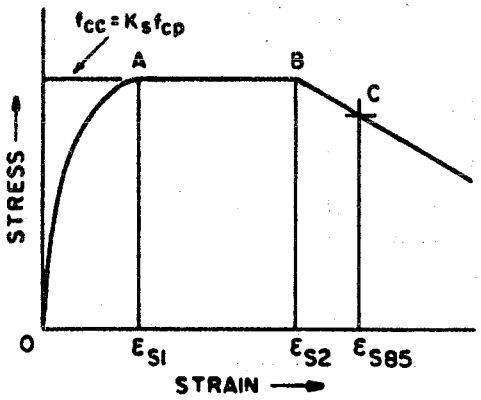

Fig. 4 : Proposed general stress-strain curve of concrete

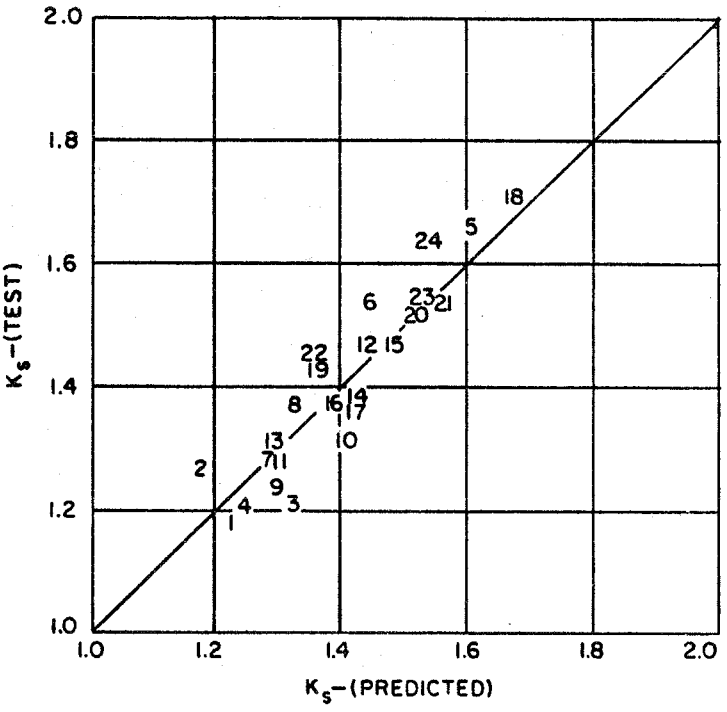

Fig. 5 : Comparison of experimental K_s values with the K_s values predicted by the proposed model

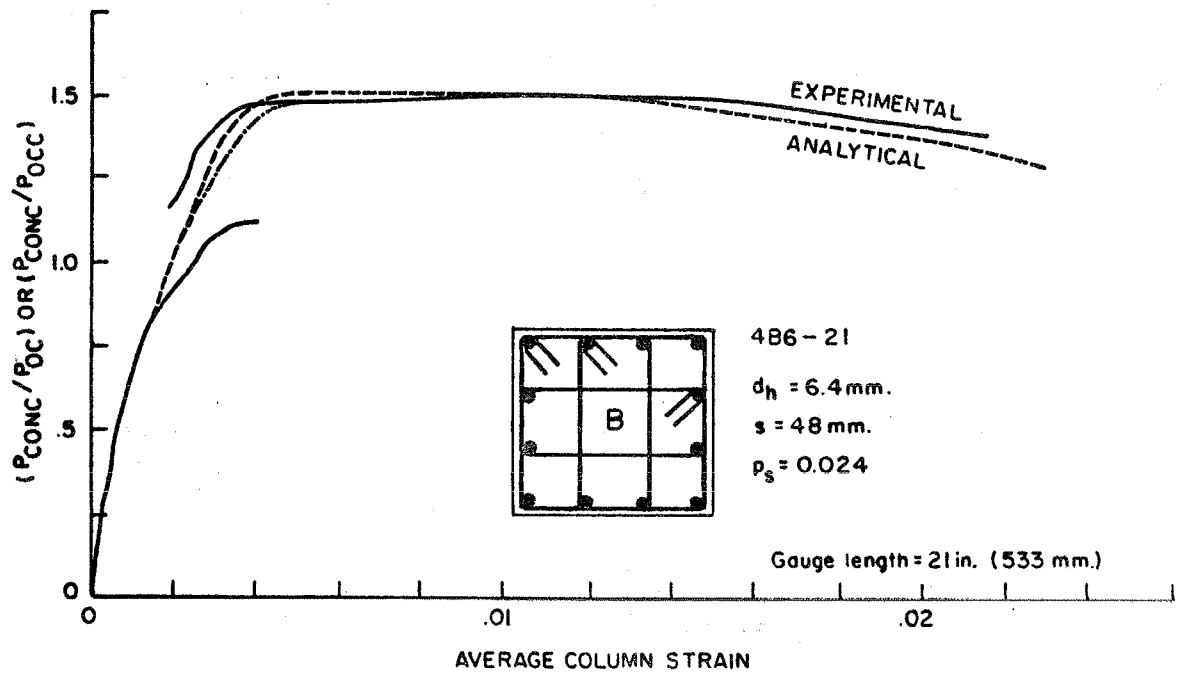

Fig. 6 . Comparison of experimental and analytical stress-strain curves

RELIABILITY IN THE CONCRETE-STEEL BOND STRENGTH UNDER REPEATED ACTIONS

Mario COLLEPARDI
Department of Material Science
University of Ancona
Ancona, Italy

Mario CORRADI
Research and Development Laboratorie
Mac Mediterranea Additivi Cemento
Treviso, Italy

Michele VALENTE
Research and Development Laboratories
Mac Mediterranea Additivi Cemento
Treviso, Italy

Abstract - The influence of the vibration time of fresh concrete on the compressive strength and the steel-concrete bond strength under repeated actions was investigated. Stiff no-slump mixes and rheoplastic concretes, with and without superplasticizers respectively,and with the same w/c ratio, were examined. Both ordinary and lightweight aggregates were used. The performances of the no-slump concretes are strongly dependent on the compaction time of fresh mixes, whereas rheoplastic concrete present a bond strength which is substantially independent of the compaction time. When concretes are not fully compacted, the difference in the steel-concrete bond strength between rheoplastic mixes and no-slump ones is much higher than that in the compressive strength of concrete. Lightweight concretes with a specific gravity of about 1600 Kg/m^3 show only a slightly lower bond strength than that of ordinary weight concretes because of the lower w/c ratio used.

Resumé - On a etudié l'influence du temps de vibration du béton frais sur la résistance à la compréssion et sur l'adherence du béton à l'acier sous charges répetées. On a examiné des bétons peu ouvrables sans affaissement au cône de Abrams et des bétons rhéoplastiques respectivement sans et avec des adjuvants superplastifiants et avec le même rapport e/c. On a utilisé les aggrégats normals ou légers. Les résultats obtenus avec le béton sans affaissement dépendent énormément du temps de vibration, tandis que l'adhérence des betons rhéoplastiques à l'acier est pratiquement indépendent du temps de vibration. La différence dans l'adhérence à l'acier entre le béton sans affaissement et rhéoplastique, tous les deux sans ou avec peu de vibration, est plus grande que la différence dans la résistance à la compréssion. Les bétons légers, avec un poid specifique de 1600 Kg/m^3, ont une adhérence à l'acier qui est seulement un peu plus basse que celle des bétons normals, et ceci peut-être attribué au bas rapport e/c.

INTRODUCTION

Concrete-steel bond strength depends on the composition of the concrete, particularly on the water/cement (w/c) ratio of the mix, and the type of aggregates. A lower w/c ratio increases the adhesion between cement paste and steel, whilst a more rigid aggregate favors the bond resistance due to the grip.

However, too stiff mixes with relatively low w/c ratios could cause a lower bond strength due to the incomplete compaction of the fresh concrete and then to the lower contact area between steel and concrete. This aspect is particularly important for the high-density reinforcement used in concrete structures in seismic regions. On the other hand, lightweight concretes, which would be very interesting for structures in seismic regions because of the lower elastic modulus and specific gravity, could cause also a decrease in the concrete-steel bond strength for the lower rigidness of the aggregates.

EXPERIMENTAL

Stiff and flowing concretes, both containing ordinary weight aggregates, were prepared. An improved superplasticizer NSF polymer based (Rheomac)was used in order to transform the stiff control mix into a rheoplastic (flowing and unsegregable) concrete (I-4) with the same w/c ratio (Table I).

Table I - Composition (Kg/m^3) of concretes

Composition	No-slump concrete	Rheoplastic concrete	No-slump concrete	Rheoplastic concrete
	ordinary weight		lightweight	
Type I Cement	355	358	350	347
Sand	990	995	493	638
Gravel (5-19 mm)	990	995	-	-
water	174	172	140	140
w/c	0,49	0,48	0,40	0,40
Expanded clay (1-3 mm)	-	-	380	194
Expanded clay (3-8 mm)	-	-	250	291
Rheomac	-	5,9	-	-
Tiamac	-	-	-	5,9
slump	15 mm	210 mm	10 mm	230 mm
air (% by volume)	1,2	1,3	1,5	7
specific gravity	2509	2520	1613	1619

The stiff control mix was a no-slump concrete (5) with a slump of 15 mm, whereas the rheoplastic concrete was a selflevelling mix with a slump of 210 mm. Both the mixes appeared unsegregable with a bleeding capacity lower than 0,003.

From the same batch of fresh concrete several specimens were compacted in cubic moulds (100 mm) for different periods of time (0-5-15-40 sec) on a rigid vibrating table. A frequency of 6000 vibrations per min and an amplitude of 0,15 mm were used. For each period of vibration, concrete compressive strength and steel-concrete bond strength under repeated actions were measured after a curing of 28 days at 20°C with a R.H. of 95%.

For the steel-concrete bond strength measurements, plain or deformed bars (diameter=10 mm) were used and the same specimens recommended by RILEM-CEB-FIP pull-out test (Fig.1) were utilized. A repeated tensile stress varying from a minimun of 6.5 N/mm^2 and a maximum of 58.5 N/mm^2 was applied to the bar for 300 cycles with a frequency of 3 Hertz. By taking into account the contact area between steel and concrete this resulted in a bond stress varying from a minimun of 0.32 N/m^2 to a maximum of 2.92 N/mm^2. If the bar was not pulled-out the maximum bond stress was increased by 1.3 N/mm^2 for other 300 cycles, while the minimum was mantained at the same level of 0.32 N/mm^2. Further increases by 1.3 N/mm^2 in the maximum bond stress for every 300 cycles were made till to pull-out the bar.

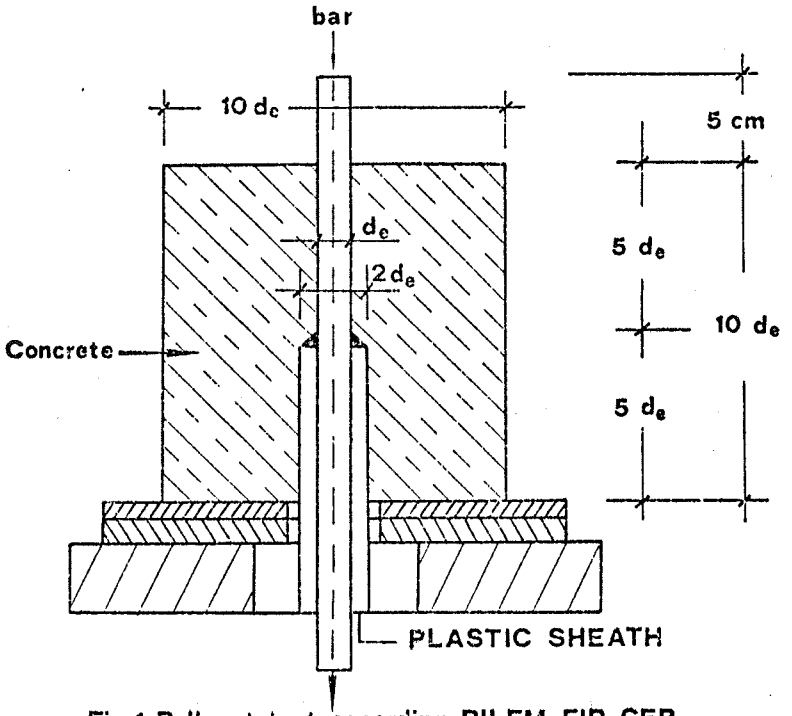

Fig.1 Pull-out test according RILEM-FIP-CEB

Similar tests were carried out on stiff and superplasticized rheoplastic concretes both prepared with lightweight aggregates and by using the same w/c ratio (Table I). A modified superplasticizer NSF polymer based (Tiamac) was used.

RESULTS AND DISCUSSION

In Fig.2 the influence of vibration time of fresh mixes on the compressive strength of hardened concretes is shown. these data confirm (2-4)that,

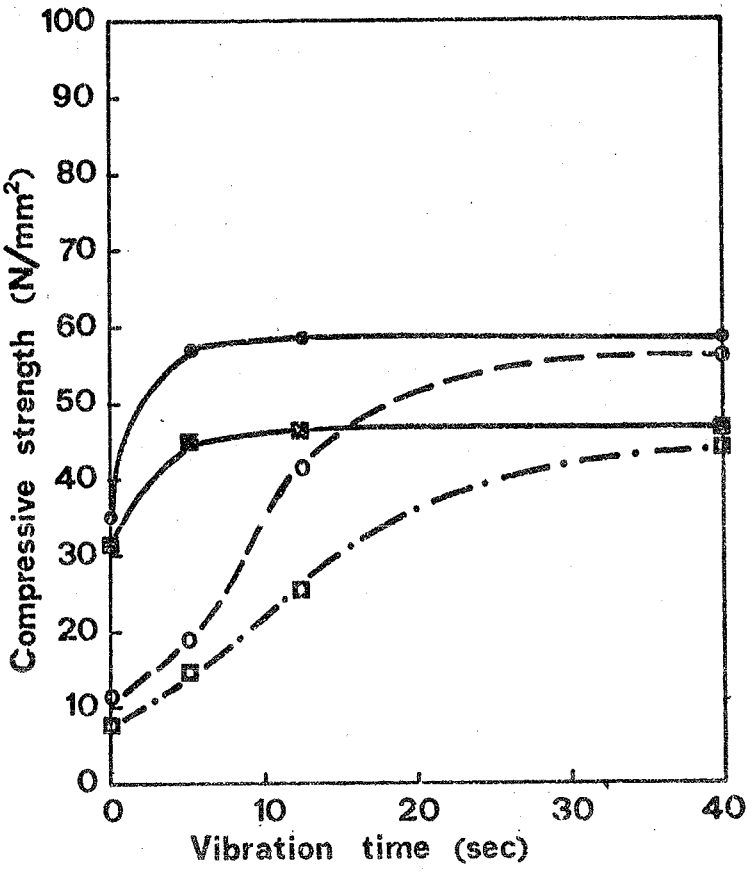

Fig.2 - Compressive strength as a function of the vibration time of fresh concrete.

- o ordinary weight no-slump concrete
- ▫ lightweight no-slump concrete
- • ordinary weight rheoplastic concrete
- ▪ lightweight rheoplastic concrete

for both ordinary and lightweight no-slump concretes, the compressive strength is strongly dependent on the way fresh mixes are compacted. Therefore, the compressive strength of the well compacted specimens prepared for laboratory tests is generally higher than those of the concretes placed into the elements, the difference beeing higher for stiffer mixes and congestioned structures. In the experimental conditions of the present work the highest compressive strength is attained with 40 sec of vibration for no-slump mixes, whereas only 5 sec are required for rheoplastic concretes. A lower vibration time, or possibly no vibration at all, could be required to fully compact when a still more flowable concretes is used, however segre-

gation must be accurately avoided for such a fluid concrete.

In Fig.3-6 the steel-concrete bond strength and the number of repeated cycles to pull-out the bar are shown

The influence of the vibration time on the bond strength between steel and ordinary weight no-slump concrete (Fig.3-4) is approximately the same as that on the compressive strength (Fig.2). For unvibrated ordinary weight

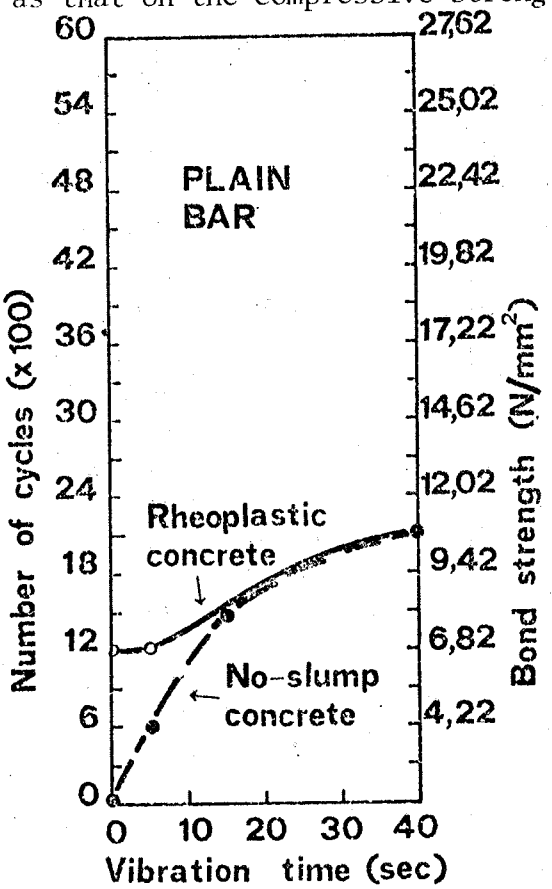

Fig.3 - Number of cycles and bond as a function of the vibration time of ordinary weight fresh concretes (plain bar).

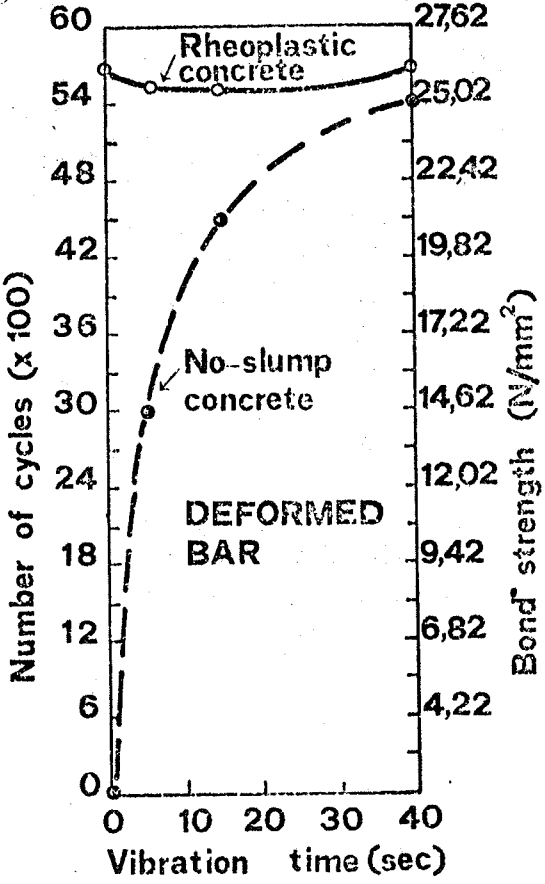

Fig.4 - Number of cycles and bond strength as a function of vibration time of ordinary weight fresh (deformed bar).

no-slump concrete, both plain (Fig.3) and deformed bar (Fig.4) are pulled-out on applying a bond stress much lower than 2.92 N/mm^2 during the first cycle. By increasing the vibration time from 0 to 40 sec, the bond strength and the number of cycles are increased till to attain the values of 10.72 N/mm^2 and 2100 cycles respectivelly when the plain bar is used, and the values of 25.02 N/mm^2 and 5400 cycles for the deformed bar. This means that stiff mixes, prepared with a relatively low w/c ratio, are not reliable not only in the compressive strength but also in the concrete-steel bond strength, and this is particularly important when a high-density reinforcement is used as in the concrete structures in seismic regions.

A similar trend is recorded for lightweight no-slump concretes with both

plain (Fig.5) and deformed bar (Fig.6). The bond strength and the number

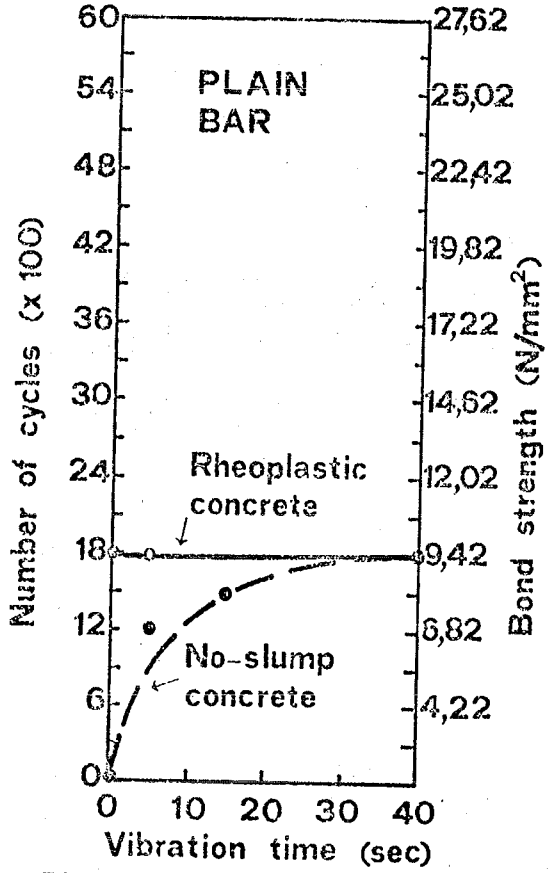

Fig.5 - Number of cycles and strength as a function of the vibration time of lightweight fresh concretes (plain bar).

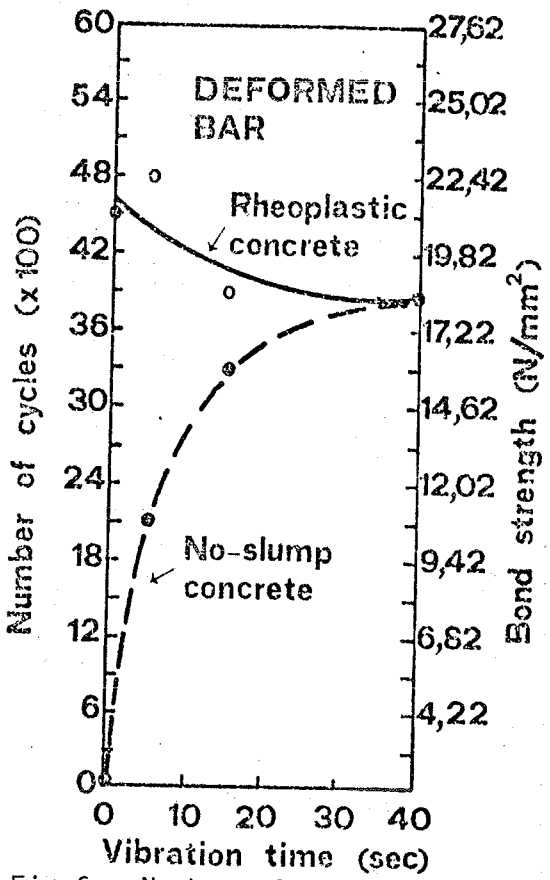

Fig.6 - Number of cycles and bond strength as a function of the vibration time of lightweigth fresh concretes (deformed bar).

of cycles to pull-out the bar in lightweight concrete is not much lower than the corresponding values for ordinary no-slump concrete. Possibily, the lower w/c ratio of lightweight mix (Table I) partially counterbalance the lower rigidness of expanded clay, so that the bond strength between still and ordinary or lightweight concrete are of the same order of magnifitude for the mixes examined in the present work.

Vibration of fresh rheoplastic mixes appears to affect the bond strength (Fig.3-6) to a still lower extent than the compressive strength (Fig.2). This indicates that rheoplastic mixes are much more reliable in the concrete-steel bond strength than the corresponding no-slump concretes with the same w/c ratio. However slightly different behaviour are found depending on the type of bar and the specific gravity of concrete. For example, by increasing the compaction time of the fresh mix, a certain increase in the bond strength is observed when ordinary weight rheoplastic concrete is reinforced plain bar (Fig.3), whereas the same concrete reinforced by a deformed bar seems to be about independent of the vibration time of the fresh mix (Fig.4). When a lightweight rheoplastic concrete is

reinforced by a plain bar, the bond strength does not change with the compaction time (Fig.5), whereas for the same concrete reinforced by a deformed bar the bond strength appears to be slightly reduced by a prolonged compaction time of the fresh mix. At the moment it seems to be very difficult to find a theoretical explanation for these different behaviours. Possibly, there are some factors that counterbalance the positive effect of the compaction on the bond strength when rheoplastic concrete are used. These factors could be emphasized when lightweight aggregates instead of ordinary weight aggregates are used or when a deformed bar replaces a plain one. However, from a practical point of view both ordinary and lightweight rheoplastic concretes present a higher bond strength under repeated actions than the corresponding no-slump concrete with the same w/c ratio. The difference is higher for shorter compaction times and is canceled only for fully compacted mixes.

CONCLUSIONS

Concretes prepared with a relatively low w/c ratio show very high bond strength under repeated actions. However, the performances of reinforced stiff mixes such as no-slump concretes are strongly dependant on the compaction time of fresh mixes, whereas rheoplastic concretes containing NSF polymer based superplasticizers show a bond strength which is substantially independent of the vibration time of fresh mixes.

The difference in the bond strength between uncompacted rheoplastic mixes and no-slump concretes is much higher than that in the compressive strength.

Lightweight concretes with a specific gravity of about 1600 Kg/m^3 show only a slightly lower bond strength than that of ordinary weight concretes when the w/c ratio is very low (0,40) as in the case of the present work.

ACKNOWLEDGEMENT

The authors are very grateful to Mr. Maniscalco, Mr. Alverà and the Laboratory of Civil Engineering Department of Florence University for their contribution to the experimental work.

REFERENCES

1) Mario Collepardi, "Assessment of the Rheoplasticity of Concretes", Cement and Concrete Research, 6, 401-408, (1976).

2) Mario Collepardi and Mario Corradi, "High-Strength an Reliable Concretes", Intern. Conference on "Cement and Concrete Admixtures and Improving Additives", publication pending on Silicates Industriels.

3) Mario Collepardi and Mario Corradi, "Influence of Naphtalene-Sulphonated Polymer Based Superplasticizers on the Strength of Ordinary and Lightweight Concrete", Proceedings of the International Symposium "Superplasticizers in Concrete", Vol.II, 451-480, Ottawa, May, (1978).

4) Mario Collepardi, Mario Corradi and Michele Valente, "Low Slump Loss Superplasticized Concrete", Transportation Research Board Symposium, Washington D.C., January, (1979).

BOND AND SPLICES IN REINFORCED CONCRETE FOR SEISMIC LOADING

Peter GERGELY
Cornell University
Ithaca, NY, USA

Fernando FAGUNDO
University of Puerto Rico
Mayaguez, Puerto Rico

Richard N. WHITE
Cornell University
Ithaca, NY, USA

SUMMARY

A series of half-scale and full-scale beams with third-point loading was tested to study the effects of repeated loading on lapped splices. Stirrups at the ends of the splices were found to be effective and highly strained. The distribution of stirrups appears to have little effect on the stress distribution in the main bars but considerable effect on splice strength.

RESUME

Des poutres en vraie grandeur, et à l'échelle un demi, ont été testées avec deux charges concentrées symétriques, pour déterminer l'effet de chargements répétés sur les recouvrements d'armatures. On a constaté la forte déformation des étriers aux extrémités des recouvrements, et leur efficacité. Il apparaît que la répartition des armatures transversales a peu d'effet sur la distribution des constraintes dans les armatures principales, mais modifie grandement la résistance du recouvrement.

INTRODUCTION

It has been stated by researchers and designers that bond and splice deterioration of reinforcing bars is one of the weakest links in earthquake-resistant design (Bertero and Vallenas [1977]). High-level reversed loading places severe demands on the strength and ductility of the anchorage and splice regions in concrete structures. Significant deformations (slip) may develop during cyclic loading but sudden failure is also a possibility.

Limited (and mostly indirect) evidence shows bond deterioration in a variety of conditions in reinforced concrete structures. Bond slip can account for as much as 30% of the total deformation at the column face of a beam-column joint if reversing yielding develops (Takeda, Sozen, and Nielsen [1970]). Significant stiffness reduction due to bond deterioration was also found by Bresler and Bertero [1968]. Yielding of anchored bars can penetrate to a considerable distance into an anchorage block at the end of a beam, especially if the load is reversed (Ismail and Jirsa [1972]).

Only a few investigations have applied repeated loading to splices; for example Rehm and Eligehausen [1979] and Tepfers [1973]. Repeated loading has little effect on bond strength as long as the level of force is less than about 60% of monotonic load capacity, but this information is of little use in earthquake-resistant design. The effects of repeated loading on bond are similar to that on plain concrete. If the loading exceeds about 80% of the monotonic capacity, subsequent strength is reduced.

Tests by Perry and Jundi [1969] show that for repeated loads bond damage seemed to stabilize after several hundred cycles and that no failure should be expected unless the applied load is at least 80% of the monotonic ultimate load.

Tests on anchored bars by Hassan and Hawkins [1977] show the detrimental effect of reversed cyclic loads on bond deterioration. They show that the loading history has a significant effect on the rate of bond deterioration and mode of failure. Contrary to the case of monotonic loading, they also show that the surface geometry of the reinforcement has a marked effect on the rate of bond deterioration.

It seems that the most significant effect of high-level repeated loads is to reduce the bond at failure while reversed cyclic stresses tend to deteriorate bond at a higher rate and to precipitate failure even at a smaller number of cycles or at lower loads.

Recent work has established the influence of concrete cover, bar spacing, and transverse reinforcement on static bond and splice strength (Orangun, Jirsa, and Breen [1977]). However, very little is known about the effects of reversed cyclic loading on bond strength and even less about the behavior of splices for such loading.

The fact that little work has been done on high-level reversed loading of splices is reflected in the fact that seismic codes vary in their splice requirements. Following an early study by Mublenbruch [1945], some codes specify a splice length that is much greater than that required for static loading. Also, the required stirrup spacing is small (a quarter of the depth). Recent evidence and understanding seems to indicate that this requirement might be too conservative; there is an amount of trasverse reinforcement above which further benefit cannot be obtained. Stirrups near the ends of a splice are much more effective than those toward the center.

It is obvious that information is needed on the earthquake-resistant design of lapped splices. The main questions to be answered are: (a) what is the required stirrup transverse reinforcement to assure sufficient strength and ductility for high-level reversed cyclic loading? (b) what is the stiffness degradation?

It is well known that two types of splice or bond failures can occur: direct pullout of the bar if ample confinement is provided, or splitting along the bar if the confinement is insufficient. However, small internal cracks initiate at bar deformations at relatively low loads (Lutz and Gergely [1968]). The small inclined cracks at the bars extend in both directions for reversed loading and this can lead to significant deterioration of the concrete around the splice, especially for large-diameter bars. Thus the overall effects of reversed cyclic loading on bond and splice behavior are probably not related closely to tensile strength of concrete, as is the case for monotonic loading.

PURPOSE OF INVESTIGATION

A study was initiated at Cornell University during the summer of 1978 to study the behavior and design of lapped splices, with the sponsorship of the National Science Foundation. The objectives of the investigation are to evaluate the effects of transverse reinforcement, splice length, bar spacing, bar size, and loading history on the behavior of lapped splices. The primary aim is the comparison of cyclic response with behavior for monotonic loading which is now quite well established. The first phase of the work has concentrated on beam splices but subsequent

research will include columns with square cross sections and symmetrical spliced reinforcement.

TYPES OF TESTS

A series of reduced scale beams (Series H) were tested during the summer of 1978 before the formal beginning of the sponsored project. Eight beams of about one-half scale were tested. The loading and cross section are shown in Fig. 1 and the properties are summarized in Table 1.

Series H tests were undertaken to assess the influence of stirrups, repeated-reversed loading, and cover on the behavior of splices. The results of these preliminary tests were used in planning the full-scale test series.

The beams were 6 ft (1.83 m) long with a cross section of 6 in. by 10 in. (152 mm by 254 mm). Reinforcement consisted of two #4 bars (13 mm diameter) with an actual yield strength of 61.2 ksi (422 MPa) and the stirrup size was #3 (9.5 mm) with actual yield strength of 58 ksi (400 MPa). The concrete cylinder strength was 4.0 ksi (27.5 MPa) except for beams H3M and H4R it was 2.9 ksi (20 MPa). The bottom bars were spliced using a splice length of 14 in. (355 mm) and the top reinforcement consisted of two #4 (13 mm) continuous bars.

Current and future phases of the investigation utilize full size specimens (Series F), reinforced with large deformed bars. Four Series F beams have been tested to date and tentative results and conclusions are summarized in this paper. The beams were 23 ft (7.0 m) long with a 12 in. by 20 in. (305 mm by 508 mm) cross section. The longitudinal reinforcement consisted of two #10 (32 mm diameter) bars with a yield strength of 67.0 ksi (460 MPa). The stirrup size was #3 (9.5 mm) with yield strength of 76.4 ksi (527 MPa). The concrete strength was 3.5 ksi (24 MPa) except for beam F1M it was 3.1 ksi (21 MPa). Two #5 (16 mm) continuous top bars were used.

The splice length was designed by a method currently being developed by the Bond and Development of Reinforcement Committee of the American Concrete Institute; the approach is based on the work of Orangun, Jirsa, and Breen [1977]. The splice length was 14 in (356 mm) for Series H and 46 in. (1170 mm) for Series F.

All beams in both test series were loaded with two equal loads at approximately the third points of the span (Fig. 1). The splices were located in the center constant-moment region. Measurements included deflections, loads, selected crack widths, and strains in the spliced bars and in some of the stirrups.

TEST RESULTS

The type of loading in each of the specimens is given in the beam designations: M = monotonic, R = repeated, and S = reversing (see Table 1).

Series H

The effect of stirrups is indicated by the fact that beam H1M of Series H (without stirrups) failed at 88% of the flexural strength of the beam, whereas H5M (with stirrups at 150 mm) reached about three times the yield deflection and failed in flexure by concrete crushing.

The effect of repeated loading is revealed by a comparison of beams H5M and H6R. Beam H6R was cycled at 78% of the monotonic strength of an identical beam (H5M). During about 12 cycles the deflections increased by a total of 13% and additional 6 cycles did not cause appreciable increase

in deformations. Then the load was cycled at 90% of the strength of beam H5M and the deflections increased continuously until splice failure occurred after 20 cycles at this load. The deflection at failure was 3.85 in. (98 mm); as a comparison, beam H5M deflected 2.7 in. (68 mm) at yielding and over 6 in. (150 mm) at flexural crushing.

Beam H7S was subjected to one fully reversed load cycle at equal load levels in both directions of 0.4, 0.5, 0.6, 0.7, 0.8, and 0.9 times the strength of beam H5M. The beam failed similarly to beam H6R, except it failed during the first cycle at the 0.9 relative load level, whereas beam H6R failed during the 20th cycle at the 0.9 load level.

Beam H8S was subjected to reversed cyclic loading to 0.8 times the strength of beam H5M in both directions. The deflections increased continuously with cycling until failure occurred during the 6th cycle.

Beam H4R had no stirrups and was loaded in one direction at 80% of the failure load of beam H3M. Deflections increased continuously with cycling and failure occurred in the 10th cycle.

The size of the concrete cover over the main bars affected the location of the splitting crack, as predicted for monotonic loading (Orangun, Jirsa, and Breen [1977]); splitting developed at the location of least cover. For equal side and bottom covers splitting develops at the bottom because of the bending of the spliced bars. Stirrups can reduce the bending of the free end of the bars and force the splitting failure to occur at the location of the smaller cover. This effect is especially important for large-diameter bars.

Series F

Beam F1M was loaded monotonically to failure, which occurred suddenly when longitudinal cracks developed at the bottom and the side of the beam. The deflection at failure was 1.65 in. (42 mm) and the steel stress was only 72% of the yield stress. Longitudinal cracks appeared on the bottom face at a deflection of 1 in. (25 mm), when the steel stress at the end of the splice was 33 ksi (227 MPa). This beam served as a reference for the other three beams that were tested under repeated loading. The estimated deflection at yield is about 1.9 in. (48 mm).

Beam F2R was subjected to 5 load cycles at load levels corresponding to 0.4 in., 0.8 in., 1.2 in., and 1.4 in. (10, 20, 30, and 36 mm) deflection. It failed during the 5th cycle at 1.4 in. (36 mm) displacement. The steel stress at failure was 68% of the yield. Failure was sudden and occurred when longitudinal cracks spread on the bottom and side faces of the beam.

Beam F3R contained #3 (9.5 mm) stirrups spaced at d/2 or 9 in. (229 mm) along the splice. Again, loading consisted of 5 cycles at 0.4 in. (10 mm) deflection increments. Deterioration, measured by increased deflection and strains during cycling, was insignificant to a deflection of 1.2 in. (30 mm). At the peak load during the first cycle at a deflection of 1.6 in. (41 mm) the stirrups at the end of the splice started to yield at the bottom of their vertical legs. Yielding also began in the horizontal legs of the end stirrups during the 5th cycle. The stress in the spliced bars was 50 ksi (345 MPa) at this stage. Beam F3R failed during the next load cycle at a steel stress of 59 ksi (407 MPa), which is 88% of yield.

Beam F4R had two stirrups at each end of the splice and one at the center. Thus about the same amount of transverse steel was provided as in beam F3R. The contribution of stirrups is measured by the quantity Af_y/sd_b, where in this case A is the area of one leg of a stirrup, f_y the yield

strength, s the spacing of stirrups, and d_b the diameter of the main bar (Orangun, Jirsa, and Breen [1977]). The value of this quantity was 577 for beam F3R and 473 for F4R.

The sequence of loading was identical to that for beams F2R and F3R. The behavior of the stirrups was markedly different for beam F4R than for the other beams. The two stirrups at the end of the splice did not yield until after the main steel began to yield. In fact, the stirrup stresses were less than 20 ksi (138 MPa) when the main bar started to yield. The beam failed at about the same deflection (1.92 in. or 49 mm) as beam F3R but the yield moment was reached. Failure occurred when small longitudinal cracks along the bar on the bottom face suddenly joined. The variation of stirrup stress in the stirrup at the end of the splice with the stress in the longitudinal bar is shown in Fig. 2. The curves show that two stirrups at the end of the splice shared the bursting forces well. The hysteresis curves have increasing enclosed areas as the number of cycles and the load increase, as can be seen in Fig. 3.

Fig. 4 shows the variation of stresses in the spliced bars at various load levels for beams F3R and F4R. The differences are not great until higher loads are reached; thus stirrups away from the ends of the splice are not effective.

CONCLUSIONS

A series of half-scale and full-scale beams were tested to study the behavior of lapped splices for repeated loads. The splice lengths were designed for monotonic loading by a new method which is based on the work of Orangun, Jirsa, and Breen [1977].

1. Stirrups concentrated near the ends of the splice are much more effective than stirrups away from the ends.
2. A beam with two stirrups near the end of the splice reached the yield deflection when considerable slip developed between the steel and the concrete. A similar beam with about the same amount of stirrups spaced at d/2 and only one stirrup at the end of the splice did not reach yield.
3. Repeated loading below about 80% of the monotonic strength has little effect on capacity and deformations.
4. Cycling at 90% of the monotonic strength caused failure.
5. Although the design of splices for static loading is insufficient for high-level cyclic loading, it seems that provisions of several codes require too long splices and too many stirrups.
6. Additional experiments are underway to establish design guidelines for splices in beams and columns in earthquake-resistant construction.

ACKNOWLEDGEMENTS

This research is sponsored by the National Science Foundation.

REFERENCES

Bertero, V.V., and Vallenas, J., "Confined Concrete: Research and Development Needs," Proceedings of a Workshop on Earthquake Resistant Reinforced Concrete Building Construction, Vol. II, Berkeley, 1978.

Bresler, B., and Bertero, V.V., "Behavior of Reinforced Concrete Under Repeated Loads," Jou. Structural Div. ASCE, Proc. V. 94, No. ST6, June 1968.

Hassan, F.M. and Hawkins, N.M., "Anchorage of Reinforcing Bars for Seismic Forces," Special Publication SP-53, American Concrete Institute, 1977.

Ismail, M.A.F., and Jirsa, J.O., "Behavior of Anchored Bars Under Low Cycle Overloads Producing Inelastic Strains," ACI Journal, Vol. 69, No. 7, July 1972.

Lutz, L.A., and Gergely, P., "Mechanics of Bond and Slip of Deformed Bars in Concrete," ACI Journal, Vol. 64, No. 11, November 1967.
Muhlenbruch, C.W., "The Effect of Repeated Loading on the Bond Strength of Concrete," American Society for Testing Materials, Proc. Vol. 45, 1945.
Orangun, C.O., Jirsa, J.O., and Breen, J.E., "A Reevaluation of Test Data on Development Length and Splices," ACI Journal, Vol. 74, No. 3, March 1977.
Perry, E.S., and Jundi, N., "Pullout Bond Stress Distribution Under Static and Dynamic Repeated Loading," ACI Journal, Vol. 66, No. 5, May 1969.
Rehm, G. and Eligehausen, R., "Bond of Ribbed Bars Under High-cycle Repeated Loads," ACI Journal, Vol. 76, No. 2, February 1979.
Takeda, T., Sozen, M.A., and Nielsen, N.N., "Reinforced Concrete Response to Simulated Earthquakes," Jou. Structural Division, ASCE, Proc. Vol. 96, No. ST12, December 1970.
Tepfer, R., "A Theory of Bond Applied to Overlapped Tensile Reinforcement Splices for Deformed Bars," Publication No. 73:2, Division of Concrete Structures, Chalmers University of Technology, Goteborg, 1973.

Beam	c_s in(mm)	c_b in(mm)	d in(mm)	$\frac{Af_y}{sd_b}$ ksi(MPa)	s in(mm)	u psi(MPa)	f_s ksi(MPa)
			H Series				
H1M	1.0(25)	1.0(25)	8.7(221)	-	-	480(3.3)	54(370)
H2R	1.0(25)	1.0(25)	8.7(221)	-	-	440(3.0)	50(340)
H3M	1.0(25)	1.5(38)	8.2(208)	-	-	470(3.2)	53(360)
H4R	1.0(25)	1.5(38)	8.2(208)	-	-	390(2.7)	44(300)
H5M	0.8(20)	1.1(28)	8.6(218)	1.5(10)	6(150)	560(3.8)	61(420)
H6R	0.8(20)	1.1(28)	8.6(218)	1.5(10)	6(150)	500(3.4)	56(380)
H7S	0.8(20)	1.1(28)	8.6(218)	1.5(10)	6(150)	500(3.4)	56(380)
H8S	0.8(20)	1.1(28)	8.6(218)	1.5(10)	6(150)	440(3.0)	48(330)
			F Series				
F1M	1.6(40)	1.9(48)	17.5(445)	.24(1.6)	22(560)	335(2.3)	48(330)
F2R	1.6(40)	1.9(48)	17.5(445)	.24(1.6)	22(560)	325(2.2)	46(320)
F3R	1.6(40)	1.9(48)	17.5(445)	.58(4.0)	9(230)	410(2.8)	59(405)
F4R	1.6(40)	1.9(48)	17.5(445)	.47(3.2)	22(560)	460(3.2)	67(460)

s = stirrup spacing, u = average bond stress at failure

Table 1. Properties of Beams

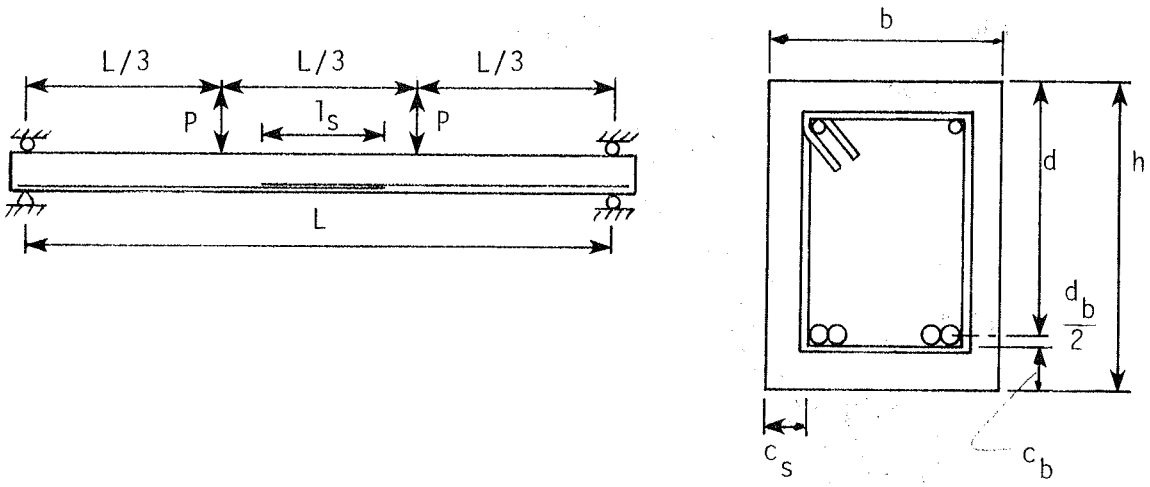

Fig. 1 Loading and Typical Cross Section

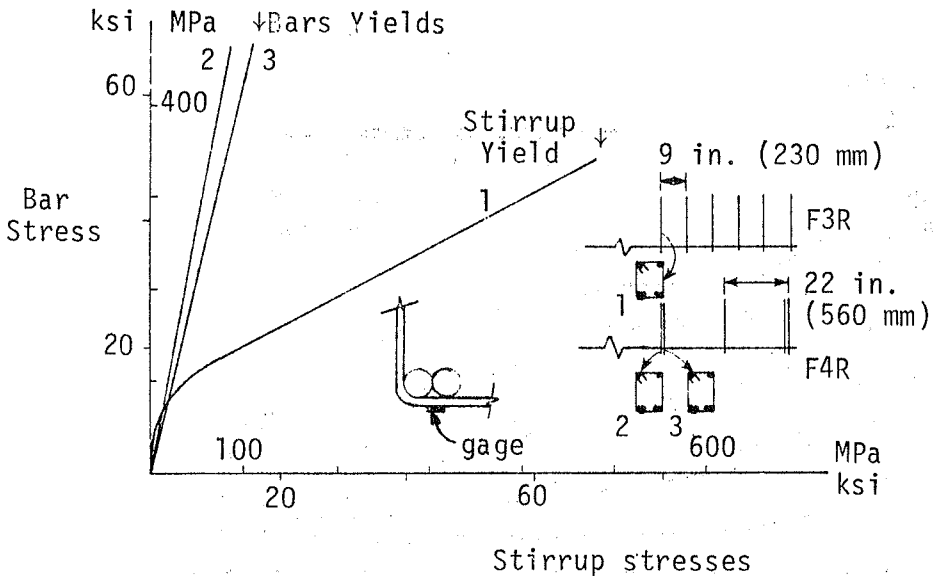

Fig. 2 Stirrups Stresses versus Stress in Longitudinal Bars.

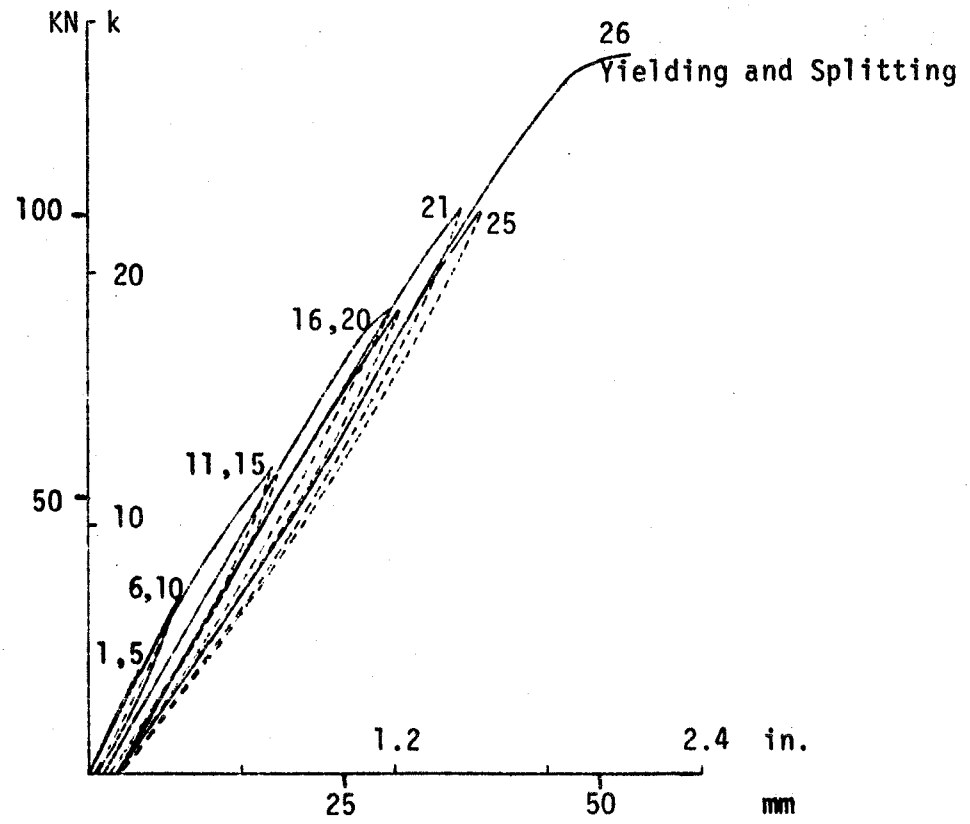

Fig. 3 Load-deflection Curve for Beam F4R

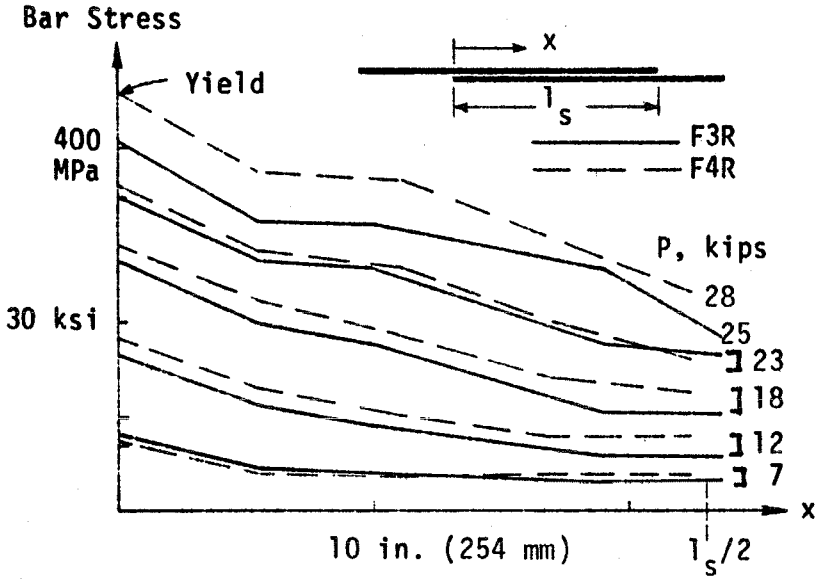

Fig. 4 Stresses Along Bar in Beams F3R and F4R.

SLIDING SHEAR AND DOWEL FORCES IN CRACKED REINFORCED CONCRETE SUBJECTED TO SEISMIC LOADING

Richard N.WHITE
Cornell University
Ithaca, NY, USA

Peter GERGELY
Cornell University
Ithaca, NY, USA

Rafael JIMENEZ
University of Puerto Rico
Mayaguez, Puerto Rico

SUMMARY

Relationships are given for interface shear transfer stiffness and dowel action stiffness of reinforced concrete specimens that are precracked and then loaded in cyclic shear across the crack. The effects of load cycling on stiffness degradation are included. Results are based on extensive experiments conducted on large concrete specimens. Hysteresis loops for combined interface shear transfer and dowel action are also given, along with predictions of the relative amounts of shear taken by the two mechanisms. Expressions are presented for predicting the onset of splitting from axial load on the reinforcement and from dowel action.

La rapport donne, pour des éprouvettes de béton-armée déjà fissurées et puis sollicitées aux efforts cycliques de cisaillement à travers la fissure, des relations entre la rigidité liée a'la transmission des efforts de cisaillement interfacial et celle liée a l'effet de goujon. Les effets des efforts cycliques sur la perte de rigidité sont inclus. Boucles d' hystérésis pour l'effet conjugé de l'effort rasant interfacial et de l'effet de goujon sont également donnés, en plus des prédictions pour la répartition de l'effort de cisaillement entre ces deux mécanismes. Des expressions pour prédire le commencement de fendage a cause de l'effort axial dans l'armature et de l'effet de goujon ont été présentées.

INTRODUCTION AND SCOPE

This paper is on the transfer of cyclic shear forces in cracked reinforced concrete by means of interface shear transfer and dowel action mechanisms. The research was originally motivated by the need to understand the transfer of membrane shear stresses induced by seismic forces across precracked concrete surfaces in pressurized secondary nuclear containment vessels made of reinforced concrete. However, the results can be applied to other situations where shear forces have to be transferred across cracked concrete surfaces reinforced with medium to large diameter bars (#7 to #14; 22 to 43 mm diameter).

Experiments were conducted to evaluate the transfer of shear forces across cracked surfaces by (a) interface shear transfer alone, (b) dowel action alone, and (c) combined interface shear transfer and dowel action. Test specimens were large concrete blocks with shearing areas of at least 225 square inches (145,000 mm^2), with reinforcement ratios in the range of 1 to 2% and reinforcing bar sizes up to #14 (43 mm diameter). The main variables studied included (a) reinforcement percentage at the crack, (b)

the initial width of the crack along which shear is being transferred, (c) the number of cycles of shear, (d) the level of applied tension acting on the bar in addition to the shear-induced dowel forces, and (e) the intensity of shear stress. The degrading nature of the shear force-shear slip relationship and the changing character of the hysteresis loops were established for use in nonlinear analysis of behavior.

Simplified equations are presented here to describe the first loading cycle stiffness exhibited by both the interface shear transfer mechanism and the dowel action mechanism. A bilinear idealization is proposed for the experimentally determined hysteresis curve for each mechanism. These idealized hysteresis curves are combined using equilibrium and compatibility constraints to obtain the hysteresis curves for combined action of both mechanisms. The model can be used to predict the relative amounts of shear carried at a crack by dowel forces and by interface shear transfer, for any combination of variables, and in nonlinear dynamic analysis.

Equations are derived from a nonlinear regression analysis for the splitting failure force for axial or dowel forces, and for their interaction.

INTERFACE SHEAR TRANSFER

A large number of experiments on interface shear transfer (IST) were conducted by Laible, et al (1977) and by White and Holley (1972) on the type of specimen shown in Fig. 1, except that the reinforcing bars in these specimens were external, anchored to steel beams that in turn were fastened to the top and bottom surfaces of the specimen. The specimens were precracked and then cycled at shear stresses on the order of ±160 psi (1.10 MPa). Typical results are shown in Fig. 2 for a specimen with an initial crack width of 0.03 inches (0.76 mm) and a total restraining bar stiffness K_r of 3420 k/in (600 kN/mm). Both shear displacement and crack width continue to grow with cycling, and the shear stress vs. shear displacement relationship becomes very soft at low shear stresses (see cycle 15 results in Fig. 2) and increasingly stiffer at higher shear stresses, with extremely high unloading stiffnesses. The first cycle of shear loading produced essentially linear response.

The basic model used in developing numerical expressions for IST is given in Fig. 3. A restraint stiffness normal to the crack is supplied by steel bars. The slightly open crack must have some shearing displacement to initiate contact and hence development of shear stiffness. An equilibrium equation can be written (see Jimenez, et al [1978]) in terms of the frictional stress generated at the crack, the contact area, and the change in axial force in the restraining steel bars. Similarly, a general relationship for the IST displacement can be written in terms of contact area and the frictional and bearing stresses generated at the crack. The bearing mode of shear transfer is predominant at low values of initial crack width, and the frictional mode dominates for larger initial crack widths.

A stiffness expression for the first cycle of shear loading for the case of constant crack width (which corresponds to a very large restraining stiffness K_r) results from this analysis, where the constants in the general expression are determined by regression analysis of experimental data from Fenwick (1966) and Houde (1973):

$$K_{IST} = \frac{1}{3.9\ (c-0.002)} \qquad (1)$$

where c is the crack width in inches and K_{IST} is in k/in. This equation gives an excellent prediction of first cycle stiffness for crack widths greater than 0.005 inches (0.13 mm).

Shear stiffness in the IST mode is a function of the normal restraint stiffness K_r when the opening of the crack during shearing is controlled by the restraint bars. Test results indicate that the value of K_r becomes significant in defining shear stiffness when it drops below the value $K_r = 3.4\ (10^5)$ c k/in. A regression analysis of Laible's data leads to the following first cycle stiffness expression for shear stress levels less than 300 psi (2.07 MPa):

$$K_{IST} = \frac{1}{fa} \tag{2}$$

where

$$f_a = 3.9\ (c - 0.002) - 1.09\ (10^{-7})\ \frac{K_r}{c} + 0.0367 \tag{3}$$

The ratios of calculated to experimental IST first cycle stiffnesses for Laible's data ranged from 0.73 to 1.17, with an average value of 0.98.

Shear load cycling increases the peak shear displacement. The main parameters controlling this increase are the number of cycles, n, and the restraint stiffness, K_r. Further analysis of Laible's data produces the following expression for predicting the peak shear displacement at shear stress v_a for load cycle n:

$$\Delta_a^{(n)} = \frac{v_a\ f_a\ \phi_a^{(n)}}{\phi K_r} \tag{4}$$

where

$$\phi_a^{(n)} = n^{(5.2c + 0.12)} \tag{5}$$

and

$$\phi K_r = 0.026\ K_r^{0.45} \leq 1.8 \tag{6}$$

The ratios of calculated to experimental shear displacements at the 15th and 25th cycles range between 0.85 and 1.10, with an average value of 0.96.

These expressions can now be used as a basis for establishing idealized IST hysteresis curves, as shown in Fig. 4. The details of this formulation are given by Jimenez, et al (1978).

DOWEL ACTION

Five specimens were tested to study dowel stiffness and strength of #9 (28 mm) and #14 (43 mm) reinforcing bars subjected to cyclic shear. The specimens were cast with either 4 - #9 bars or 2 - #14 bars and with greased plates at the crack plane to eliminate any IST action. The cyclic shear loading on the bars produced pure dowel action which is expressed in terms of the average shear stress acting on the bars.

The first cycle stiffness can be approximated by a straight line up to a dowel shear stress of approximately 5 ksi (34.5 MPa); for higher stress the dowel stiffness decreases significantly. In subsequent cycles the dowel stiffness is highly nonlinear and exhibits the same general behavior as IST (compare Fig. 5, where the 11th cycle and 15th cycle are shown for specimens with #14 and #9 bars, respectively, with the 15th load cycle in Fig. 2). The major difference from IST behavior is the almost negligible area enclosed by the hysteresis curve for the dowel tests. The latter fact enables one to idealize the dowel action with the curves shown in Fig. 6.

The dowel stiffness for the first load cycle, for dowel shear stress not exceeding 5 ksi (34.5 MPa), may be represented by:

$$K_D = 312\ n_b\ d_b^{1.75} \tag{7}$$

where n_b is the number of bars per layer and d_b is the bar diameter in inches, and K_D is in k/in. The 5 ksi (34.5 MPa) limitation on dowel shear stress is not severe in that in most practical situations with shear stresses on the order of 200 psi (1.4 MPa) the portion of total shear taken by dowel action will lead to shear stresses less than 5 ksi (34.5 MPa).

This equation was derived by Jimenez, et al (1978) from the classical beam on elastic foundation approach, using an average value of 750 ksi/in (204 MPa/mm) for the foundation modulus as determined from the experiments with #9 and #14 bars.

Load cycling increases peak dowel displacements according to the following equation:

$$\Delta_d^{(n)} = \phi_d^{(n)} \frac{V_d}{312\, n_b\, d_b^{1.75}} \tag{8}$$

where

$$\phi_d^{(n)} = 0.029\, n + 0.97 \tag{9}$$

and V_d is the dowel force in kips.

After designating the point of stiffness change for the nth cycle, the foregoing equations enable the complete definition of the idealized hysteresis curve in Fig. 6.

COMBINED IST AND DOWEL ACTION

Results for load cycles 1 and 15 for a specimen with two #14 reinforcing bars embedded in it are given in Fig. 7. A series of specimens of this type were tested by first tensioning the reinforcement to produce a crack of about 0.020 inch (0.51 mm) width and then applying cyclic shear forces with a tension of about 35 ksi (241 MPa) on the bar. Increase of shear displacement with cycling for four different specimens is plotted in Fig. 8.

The stiffness and displacement relations given earlier in the paper for IST alone and for dowel action alone were combined using equilibrium and compatibility equations. The resulting computer program, given in the reference by Jimenez, et al (1978), can be used to general load-displacement curves for any combination of reinforcing bars. A typical set of curves for load cycles 1, 9, and 15 for specimens with 2 - #14 bars is given in Fig. 9.

The analysis predicts the percentage of total shear taken by IST and by dowel action. For specimens with an initial crack width of 0.02 in. (0.51 mm), the IST mechanism accounts for about 75% of the total shear in specimens reinforced with #14 bars, and about 85% in specimens with 4 - #9 bars. The IST share tends to decrease slightly (several percent) during the first five load cycles and then increases very slightly in subsequent cycles.

The combined model also gives predicted values of peak shear displacement as a function of cycling. Typical results are given in Fig. 10.

SPLITTING EFFECTS

Except for one specimen made with 4 - #7 bars, all specimens used for dowel action and for combined IST and dowel action failed by splitting of the concrete along the longitudinal axes of the reinforcing bars.

The axial and dowel loads (in kips) required to produce a concrete splitting failure are:

$$\text{Axial:}\quad T_o = \frac{d_b\, L\, c_m \sqrt{f'_c}}{35.4\, d_b + 0.57L} \tag{10}$$

$$\text{Dowel:} \quad V_{do} = \frac{d_b b_n}{n_b} \left[0.47 + \frac{0.54 c_m}{(b_n/n_b^2)+d_b}\right] \qquad (11)$$

where L = bar length, c_m = minimum concrete cover, f'_c = concrete strength in psi, d_b = bar diameter, b_n = net width at a layer of bars (perpendicular to shear force), and n_b = number of bars in a layer, with all dimensions in inches.

The interaction of these two effects is tentatively proposed to be represented by an elliptical equation, but further experiments are needed to confirm this.

The reader is urged to consult the references by Jimenez, et al (1978) and by Jimenez, et al (1979) before applying Equations 10 and 11 to any situation other than that used in the experiments discussed in this paper. The influence of specimen geometry and method of load application are particularly crucial parameters in either enhancing or hindering the onset of splitting type failures.

CONCLUSIONS

1. Shear forces can be transmitted efficiently across cracks in reinforced concrete by the combined action of interface shear transfer and dowel action.
2. Cyclic shear loading increases the shear displacement at the crack, the crack width, and the reinforcing bar strains. The rates of increase are strong functions of the reinforcement percentage (restraint stiffness), the initial crack width, and the level of applied shear stress.
3. The size of the reinforcing bar crossing the crack is important in determining the fraction of total shear taken by dowel action and in influencing possible splitting action; the larger the bar, the greater the tendency to fail by splitting when the specimen is subjected to combined shear on the crack and axial tension in the reinforcement. Hence test results using small bars are not necessarily applicable to situations utilizing large bars.
4. Interface shear transfer stiffness and the effects of cyclic shear loading on increasing peak shear displacements are predicted by Equations 1-6.
5. Dowel action stiffness and the effects of cyclic shear loading on increasing peak dowel displacements are predicted by Equations 7-9.
6. The models implied by Equations 1-9, along with experimentally determined points for change in stiffness in cycles past the first cycle, may be combined to give a valid model for predicting stiffness, peak displacements, effects of cycling, and relative contribution of IST and dowel action for cracked reinforced concrete where both IST and dowel action are present.
7. Expressions for predicting splitting failures by dowel forces and by axial load are given in Equations 10 and 11.
8. The IST mechanism accounts for about 75-85% of the total shear force transmitted across cracked reinforced concrete under the conditions met in this research project; the remaining 15-25% is transmitted by dowel action.

ACKNOWLEDGEMENTS

This research was sponsored by the National Science Foundation and the Nuclear Regulatory Commission, and is part of a comprehensive, continuing investigation at Cornell University of shear transfer and related problems in reinforced concrete structures subjected to seismic loadings.

REFERENCES

Fenwick, R. C., "The Shear Strength of Reinforced Concrete Beams," Ph.D. Thesis, University of Canterbury, Christchurch, New Zealand, 1966.

Houde, J., "Study of Force-Displacement Relationship for the Finite Element Analysis of Reinforced Concrete," Structural Concrete Series, No. 73-2, McGill University, Montreal, December 1973.

Jimenez, R., Gergely, P., and White, R.N., "Shear Transfer Across Cracks in Reinforced Concrete," Report 78-4, Department of Structural Engineering, Cornell University, Ithaca, N.Y., August 1978.

Jimenez, R., White, R.N., and Gergely, P., "Bond and Dowel Capacities of Reinforced Concrete," ACI Journal, Proc. V. 76, No. 1, January 1979.

Laible, J.P., White, R.N., and Gergely, P., "An Experimental Investigation of Seismic Shear Transfer Across Cracks in Concrete Nuclear Containment Vessels," Reinforced Concrete Structures in Seismic Zones, ACI Special Publication, SP-53, 1977.

White, R.N., and Holley, M.J., Jr., "Experimental Studies of Membrane Shear Transfer," Journal of the Structural Division, ASCE, August 1972.

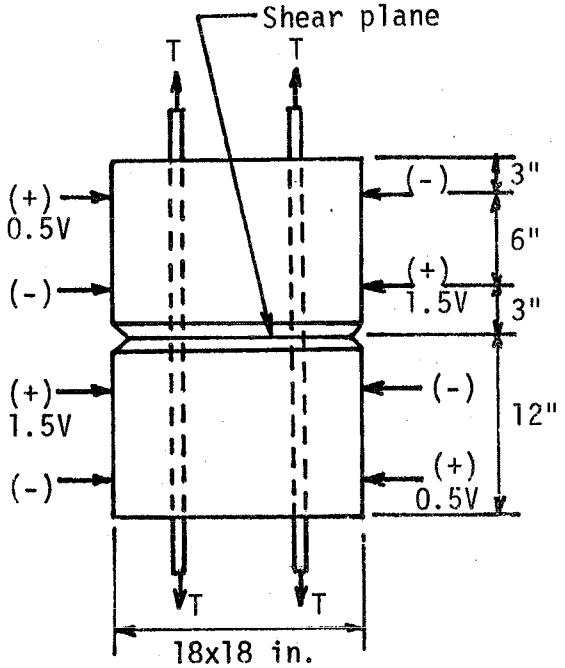

Fig. 1 - Specimen Dimensions

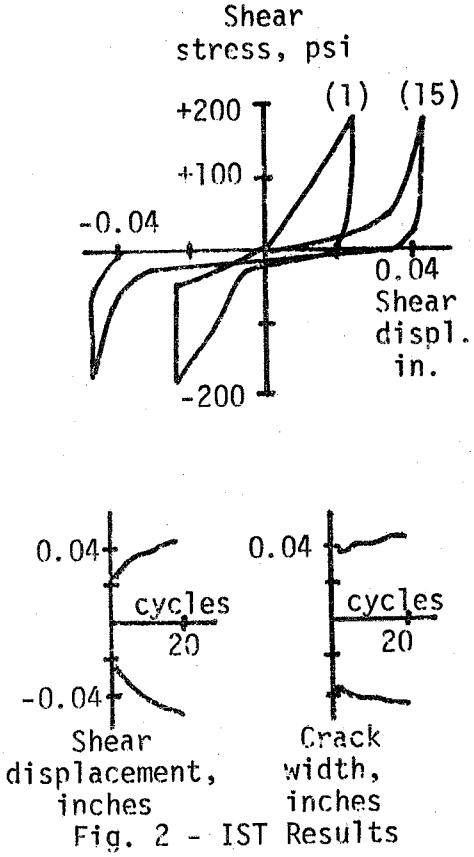

Fig. 2 - IST Results

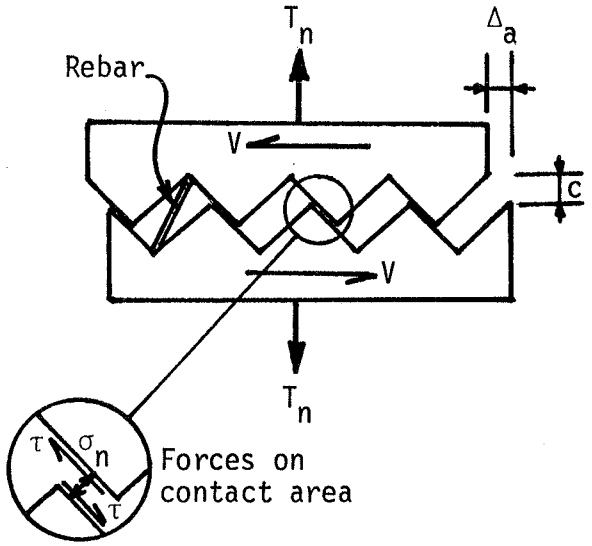

Fig. 3 - Interface
Shear Transfer Model

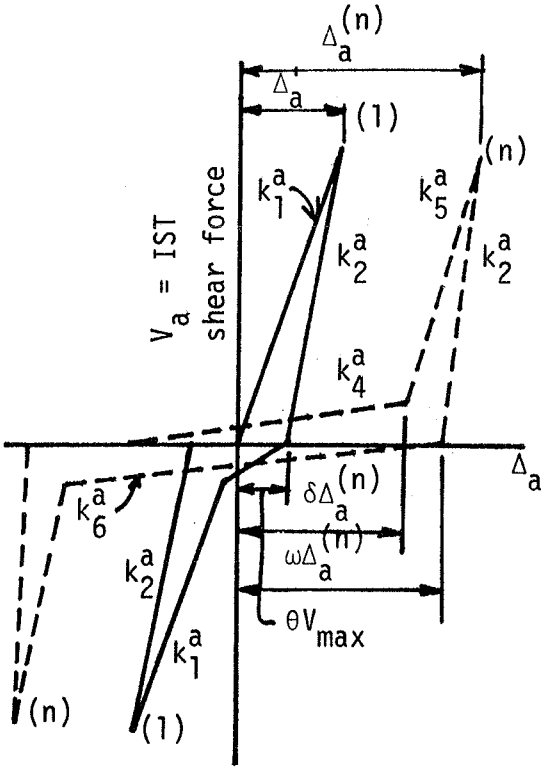

Fig. 4 - Idealized Model
for IST Hysteresis Curves

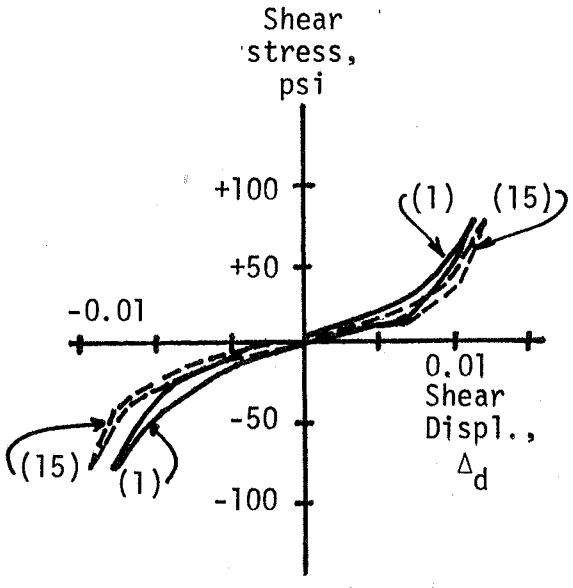

Fig. 5 - Dowel Action
Results

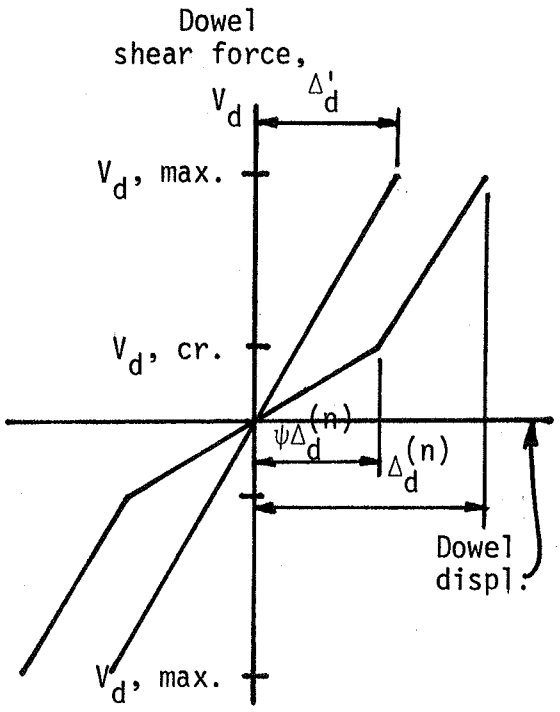

Fig. 6 - Idealized
Dowel Action Hysteresis Curves

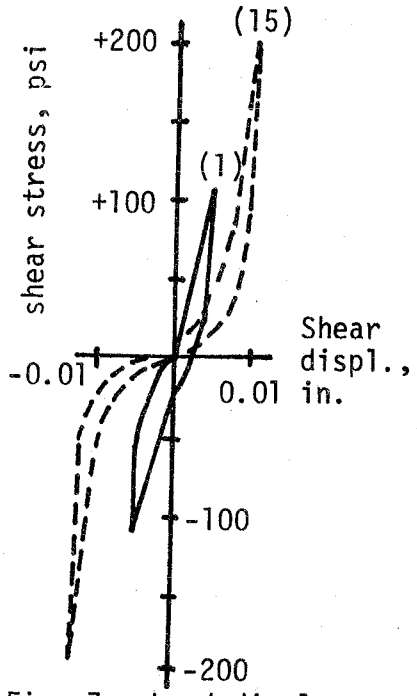

Fig. 7 - Load-displ. Curves

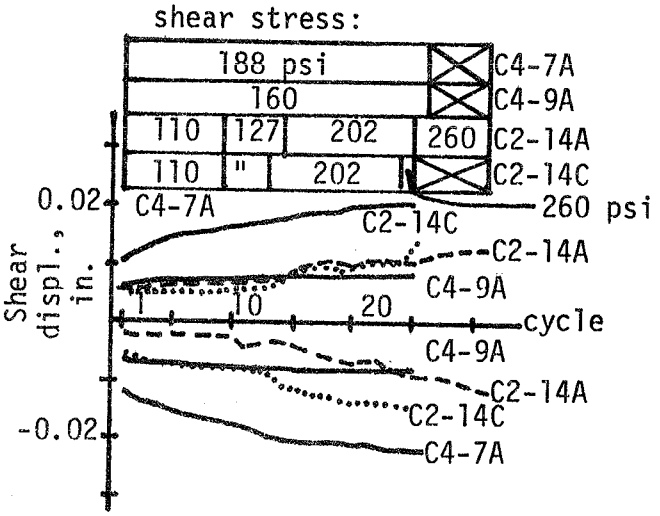

Fig. 8 - Maximum Shear Displacement As A Function of Cycle Number

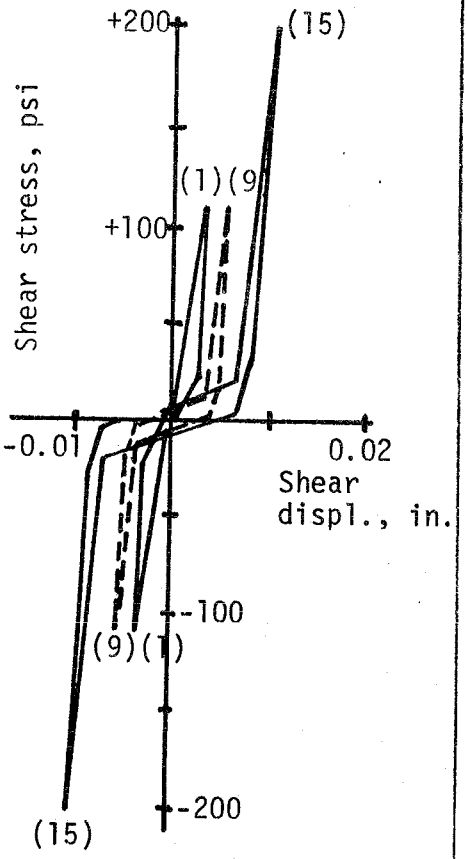

Fig. 9 - Calculated Load-Displ. Curves

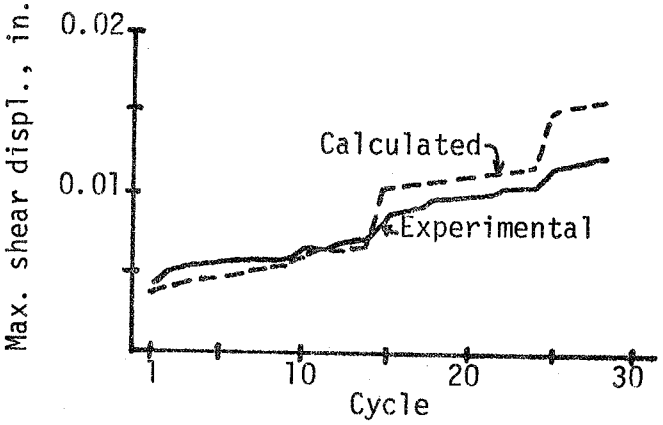

Fig. 10 - Increase in Maximum Shear Displacement Cycling

PRELIMINARY RESULTS OF LOCAL BOND-SLIP RELATIONSHIPS BY MEANS OF MOIRE METHOD

T.P.TASSIOS
National Technical University
Athens, Greece

E.G. KORONEOS
National Technical University
Athens, Greece

S U M M A R Y

An overall optical method (the differential Moiré method) is used in order to visualize the full field of stresses, strains and slips at the interface between concrete and a steel sheet tensioned from outside. The interface is simultaneously loaded in the transversal direction by a compressive stress equal to approx. 1,2 MPa. From the induced mechanical interference pattern between a 20 lines per mm grating, glued on the specimen, and an external (undeformed) grating, the longitudinal displacements "s" are determined on every point of the interface. Similarly, the steel strains are determined, allowing for steel stress evaluation. Consequently, by derivation of the steel stress diagrams, local bond stresses "τ" are evaluated. By compilation of coupled "τ" and "s" values, a local-bond vs local-slip curve is found which constitutes a basic tool for analytic treatment of a series of stiffness degradation problems.

R E S U M É

Une méthode optique d'ensemble (la méthode Moiré différentielle) fut utilisée afin de rendre visible le domaine complet des contraintes, déformations et glissements sur l'interface entre le béton et une lame d'acier chargée axiallement de ses deux côtés. L'interface etait simultanément chargée transversalement en compression (1,2 MPa). Les franges formées entre un

réseau collé sur l'éprouvette (20 lignes par mm) et un réseau de référence non déformé, servent à determiner les déplacements longitudinaux a tout point de l'interface. De la même façon les allongements de l'acier sont également trouvés. Leur dérivation conduit aux valeurs des contraintes d'adhérence le long de l'interface. C'est ainsi que, en combinant les pairs des valeurs "adhérence locale" τ et "glissement local" s, on établit une courbe unique "τ-s" qui constitue un outil fondamental pour le traitement analytique de toute une série de problèmes de diminution graduelle de rigidité.

1.-I N T R O D U C T I O N

1.1.-It is admitted that a constitutive law could be established between the local bond-stress and the corresponding local slip, at several points along a reinforcing bar, as a function of geometrical and material properties. If this would be the case, then a series of problems of structural behaviour of reinforced concrete under both monotonic and cyclic loading could be a n a l y t i c a l l y solved, such as crack widths, fixed-ends slip, stiffness degradation, hysteretic damping etc.

There is actually a considerable evidence about the possibility to establish such an approximative constitutive law, when the following data are given: concrete quality, transversal reinforcement, clear cover and the distance of the point considered from a primary crack or from an end-face. Such evidence may be found i.a in research works of Morita and Kaku [1973], Doerr [1978] and Bertero, Popov and Viwathanepa [1978].

1.2.-Except of the "short"-length pull out tests, these local bond-slip relationships are assessed by means of internally instrumented bars.

This paper reports the results of a preliminary test with a third experimental technique: An o v e r a l l

optical method (the Moiré method) is used, by means of which the f u l l f i e l d of stresses, strains and slips is visualized. The first results appear to be encouraging, and the potentiality of the method seem quite large: Local bond-local slip relationships under monotonic and cyclic loading, overall structural behaviour of hooked steel sheets embedded in concrete, crack detection and analysis, interface behaviour of epoxy glued metals etc.

Several research projects on these topics are actually in progress in the National Technical University of Athens.

2.-E X P E R I M E N T A L S E T U P

2.1.-Materials

The specimen tested in this investigation consisted of a steel sheeton both sides of which concrete blocks of prismatic shape were casted. Form and dimensions of the specimen are given in figure 1.

The steel in the composite specimen is subjected to tensile loads, so that its deformations are transferred to the concrete. The specimen is also loaded in the transverse direction by a compressive loading system. Both external surfaces of the specimen that is steel and concrete and especially the part corresponding to the gauge area had a ground finish taken down to "0000" emery paper; the steel surface afterwards was polished with diamond paste. Thus, the surface of the specimen was made free from pits, scratches or other surface imperfections.

Great care was exercized in properly aligning the specimen in the grips of the testing machine.

The mechanical properties of steel and concrete used for the specimen, are as follows : Steel ; tensile strength 428 MPa, yield strength 223 MPa, modulus of elasticity 208800 MPa, elongation up to rupture 35 %,

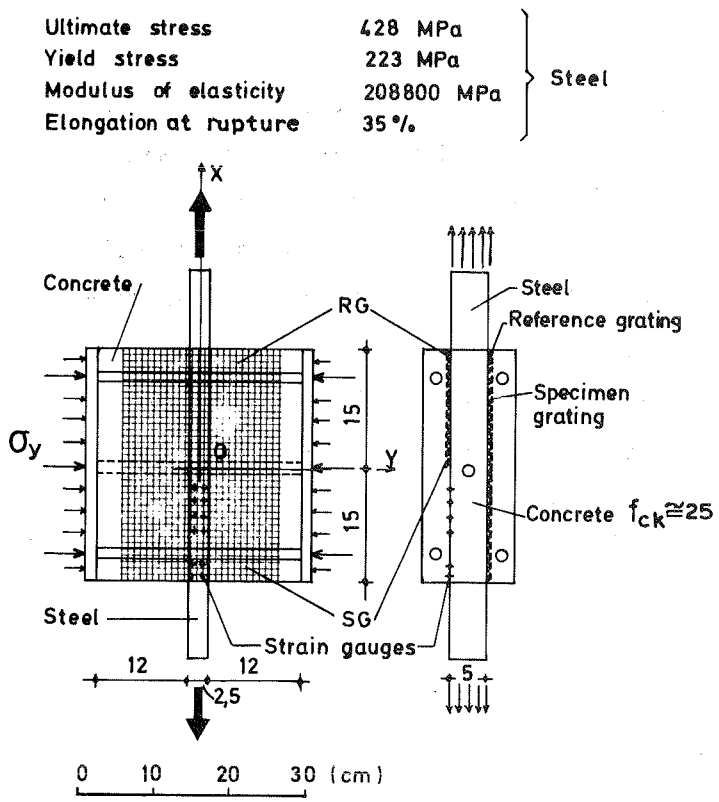

Fig.1 Test specimen

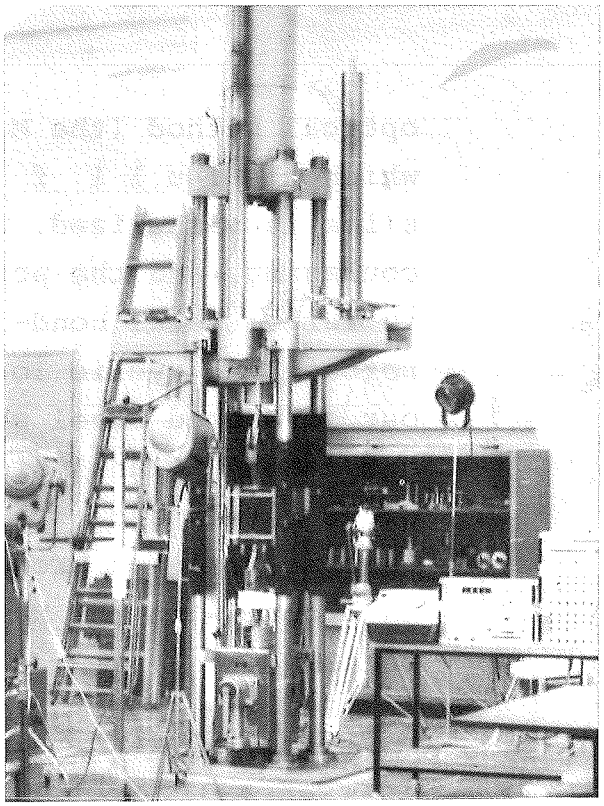

Fig.2 Test set-up

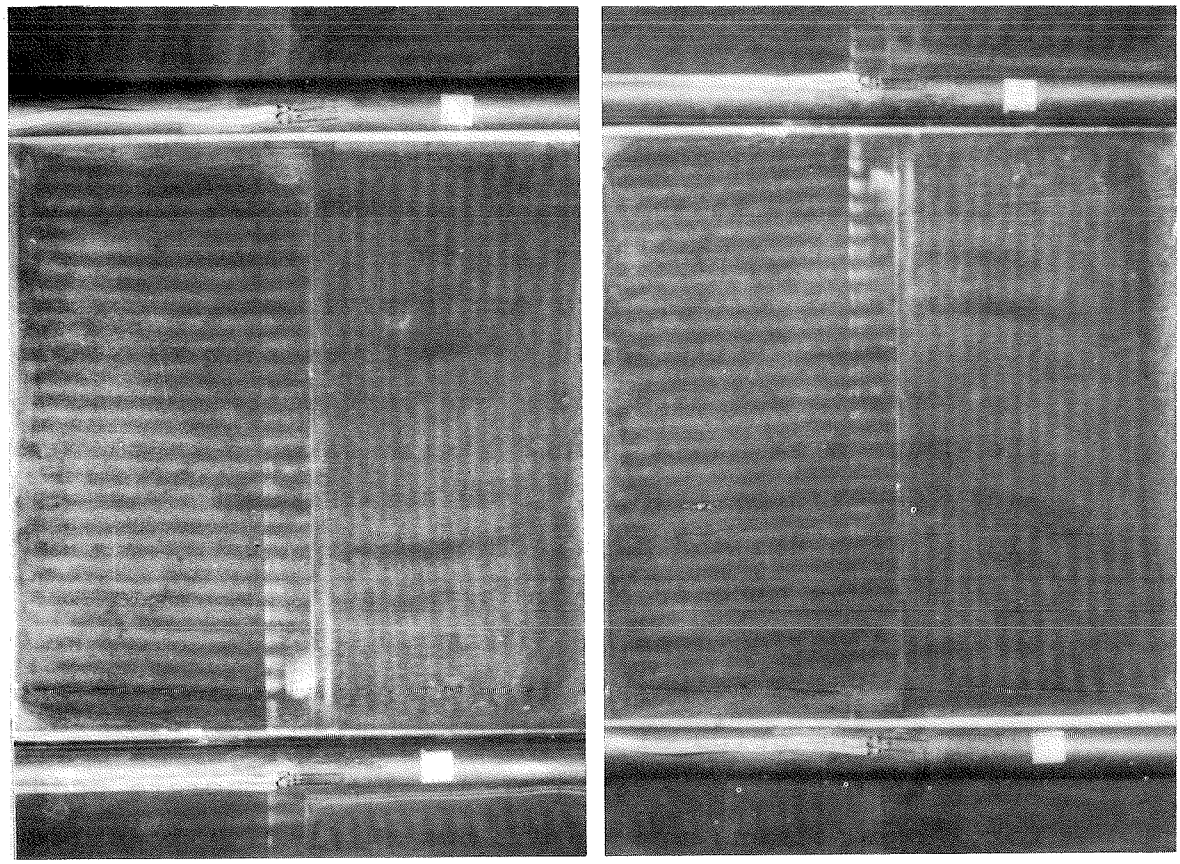

Fig.3 Longitudinal and transverse interference moiré patterns for two loading levels

Concrete: compression strength $f_{ck} \cong 25$, granulation 0-15 mm

2.2.-Testing Technique

Tests were run in a 100 ton. Amsler hydraulic testing machine. Crosshead speeds were kept constant all over each test, interrupted by constant time intervals for taking photographs of each step of loading.

The Moiré method of measuring strains, Theocaris [1969], is based on the mechanical interference produced by the superposition of a line master grating on the crossed model grating.

The interference of the two grating produces fringes, measuring the relative displacement between the two gratings. Hence, the components of strain can be calculated over the entire gauge area of the specimen through graphical differentiation of the field of displacements.

For the accurate measurement of the elastic strains the master and model gratings are chosen to have slightly different pitches, producing an initial moiré pattern before any loading of the specimen. This initial moiré pattern is added vectorially to the moiré produced by the progressive deformation of the specimen. This is the so called differential moiré method.

An orthogonally crossed grating of a density of 20 lines per mm was fixed on both sides of the specimen for the measurement of longitudinal and transverse strains as well as relative displacements.

Master line gratings were reproduced on photographic sheets with different pitch values. The master grating was superimposed on the model grating and was applied by mean of a thin layer of a special grease resulting to an initial moiré pattern with a finite value of interfringe.

The moiré patterns produced by superposition in both directions of the suitably reduced or enlarged master gra-

tings on the model grating were photographed before loading and at each loading step with a fine grain polystyrene-base film. Positives of these photographs were prepared on the same scale as the specimen dimensions. The quantity of light and the exposure time were selected to yield slightly underexposed photographs showing the darkest parts of moiré fringes.

In the specimen the elastic strains were also determined by means of electric strain gauges, disposed in longitudinal direction along the steel sheet at the vicinity of the interface between steel and concrete (Fig. 1)

The arrangement of the experimental apparatus used is shown in figure 2.

3.-D A T A E V A L U A T I O N

From the results after the evaluation of the moiré patterns (Fig.3) as well as the elastic strain values determined by means of the electric strain gauges, the variation of the longitudinal strain, cons/tly the normal stress "σ_{sx}" along the interface is plotted (Fig.4).

Afterwords by using the simple equilibrium equations the shear stress "τ" along the interface between steel and concrete for various loading steps is derived through graphical differentiation of the steel normal stress curves and is plotted in diagrams in figure 5.

The relative displacements between steel and concrete is determined in the region of the interface through graphical evaluation of the displacement curves. Plots of the relative displacement curves along the interface are constructed for different steps of loading (Fig.5).

Figure 6 presents the variation of the shear stress "τ" at the interface as a function of the relative displacement "s" between steel and concrete for different points on the interface and for various loading steps.

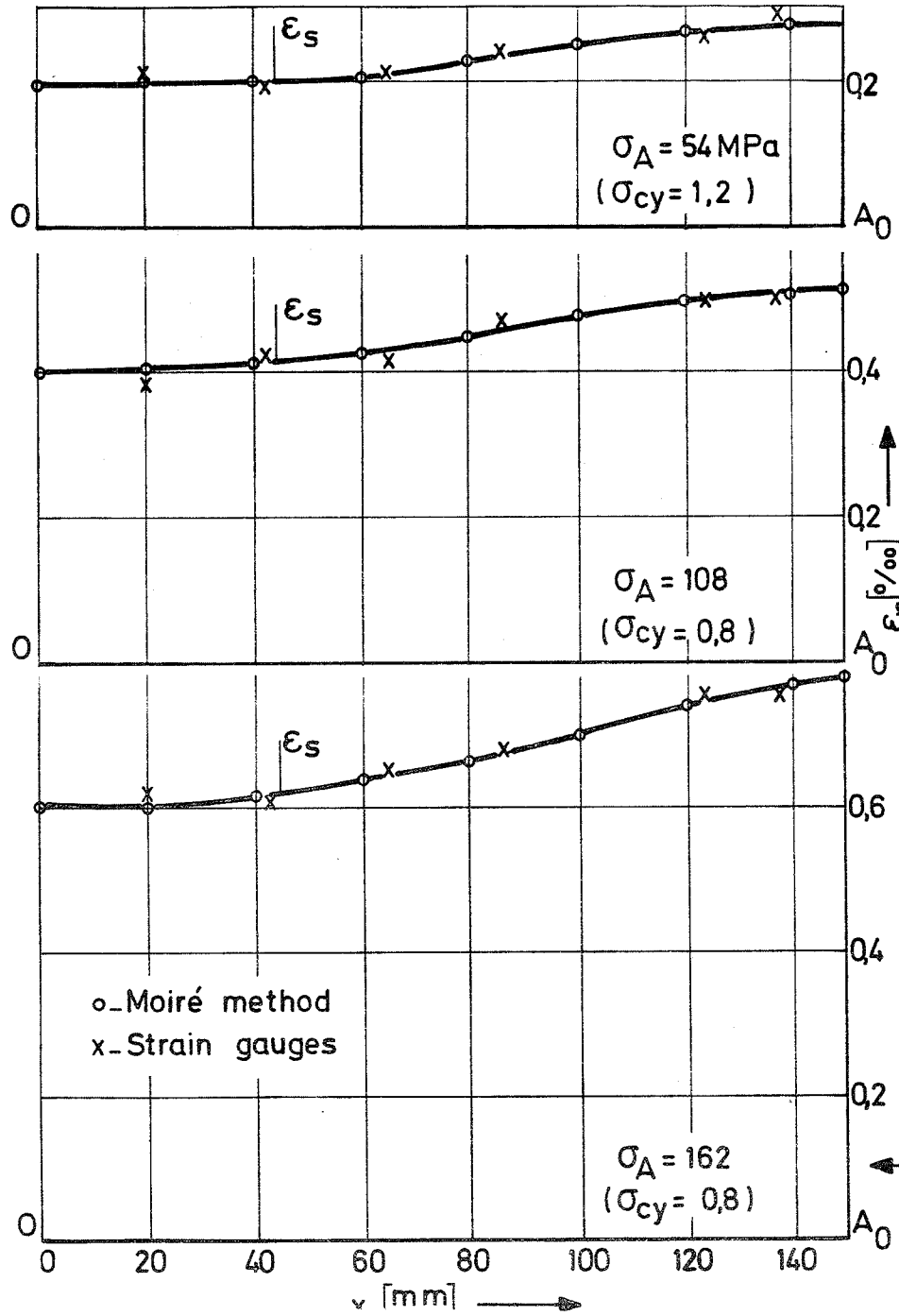

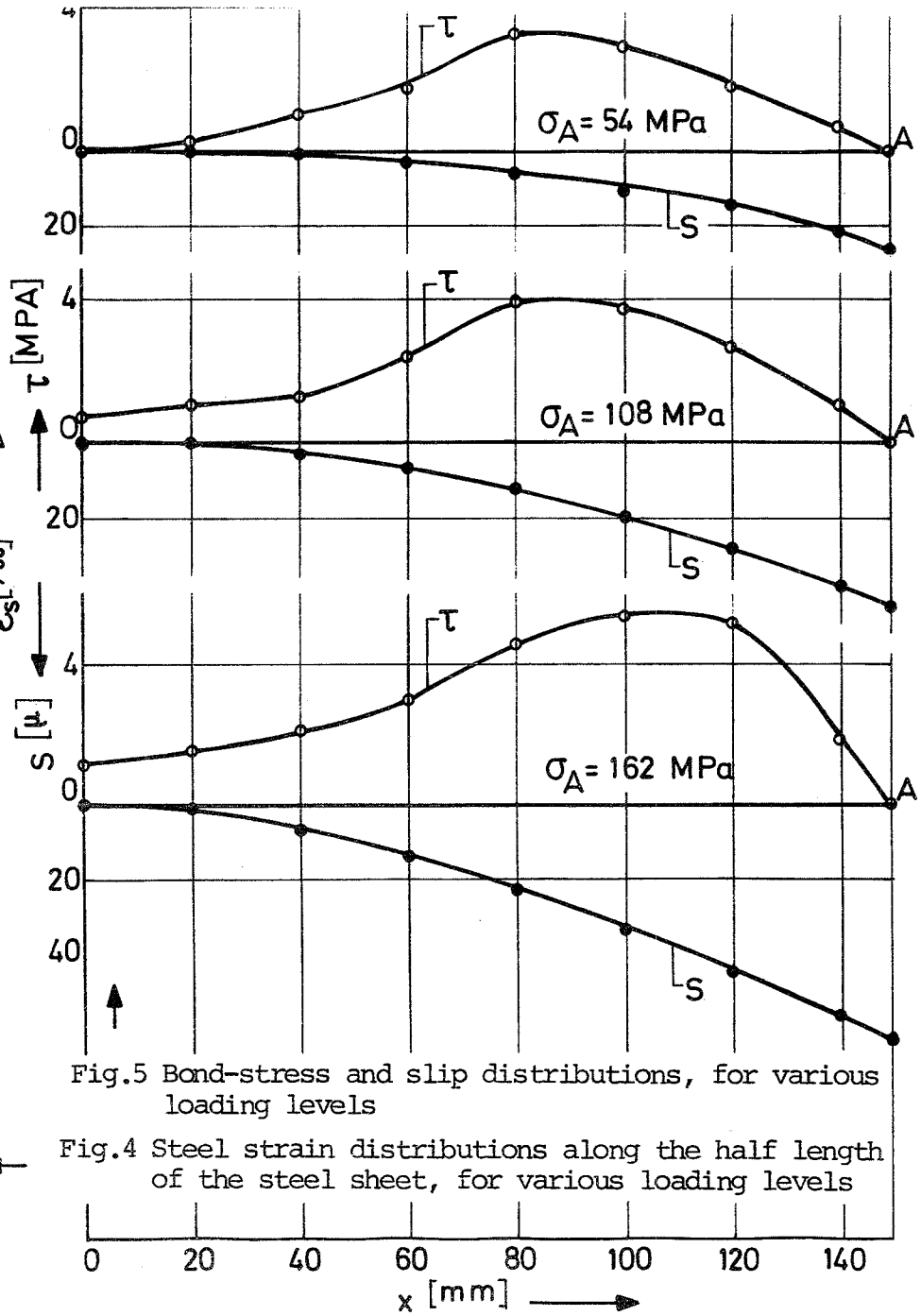

Fig.5 Bond-stress and slip distributions, for various loading levels

Fig.4 Steel strain distributions along the half length of the steel sheet, for various loading levels

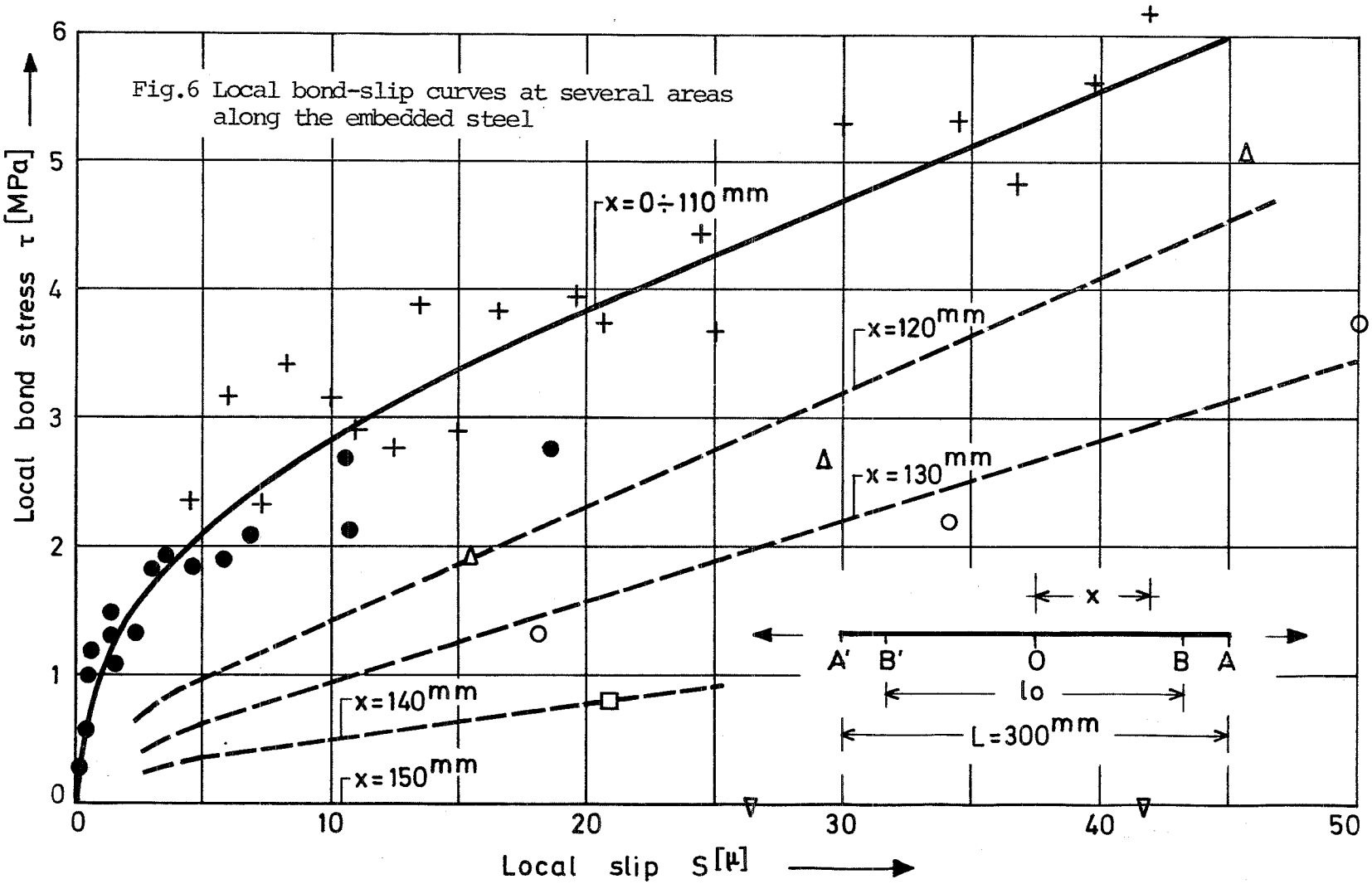

Fig.6 Local bond-slip curves at several areas along the embedded steel

4.-T E S T R E S U L T S

Detailed results along the half length of the embedded steel are shown on Fig. 4 and Fig. 5 for several loading levels of the steel.

A satisfactory agreement has been found between strain gauge measurements of steel strains and strains measured by means of Moiré fringe evaluation.

Slips were determined with a precision of ± 1μ, (10^{-3}mm).Nevertheless, the overall precision (as it may be judged on the basis of the scattering) is equal to ± 4μ.

Anyhow, this seems to be a remarkably high precision constituting the most interesting feature of the method used.

Fig. 6 is a compilation of all pairs of "τ" and "s" - values along the interface, for all loading levels considered. For points away from the end-face ($x: \frac{L}{2} < 0,75$) a common τ-s curve may be traced, with a rather reasonable scattering. Further straining levels are needed in order to complete this curve for large s-values.

On the contrary, for points near the end face ($x: \frac{L}{2} > 0,75$), much lower and distinctive τ-s curves are taken, gradually tending to zero bond-stress for finite slip-values.

Similar tests with the same method are still in progress within a broader research program in the Nat.Tech.University of Athens.

A C K N O W L E D G E M E N T S

The authors gratefully acknowledge the basic financing of this project offered by the Nat. Tech. University of Athens. They also wish to express their gratitude to Prof. P.S. Theocaris for kindly making available to the authors the testing machine and photographic equipment.

R E F E R E N C E S

Bertero, Popov and Vivathanatepa: "Bond of reinforcing steel: Experiments and a mechanical model", Proc. IASS Symp. Nonlinear

Behaviour of R.C. Spatial Structures, Darmstadt, 1978.
Doerr K.: "Bond-behaviour of ribbed reinforcements under transversal pressure", Proc. IASS Symp. Nonlinear Behaviour of R.C. Spatial Structures, Darmstadt, 1978.
Morita and Kaku: "Local bond stress-slip relationship under repeated loading", Symposium: Resistance and ultimate deformability of structures acted on by well defined repeated loads, Lisboa, 1973.
Theocaris P.S.: "Moiré fringes in strain analysis", Pergamon Press, London, 1969.